
Wayne State University Dissertations


January 2019

Gentamicin-Modified Nanocarriers For Placental Targeted Drug Delivery To Treat Pregnancy-Related Complications

Ali Alfaifi

Wayne State University, alialfaifi85@gmail.com

Follow this and additional works at: https://digitalcommons.wayne.edu/oa_dissertations

 Part of the [Medicinal Chemistry and Pharmaceutics Commons](#), and the [Nanoscience and Nanotechnology Commons](#)

Recommended Citation

Alfaifi, Ali, "Gentamicin-Modified Nanocarriers For Placental Targeted Drug Delivery To Treat Pregnancy-Related Complications" (2019). *Wayne State University Dissertations*. 2281.
https://digitalcommons.wayne.edu/oa_dissertations/2281

This Open Access Dissertation is brought to you for free and open access by DigitalCommons@WayneState. It has been accepted for inclusion in Wayne State University Dissertations by an authorized administrator of DigitalCommons@WayneState.

**GENTAMICIN-MODIFIED NANOCARRIERS FOR PLACENTAL TARGETED
DRUG DELIVERY TO TREAT PREGNANCY-RELATED COMPLICATIONS**

by

ALI ALFAIFI

DISSERTATION

Submitted to the Graduate School

of Wayne State University,

Detroit, Michigan

in partial fulfillment of requirements

for the degree of

DOCTOR OF PHILOSOPHY

2019

MAJOR: BIOMEDICAL ENGINEERING

Approved By:

Advisor

Date

ACKNOWLEDGEMENT

WOW! How can I mention every person that has helped me throughout this journey! It has been a very exciting, developing learning process. Not too long ago, I started my classes in English as a foreign language. This moment was a remote ambition and now new ambitions have been born.

I would like to thank my whole family for the continuous support, love, understanding, motivation and encouragement, especially my loving mother who called me every week asking me how far away I was from finishing! And my answer was always the same, “what I said last week minus one week”. It finally happened!

I would like to especially thank my dear PI. Prof. Sandro da Rocha for his continuous support, guidance, advice, discussions, suggestions, patience, jokes, compassion and signature emails. He has been an inspiring figure not only educationally and scientifically, but also personally. I would like to also thank Dr. Mahendra Kavdia for the continuous support and advisory throughout the PhD.

I would like to also thank every one in the da Rocha group including Qian Zhang, Elizebth Bielski, Rashed Almuqbil, Hanming Zhang, Younan Ma, Fatemhah Sunbul and Sulaiman Alhudaithi. Special thank for Dr. Philip M Gerk for the useful discussions. Many thanks to Dr. Douglas Sweet and Dean Joseph Dipiro for being very welcoming in the Pharmaceutics department, School of Pharmacy, at Virginia Commonwealth University. Many thanks are also for Keyetta Tale and Laura Georgiadis.

I would like to thank my committee members Dr. da Rocha, Dr. Kavdia, Dr. Chen, Dr. Matthew and Dr. Liu for their feedback, critique, discussions, suggestions,

and their valuable time. I would like to also thank the department of Biomedical Engineering at Wayne State University for giving me this opportunity to success. A special thanks is also for Namrata Murthy for continuous support and advisory.

Many special thanks for my family and friends, who were always there in every moment for support, guidance, laughter, understanding and time. This has made me accomplish many things including this dissertation.

Finally I am extremely thankful to the Saudi Arabian government, represented in the Saudi Ministry of Education for the financial support providing me with the scholarships for the PhD, MS and BS degrees.

TABLE OF CONTENTS

ACKNOWLEDGEMENTS	ii
LIST OF TABLES	vi
LIST OF FIGURES	vii
LIST OF ABBREVIATIONS	x
CHAPTER 1 - INTRODUCTION	1
1.2.1 OVERVIEW	1
1.2 UNDERSTANDING THE PLACENTA	3
1.2.1 FUNCTIONS.....	3
1.2.2 DEVELOPMENT AND ANATOMY	4
1.2.3 HUMAN VS RODENT PLACENTA.....	6
1.2.4 SURFACE RECEPTORS IN THE SYNT	8
1.3 NANOCARRIERS FRO PLACENTAL DRUG DELIVERY	9
1.3.1 LIPOSOMES	10
1.3.2 DENDRIMER NANOCARRIERS (DNCs)	11
1.3.3 LITERATURE REVIEW.....	13
1.4 HYPOTHESIS AND OBJECTIVES	17
1.5 RELEVENCE AND ANNOVATION.....	19
CHAPTER 2	20
ABSTRACT HUMAN VS RODENT PLACENTA.....	21
2.1 INTRODUCTION	22
2.2 MATERIALS AND METHODS.....	25
2.2.1 MATERIALS.....	25

2.2.2 SYNTHESIS AND CHARACTERIZATION OF TAGETING LIPIDS	26
2.2.3. IN VITRO STUDIES	28
2.2.3.1 LIPOSOMES PREPARATION	28
2.2.3.2 FITC LOADING IN LIPOSOMES	28
2.2.3.3 LIPOSOMES CHARACTERIZATION	29
2.2.3.4 IN VITRO RELEASE	30
2.2.3.5 PREPARATION AND CHARACTERIZATION OF THE IN VITRO MODEL.....	30
2.2.3.5.1 CELL CULTURE	30
2.2.3.5.2 BEWO MONOLAYER FORMATION AND POLARIZATION	31
2.2.3.5.3 TIGHT JUNCTIONS IN BEWO CELLS	31
2.2.3.5.4 BEWO MONOLAYER CROSS-SECTION	32
2.2.3.5.5 LIPOSOMAL TARGETING IN VITRO	32
2.2.4 IN VIVO EXPERIMENTS.....	33
2.2.4 .1 SYNTHESIS OF CY5.5-MODIFIED PEGYLATED LIPIDS	33
2.2.4.2 PREPARATION OF LIPOSOMES FOR IN VIVO STUDIES.....	33
2.2.4.3 TIMED PREGNANCY	34
2.2.4.4 BIODISTRIBUTION: EX VIVO IMAGING AND TISSUE QUANTIFICATION....	35
2.2.5 STATISTICAL ANALYSIS	36
2.3. RESULTS AND DISCUSSION.....	36
2.3.1 LIGAND DESIGN AND SYNTHESIS OF THE TARGETING LIPID	36
2.3.1.1 LIGAND DESIGN	36
2.3.1.2 SYNTHESIS OF TARGETING LIPIDS	37
2.3.2 IN VITRO STUDIES	40

2.3.2.1 FITC-LOADED LIPOSOMES PREPARATION AND CHARACTERIZATION...	40
2.3.2.2 THE IN VITRO PLACENTAL MODEL	43
2.3.2.3 TARGETING THE IN VITRO PLACENTAL MODEL.....	44
2.3.2.3.1 UPTAKE IN BEWO MONOLAYERS	44
2.3.2.3.2 UPTAKE IN HEPATOCELLULAR CARCINOMA (HEPG2).....	46
2.3.2.3.3 COMPETATIVE INHIBITION OF MEGALIN RECEPTORS	48
2.3.3 IN VIVO STUDIES	49
2.3.3.1 SYNTHESIS AND CHARACTERIZATION OF CY5.5-MODIFIED LIPIDS	49
2.3.3.2 LIPOSOMAL FORMULATION FOR IN VIVO STUDIES	50
2.3.3.3 TARGETING THE IN VIVO PLACENTAL MODEL	50
2.4 CONCLUSION	55
2.5 ACKNOWLEDGMENTS	56
CHAPTER 3	58
3.1 INTRODUCTION	59
3.2 MATERIALS AND METHODS.....	60
3.2.1 MATERIALS	60
3.2.2 SYNTHESIS AND CHARACTERIZATION OF GENTAMICIN-PEG1000DA CONJUGATED, CY5.5-MODIFIED, GENERATION 4, POLYESTER DENDRIMERS (G4OH-PEG1K-GM)	61
3.2.3 IN VIVO EXPERIMENTS	62
3.2.3.1 PHARMACOKINETICS STUDY IN NON-PREGNANT MICE	63
3.2.4 STATISTICAL ANALYSIS	63
3.3 RESULTS AND DISCUSSION.....	64

3.3.1 DENDRIMER MODIFICATION	64
3.3.2 PHARMACOKINETICS (PK)	66
3.4 CONCLUSION	68
CHAPTER 4 - CONCLUSIONS AND FUTURE WORK.....	69
APPENDIX	76
REFERENCES	89
ABSTRACT	100
AUTOBIOGRAPHICAL STATEMENT.....	102

LIST OF TABLES

Table 2.1	Hydrodynamic Diameter (HD), Zeta Potential (ζ), FITC encapsulation efficiency (EE) and percent release at 6h (pH 7.4) for the three different liposomal formulations used in the <i>in vitro</i> studies. SD = standard deviation, n = 4.....	42
Table S2.1	Hydrodynamic Diameter (HD) and Zeta Potential (ζ) of the <i>In Vivo</i> Liposomal Formulations. SD = standard deviation, n =4.....	83
Table 3.1	Characterization of the polyester dendrimer conjugates with respect to molecular weight (MW, Da, from MALDI-ToF), size (hydrodynamic diameter, HD in nm), surface charge (zeta potential, z in mV) and the number of PEG1K or PEG1K-GM conjugates and of Cy5.5 conjugates as determined by MALDI-Tof (M) and ¹ H-NMR (N).....	69

LIST OF FIGURES

- Figure 1.1** Schematic drawing of a full-term placenta with a close-up to the placental villi showing the SynT layer.....4
- Figure 1.2** Illustration of similarities between human and mouse placentas showing the analogous regions between the two species.....6
- Figure 1.3** Comparative representation of human (third trimester) and rodent (GD18.5) placentas showing their differences. Left, human placenta showing a single layer (SynT) separating maternal and fetal circulations. Right, rodent placenta showing three layers (2 SynT layers and one giant trophoblast) separating the two circulations.....7
- Figure 1.4** Illustration of a liposome (lipid bilayer vesicle) with versatile properties such as size, surface charge, surface modifications and capacity to carry small molecular weight hydrophilic and lipophilic drugs and biologics.....11
- Figure 1.5** Illustration of a fourth generation (G4) dendrimer containing 48 surface groups that can be used for conjugating different molecules such as the drug cargo, targeting moieties, tracer molecules, and other surface groups.....13
- Scheme 2.1** Schematic of the chemical synthesis of the targeting lipid DSPE-PEG2K-GM.....38
- Figure 2.1** (a) MALDI-ToF spectra showing the main three peaks of gentamicin (GM, 478, 486, 500Da), BOC-protected gentamicin (GM-BOC, 972, 986, 1000Da) and the succinic anhydride (SA) modified protected gentamicin (GM-BOC-SA, 1072, 1086, 1100Da). (b) ¹H NMR spectra showing the successful modification of gentamicin (GM, black) with BOC (GM-BOC, in red) and SA (GM-BOC-SA, green).....39
- Figure 2.2** MALDI-ToF results showing DSPE-PEG2K (2792Da, black), conjugated DSPE-PEG2K to SA-modified, protected gentamicin (DSPE-PEG2K-GM-BOC, 3961Da, red) and the deprotected final product, the targeting lipid DSPE-PEG2K-GM (3500Da, blue).....41
- Figure 2.3** Cumulative amount of FITC released from actively-loaded, non-targeting (5PEG2K-0GM, red dotted line) and targeting (5PEG2K-5GM – blue dashed line, and 10PEG2K-10GM green line), liposomes at pH 7.4 over 6 hours - incubated at 37 °C. Data represents mean ± SD (n = 4). 5PEG2K-0GM = liposomes with 5 mol% DSPE-PEG2K lipid; 5PEG2K-

5GM = liposomes with 5 mol% DSPE-PEG2K-GM lipid; 10PEG2K-10GM = liposomes with 10 mol% DSPE-PEG2K-GM lipid.....44

Figure 2.4 (a) Transepithelial electrical resistance (TEER) of BeWo monolayers cultured on 0.33 cm² Transwell® inserts as a function of time. Data represents mean ± SD (n = 4). (b) 40X optical image showing a cross-section of the BeWo monolayer on the 6th day post seeding (DPS). (c) ZO-1 staining of a confluent BeWo monolayer obtained on the 6th DPS, indicating tight junction formation.....46

Figure 2.5 Cellular internalization of FITC on polarized BeWo cells (6th day post seeding) determined by flow cytometry, as a function of time post contacting the monolayer with FITC-encapsulated liposomes. The median fluorescence intensity (MFI) data represents mean ± SD (n = 4), with at least 6,000 events (singlets). 5PEG2K-0GM = liposomes with 5 mol% DSPE-PEG2K lipid; 5PEG2K-5GM = liposomes with 5 mol% DSPE-PEG2K-GM lipid; 10PEG2K-10GM = liposomes with 10 mol% DSPE-PEG2K-GM lipid.....48

Figure 2.6 Normalized cellular Internalization of FITC on HepG2 cell monolayers determined by flow cytometry, as a function of time post contacting the monolayer with FITC-encapsulated liposomes. The median fluorescence intensity (MFI) data represents mean ± SD (n = 4) with at least 6,000 events (singlets). 5PEG2K-0GM = liposomes with 5 mol% DSPE-PEG2K lipid; 5PEG2K-5GM = liposomes with 5 mol% DSPE-PEG2K-GM lipid.....49

Figure 2.7 Normalized cellular Internalization of FITC on polarized BeWo cells (6th day post seeding) in the absence and presence of free gentamicin (Free GM; 2mM) determined by flow cytometry at 6 h post contacting the monolayer with FITC-encapsulated liposomes. The median fluorescence intensity (MFI) data represents mean ± SD (n = 4) with at least 6,000 events (singlets). 5PEG2K-0GM = liposomes with 5 mol% DSPE-PEG2K lipid; 5PEG2K-5GM = liposomes with 5 mol% DSPE-PEG2K-GM lipid; 10PEG2K-10GM = liposomes with 10 mol% DSPE-PEG2K-GM lipid.....51

Figure 2.8 (a) Total flux of Cy5.5 for free Cy5.5, 10PEG2K-0GM-CY and 10PEG2K-10GM-CY liposomes measured ex vivo by IVIS imaging showing placentas, fetuses and kidneys 4 hr post treatment. Results shown have been subtracted from background which are fluxes of tissues exposed to PBS control only; (b) representative images of the placental and fetal tissues, as well as kidneys for the various treatment groups. 10PEG2K-0GM-CY = non-targeting liposomes with 10 mol% DSPE-PEG2K lipid and 1.7 mol % DSPE-PEG2K-CY lipid; 10PEG2K-

10GM-CY = targeting liposomes with 10 mol% DSPE-PEG2K-GM lipid and 1.7 mol % DSPE-PEG2K-CY lipid.....54

Figure 2.9 (a) Quantitative analysis (ng/g tissue) of Cy5.5 for control (no exposure to Cy5.5), free Cy5.5, 10PEG2K-0GM-Cy and 10PEG2K-10GM-Cy liposomes measured from homogenized tissues 4 hr post treatment; (b) same results plotted as % initial dose (%ID) – total of 25ug in tissue. Cy5.5 assessed fluorometrically by microplate reader and concentrations obtained based on established calibration curves on spiked tissues. 10PEG2K-10GM-CY = targeting liposomes with 10 mol% DSPE-PEG2K-GM lipid and 1.7 mol % DSPE-PEG2K-CY.....57

Scheme S2.1 Schematic of the chemical synthesis of Cy5.5-modified DSPE-2KPEG lipid (DSPE-PEG2K-CY).....79

Figure S2.1 MALDI-ToF showing the peak shifts for DSPE-PEG2K-CY compared to DSPE-PEG2K (ca. 2790 Da, Figure 2). Cy5.5 with 619 Da.....80

Figure S2.2 (a) Increase in transepithelial electrical resistance (TEER) of BeWo monolayers as a function of time. The figure shows the increasing TEER values of this study compared to other previously reported work^{1, 2}. Note a shift in TEER at day 7. Based on cross section micrographs this corresponds to the formation of multilayers (b). Our work is all at day 6 when BeWo is in monolayer form and polarized...81

Figure S2.3 Cell Viability of BeWo Cell Monolayer after treatment with free gentamicin (n=3). IC₅₀ =10.09 mM.....82

Figure 3.1 Plasma concentration (C_p) analysis as a function of time after retro-orbital administration of CY-G4OH-PEG1K.....70

Figure S3. Cell Viability of BeWo Cell Monolayer after treatment with free gentamicin (n=3). IC₅₀ =10.09 mM.....83

Figure S3.1 MALDI ToF and ¹H NMR showing successful modification of polyester dendrimer with FITC and GM.....84

Figure S3.2 MALDI-ToF peak showing the successful partial conversion of –OH to –NH₂ (15), 7498 Da.....85

Figure S3.3 MADLI-ToF results showing the peak of G4OH-CY at 8600 Da.....86

Figure S3.4 MADLI-ToF results showing the peak of G4OH-CY conjugation of mPEG1K at 17000 Da.....87

Figure S3.5 Detailed ^1H NMR spectra of (a) Cy5.5, (b) dendrimer, (c) G4OH-CY, and (d) G4OH-CY-mPEG1000.....88

Figure S3.6 MALDI-ToF peak (200089 Da) showing the successful conjugation of HOOC-PEG-NH₂-BOC to the G4-CY.....91

LIST OF ABBREVIATIONS

$^1\text{H NMR}$	proton nuclear magnetic resonance
1xHBSS	1x Hank's Buffered Saline Solution
AHA-Boc	6-(Boc-amino)hexanoic acid
BOC	Di-tert-butyl dicarbonate
Bis-MPA	2,2-bis(hydroxymethyl)propionic acid
BSA	Bovine serum albumin
CHOL	Cholesterol
CY5.5	Cyanine 5.5
Da	Dalton
DCM	Dichloromethane
DHB	2,5-dihydroxybenzoic acid
DI water	deionized water
DIPEA	N,N-Diisopropylethylamine
DLS	dynamic light scattering
DMAP	4-(Dimethylamino)pyridine
DMEM	Dulbecco's Modified Eagle Medium 1x high glucose
DMF	N,N-Dimethylformamide
DMSO	Methylsulfoxide
DNCs	dendrimer nanocarriers
DSPE	1,2-Distearoyl-sn-glycero-3-phosphoethanolamine
EDC	N-(3-dimethylaminopropyl)-N'-ethylcarbodiimide

EDTA	Ethylenediaminetetraacetic acid
EE	Encapsulation efficiency
eGFP	enhanced Green Fluorescent Protein
EMEM	Eagle's Minimum Essential Medium
Ex/Em	Excitation/Emission
FACS	flow associated cell sorting (flow cytometry)
FBS	Fetal bovine serum
FITC	fluorescein isothiocyanate
G4NH2	Generation 4 amine-terminated PAMAM dendrimer
GD	Gestational day
GM	Gentamicin
G4OH	Generation 4 polyester dendrimer
HCl	Hydrochloric acid
HD	Hydrodynamic diameter
HepG2	Hepatocellular carcinoma
HSPC	Hydrogenated soybean Phosphatidylcholine
ICC	Immunocytochemistry
IUGR	Intrauterine Growth Restriction
IV	intravenous
IVIS	in vivo imaging system
LA	lauryl alcohol
LS	light scattering
MALDI-TOF	Matrix-Assisted Laser Desorption Ionization Time-of-Flight

MeOH	methanol
MFI	Median Fluorescence Intensity
mRNA	messenger RNA
MWCO	Molecular Weight Cut Off
NHS	N-Hydroxysuccinimide
PAMAM	poly(amidoamine)
PBS	Phosphate buffer saline
PE	preeclampsia
PEG	polyethylene glycol
PNCs	polymeric nanocarriers
SA	succinic anhydride
SD	Standard deviation
SEM	scanning electron microscopy
siRNA	short interfering RNA
SynT	syncytiotrophoblast
TEER	transepithelial electrical resistance
TV	tail vein
ULV	unilamellar liposomes

CHAPTER 1

INTRODUCTION

1.1 Overview

Nanomedicine has recently gained popularity as a medical application of nanotechnology in order to aid in the development of medical treatment, diagnosis, monitoring, and control of biological systems.(Moghimi et al., 2005) Drug delivery using nanocarriers has many potential advantages as for example more efficient formulation, reduced side effects, higher bioavailability, longer circulation and improved pharmacokinetics and biodistribution(Mirza and Siddiqui, 2014). Nanocarriers can be devised from natural or synthetic, organic or inorganic materials such as dendrimers, liposomes, gold nanoparticles, protein-based carriers, and viral-derived nanoparticles(Mirza and Siddiqui, 2014; Moghimi et al., 2005). Many important advances in nanotechnology have been already translated into medical research; several are FDA approved and commercially available for treatment of different types of diseases such as cancer,(Miele et al., 2009; Muggia, 2001; Wagner et al., 2006) hepatitis,(Zeuzem et al., 2000) fungal infections,(Bawa, 2008) pain and influenza(Faraji and Wipf, 2009). Despite the progress accomplished in a wide spectrum of diseases in the area of nanomedicine, there are no clinical applications of nanocarriers to prevent or treat pregnancy-related complications, which begs the question: can we use nanomedicine for the treatment of fetal and/or maternal complications? In this introductory chapter I review the human placental tissue and its contribution to pregnancy related complications; as well as a detailed comparison to mouse

placenta, an analogous in vivo model. I also review the use of nanocarriers as drug delivery tools to the placenta, focusing on the platforms we used: liposomes and dendrimers and how we aim to utilize them to enhance the delivery of therapeutics to the placenta in order to treat pregnancy related complications that are caused by placental malfunction.

Pregnancy-related complications are common, affecting more than 20% (approximately 26 million) of all pregnancies.(Duley, 2009) Some of those complications include preeclampsia (PE), intrauterine growth restriction (IUGR), gestational diabetes, fetal hypothyroidism, bacterial and viral infections(McDonagh et al., 2004; Racicot and Mor, 2017; Silasi et al., 2015). Many of such complications result from compromised functions of the placenta, some of which can lead to maternal and/or fetal mortality if not controlled(Thornburg and Marshall, 2015). Administration of medications in the maternal circulation can treat some diseases of pregnancy. Maternal steroids, for instance, are used to accelerate fetal lung maturation(Roberts et al., 2017). Cardiac drugs can also be used similarly to treat fetal arrhythmias(Oudijk et al., 2000). Levothyroxine can be invasively injected to the amniotic fluid, although being invasive and a less desirable route, to treat fetal hypothyroidism(Gulraze et al., 2013). On the other hand, no effective treatments exist to treat several other complications of the pregnancy, including PE and IUGR.(Romo et al., 2009) In the case of PE, for instance, labor is the best option to mitigate the disease,(McCoy and Baldwin, 2009) however, that is not always a possibility. Therefore, hypertension medications are currently used to lower high blood

pressure associated with PE(Roberts and Gammill, 2005). Anticonvulsant medications are used if PE is severe(Sibai, 2004; Zuspan, 1966). Life style changes such as bed rest is also often required. To understand many of those diseases and be able to devise a strategy to approach them, it is essential to understand the anatomy and physiology of the placenta as well as the pathogenesis of such diseases.

1.2 Understanding the Placenta

1.2.1 Functions:

Placenta is a specialized organ that is present only during pregnancy. At term, the human placental weight is approximately 500 g, has a diameter of 15–20 cm and thickness of 2–3 cm.(Griffiths and Campbell, 2014) It functions by separating two completely distinct circulations: maternal and fetal. It serves several functions that contribute to the synchronization between pregnant mothers, the fetus and the placenta itself.(John and Hemberger, 2012) It is responsible for gas exchange between the two circulations and providing nutrients from the maternal circulation to the fetal one as well as eliminating the waste from the fetal circulation.(Nelson, 2015) The placental tissue also serves as a barrier protecting the fetus from maternal infections and diseases, as well as certain potentially harmful molecules. It is also a major site for metabolism. It can metabolize several drugs and biologics.(Donnelly and Campling, 2014) Moreover, the placenta is also a major endocrine organ that secretes more than 100 peptide and steroid hormones to the fetal or maternal circulations in order to

modulate different functions such as fetal growth, metabolism and parturition.(Burton and Jauniaux, 2015; Gude et al., 2004)

1.2.2 Development and Anatomy:

Placentation starts after implantation of the blastocyst (a newly developed fertilized egg), where trophoblast cells begin proliferating and migrating to the decidua part of the endometrium.(Wooding and Flint, 1994) Part of the proliferating trophoblast starts fusing together to form multinucleated syncytiotrophoblast (SynT), which grow invaginations in the endometrium(Carter, 2007). Such invaginations make up independent functional vascular units called cotyledons. The villous trees located within the cotyledons separate maternal circulation from fetal circulation. The villus is composed of four layers: the SynT

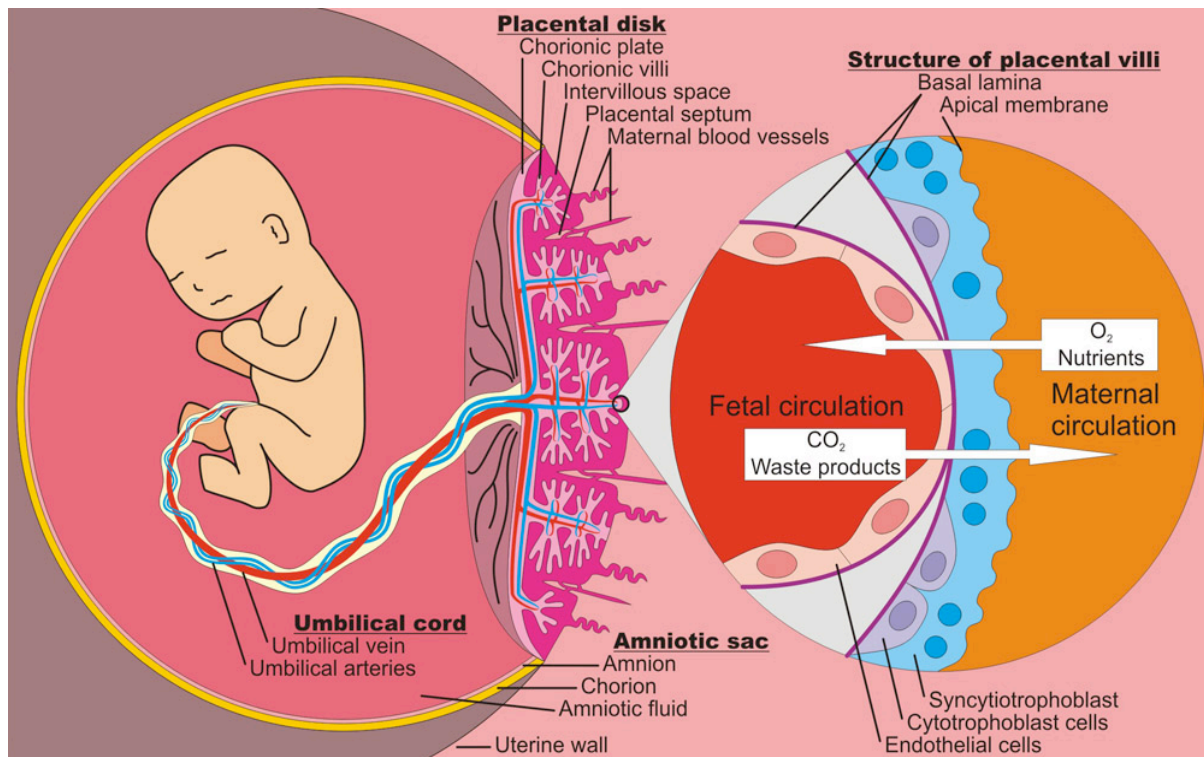


Figure 1.1 Schematic drawing of a full-term placenta with a close-up to the placental villi showing the SynT layer. <http://pimeonline.blogspot.com>

layer, cytotrophoblast cells, connective tissue of the villus and the endothelium of the fetal blood vessels arranged from the maternal to the fetal side, respectively. Such arrangement continues for the first 20 weeks of gestational period. However, after that, the cytotrophoblast layer disappears leaving the placental barrier with the remaining three layers, placing maternal and fetal circulations about 2 to 4 μm in proximity as illustrated in **Figure 1.1**. This arrangement makes the SynT layer to become the main barrier at the maternal-fetal interface.

The SynT layer is a multinucleated epithelial layer that is in direct contact with the maternal blood and is covered on the apical (maternal) side with branched microvilli that maximize the surface area for gas and nutrient/waste exchange. The blood vessels that ramify through the villous stroma carry embryonic/fetal blood, which serves as portal to fetal tissues (Robbins et al., 2010). All these arrangements are the fetal part of the placenta, which is known as the chorionic plate. The maternal part, on the other hand, is called the basal plate. The basal plate contains the endometrium and it provides the endometrial blood vessels that would pour into the space between the chorionic plate and the basal plate; this space is known as the intervillous space. The maternal side is arranged as basal plate, the decidua basalis and the endometrium from fetal to maternal side, respectively. **Figure 1.1** provides an illustration of the arrangements of different parts of the human placenta.

1.2.3 Human VS Rodent Placenta:

The placenta in both humans and rodents serves the main purpose of providing the interface between the mother and the fetus. It is through this

interface all the functions mentioned above are accomplished. While there are many differences between the two species, there are many similarities in terms of placental development, anatomy and functions as illustrated in **Figure 1.2** (Krishnan et al., 2013). From the maternal to the fetal side, the arrangement is as follows: **First region** is the decidua basalis, which is the maternal portion of the placenta that is in direct contact with the myometrium. **Second region** is the *junctional zone* (*jz*, also known as *basal zone*) in mice and basal plate (*bp*, also known as *cytotrophoblastic shell*) in humans.

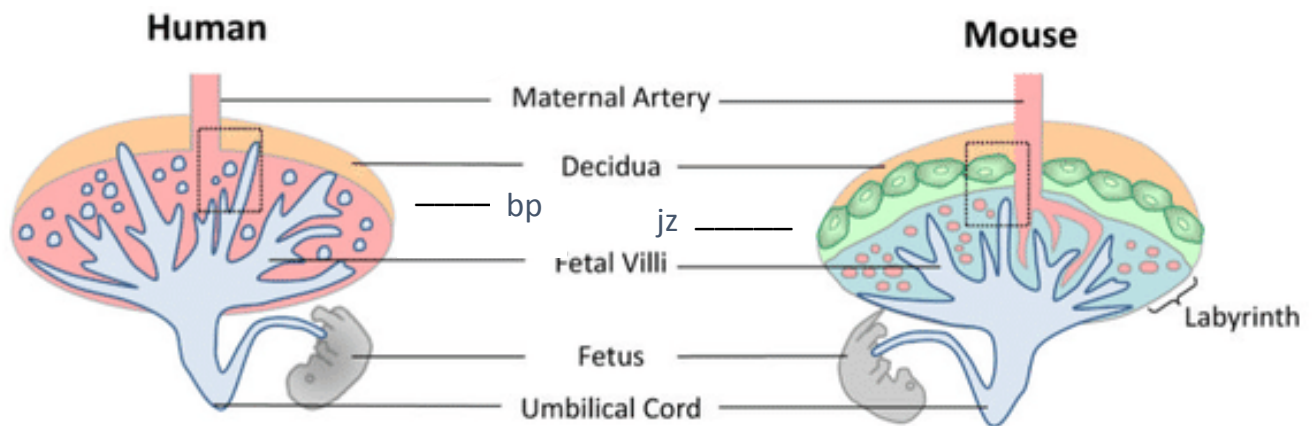


Figure 1.2 Illustration of similarities between human and mouse placentas showing the analogous regions between the two species.(Krishnan et al., 2013)

Third region is known as the *fetal placenta* in humans and *labyrinth* in mice. This region is the fetal part of the placenta and it develops from the zygote. It is within the chorionic plate and is the region at which the villous trees (chorionic villi) bathe in maternal blood within the intervillous space, as shown in **Figure 1.3** (Kulvietis et al., 2011). Within the core of the chorionic villi are the fetal blood vessels that make up the umbilical arteries and veins.

The human fetal placenta is functionally analogous to the mouse labyrinth despite slight structural differences (Georgiades et al., 2002). In mice, the labyrinth consists of 3 layers of cells, and is therefore known as trichorial placenta. On the other hand, human fetal placenta has one layer and is known as monochorial placenta. The three layers of the labyrinth are arranged as Layer I, (cytotrophoblast) Layer II, and III SynT from maternal to fetal side, respectively (Georgiades et al., 2002). It is important to emphasize that both Layers I and II are in contact with the maternal blood. In the human fetal placenta, which is analogous to mouse labyrinth, only one SynT is present.

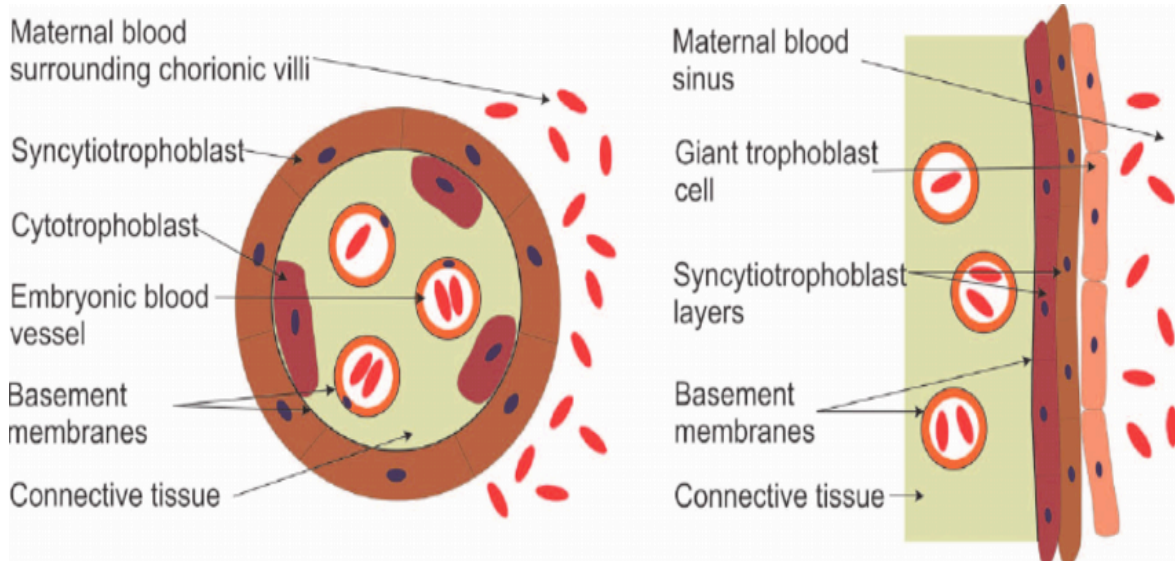


Figure 1.3 Comparative representation of human (third trimester) and rodent (GD18.5) placentas showing their differences. Left, human placenta showing a single layer (SynT) separating maternal and fetal circulations. Right, rodent placenta showing three layers (2 SynT layers and one giant trophoblast)

1.2.4 Surface Receptors in the SynT Layer and Aminoglycosides as a Targeting Moiety to SynT

The SynT layer, as explained above, determines the possibility of uptake of materials present in the maternal circulation and potentially transport to the fetal circulation. Some molecules can pass freely via simple diffusion such as gasses. Other molecules can pass via facilitated diffusion such as glucose. Several other biomolecules including amino acids can only be taken up through active transport (Jansson, 2001). Many other substances including riboflavin, folic acid, cobalt and immunoglobulin G (IgG) are taken up via receptor-mediated endocytosis. Hence, many receptors are expressed on the maternal side of the SynT layer including megalin receptors,(Akour et al., 2015a; Akour et al., 2013; Akour et al., 2015b) transferrin receptors,(Bergamaschi et al., 1990) porcine growth hormone (pGH) and human growth hormone (GH) receptors (Velegrakis et al., 2017).

Megaline receptors are also expressed on the apical surface of renal proximal tubular epithelial cells and mainly responsible for the reabsorption of proteins and vitamins (Akour et al., 2015b; Verroust et al., 2002; Verroust and Christensen, 2002) via clathrin-dependent RME.(Verroust et al., 2002; Verroust and Christensen, 2002) They are also expressed on the maternal side of the placenta and responsible for uptake of vitamins, lipids, and hormones. Megalin is thus a valuable target for ligand-modified nanocarriers to actively deliver drugs and biologics to the placenta for the treatment of diseases of the pregnancy. Such receptors have been shown to be expressed on the SynT layer of the placenta of human and mice, as well as on human choriocarcinoma (BeWo) cells, an *in vitro* placental cell model (Akour et al., 2015b; Lybbert et al., 2016; Saito et

al., 1994; Storm et al., 2016).

Recent studies have shown Megalin to be receptors for gentamicin (GM), an antimicrobial aminoglycoside (AG) that is produced naturally by bacteria, (Weinstein et al., 1963) and such megalin-based endocytic processes to follow Michaelis-Menten kinetics (Akour et al., 2015b). AGs are also known to have low protein binding (Mehrotra et al., 2004). AG may thus serve as potential targeting agents that modify the surface of drug containing nanocarriers so as to improve targeting of the maternal-fetal interface.

1.3 Nanocarriers for Placental Drug Delivery:

Various platforms can be used as nanocarriers in drug containing nanomedicines including liposomes, dendrimers, polymeric micelles, gold nanoparticles, linear polymers (synthetic or natural), protein-based carriers, viral-derived nanoparticles and many others (Mirza and Siddiqui, 2014; Moghimi et al., 2005). In this dissertation, two different nanocarrier platforms (liposomes and dendrimers) were used and therefore turn our focus on those nanocarriers, which have different strengths as they relate to drug delivery and targeting to the placenta and their translational potential.

Liposomes are the most widely used nanocarriers in drug containing nanomedicine in the clinic and under clinical trials, and thus have well known toxicity profiles, which is paramount for applications involving pregnant mothers. Biodegradable dendrimers on the other hand provide an opportunity for improved release profiles and thus PK and biodistribution of conjugated drug products, and also provide for an opportunity to deliver high payloads and tailoring of surface

properties to control their interaction with different physiological environments including the blood and the cytosol.

1.3.1 Liposomes: are spherical lipid bilayer vesicles that can be used as vehicles to carry hydrophilic and lipophilic small molecular weight drugs and biologics within their hydrophilic core or hydrophobic lipid bilayer (Bozzuto and Molinari, 2015a). The physicochemical properties of liposomes can be manipulated so as to optimize their function. Size, for instance, can vary depending on the method of preparation and can range from 20 nm to >1000 nm (Akbarzadeh et al., 2013a; Bozzuto and Molinari, 2015a; Pattni et al., 2015) Surface charge can also be modulated and is usually determined by the type lipids used (Miller et al., 1998b) The length and saturation of the lipid tails affect the transition temperature of the lipid itself leading to different release profiles and stability (Wolfram et al., 2014). Thus, the type of lipid is usually selected prudently. Many different molecules can be added to the surface of the lipids that eventually form liposomes, including masking agents such as polyethylene glycol (PEG) (decrease serum protein binding), (Papahadjopoulos et al., 1991) imaging agents such as fluorescent dyes including cyanine and FITC (Gao et al., 2018; Portnoy et al., 2011), and/or targeting moieties such as peptides, (Huang et al., 2008; Yang et al., 2014) carbohydrates (Zhang et al., 2010), antibodies (Heath et al., 1980; Heath et al., 1983) or other functional groups (Sercombe et al., 2015). Moreover, several different drugs and biologics, can be encapsulated within the liposomes including peptides, nucleic acids and small molecular weight

drugs (Tiwari et al., 2012) as schematically illustrated in **Figure 1.4** (Robson et al., 2018).

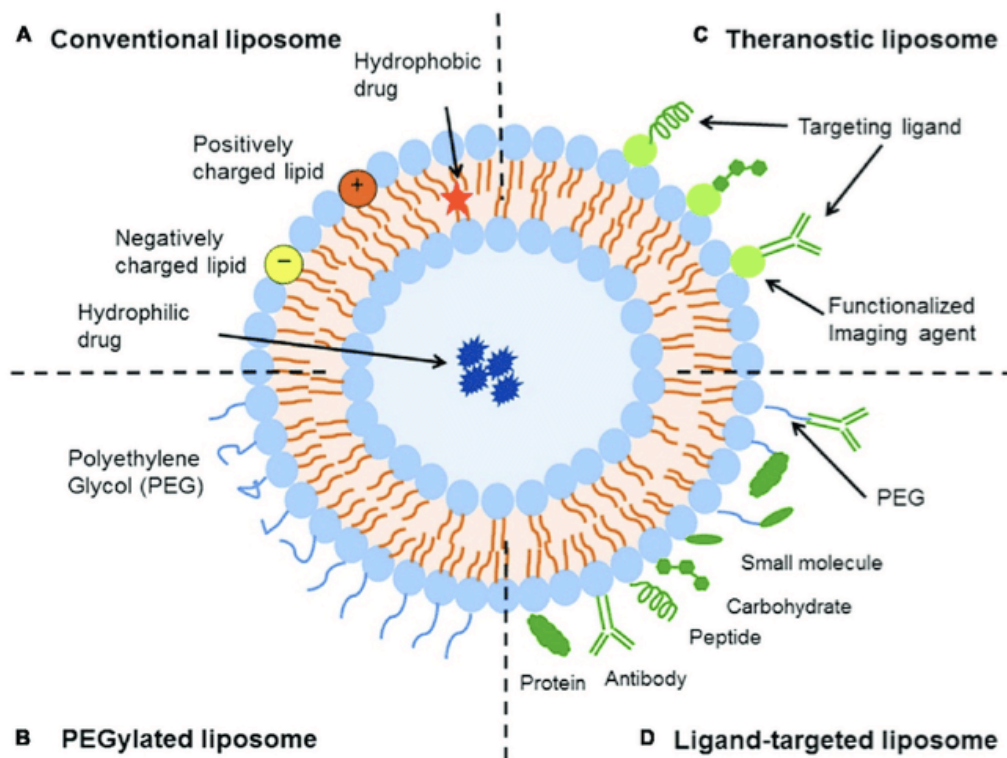


Figure 1.4 Illustration of a liposome (lipid bilayer vesicle) with versatile properties such as size, surface charge, surface modifications and capacity to carry small molecular weight hydrophilic and lipophilic drugs and biologics.

1.3.2 Dendrimer Nanocarriers (DNCs): are hyper-branched synthetic polymers made structured in a tree-like shape as illustrated in **Figure 1.5**. Each added layer of branches is considered a generation starting with the core, generation 1 (G1), G2, G3, G4 and so on. As the generation grows, so does the molecular weight and size. Because of the synthetic approach used to synthesize such systems, they are the most monodisperse polymers available in our toolbox (Biswas et al., 2012; Cheng and Xu, 2008; Nanjwade et al., 2009).

They have unique properties including small nanoscale size (a few nanometers) (Kolhe et al., 2006), high monodispersity, and a large number of functional groups that can be used to conjugate the drug payload through liable bonds, or other ligands so as to modulate their interaction with the physiological environment (Duncan and Izzo, 2005; Yellepeddi et al., 2011), as well as other probes that allow us to track such systems in vitro and in vivo (Wijagkanalan et al., 2011; Zhu et al., 2010). Dendrimers can be prepared from a large variety of chemistries including polyamidoamine (PAMAM), polypropyleneimine (PPI), poly-L-lysine (PLL), poly(glycerol-co-succinic acid), melamine, poly(glycerol), 2,2-bis(hydroxymethyl)propionic acid (Bis-MPA), poly(ethylene glycol) (PEG), and others (Kesharwani and Iyer, 2015). Biodegradable polyester dendrimers are very promising given they reduced toxicity profiles (Heyder et al., 2017; Kolhe et al., 2006; Wijagkanalan et al., 2011) as the polyester bonds that connect the branches lead to the slow disintegration of the polymer into fragments that can be easily eliminated from the physiological environment (in a predictable way)(Heyder et al., 2017) after delivery the payload to the intended tissue.

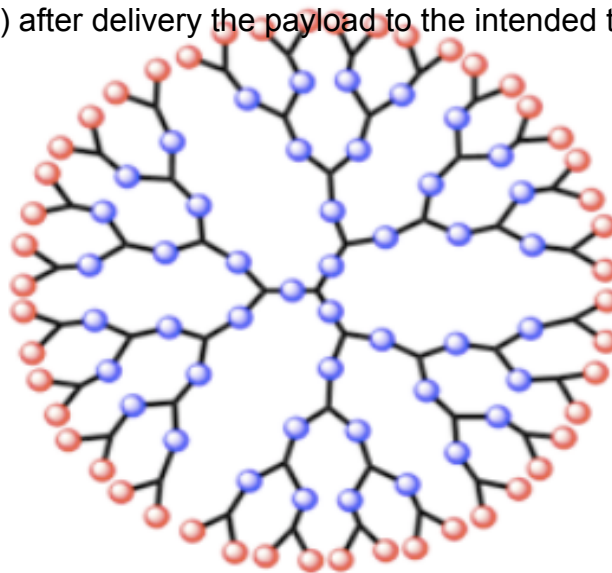


Figure 1.5. Illustration of a fourth generation (G4) dendrimer containing 48 surface groups that can be used for conjugating different molecules such as the drug cargo, targeting moieties, fluorescent molecules, and other surface groups.

1.3.3 Nanocarriers for Placental Drug Delivery (literature Review)

There have been several *in vivo* pre-clinical and *ex vivo* studies that discuss the use of nanocarriers for the placental drug delivery (Bajoria et al., 1997a; Bajoria et al., 2013; Menjoge et al., 2011; Soininen et al., 2015; Valero et al., 2018; Valero et al., 2017; Yu et al., 2017). The effect of certain physical properties of (non-targeting) liposome including size (Bajoria and Contractor, 1997), surface charge, (Bajoria et al., 2013; Miller et al., 1998a) and physical properties of the lipids (Grazia Calvagno et al., 2007) on the transport across the maternal-fetal interface has been investigated. It was observed that small (70nm) unilamellar liposomes showed enhanced uptake of a fluorescent dye in perfused human term placenta compared to larger liposomes (>300nm), as measured fluorometrically (Bajoria and Contractor, 1997). In terms of the surface charge of liposomes, it was determined that anionic liposomes have increased placental uptake of a encapsulated carboxyfluorescein *in vitro* (trophoblast cells) that was quantified fluorometrically (Bajoria et al., 1997b). Another study by the same group was done in perfused human term placenta in order to deliver thyroxine (T₄) to the fetus by encapsulating it in anionic small unilamellar liposomes where results showed enhanced delivery compared to free T₄, which was metabolized to reverse triiodothyronine (rT₃) (Bajoria et al., 1997a). This placental uptake on anionic small unilamellar liposomes were also demonstrated in *in vivo* models (Tuzel-Kox et al., 1995). On the other hand, cationic liposomes have been shown to reduce drug uptake. A study showed that encapsulating warfarin, a drug that passes the placenta freely, in cationic liposomes significantly reduced its

passage to the fetus in perfused human term placenta (Bajoria et al., 2013). Moreover, indomethacin (IND), a prostaglandin production inhibitor that reduces uterine contractions and can pass the placenta freely causing fetal toxicity, was encapsulated in cationic multilamellar liposomes in order to reduce transplacental crossing. Results showed that cationic liposomes reduced the passage to the fetus 7.6 folds compared to free IND (Refuerzo et al., 2015). All these studies demonstrate that manipulating liposomal properties can serve different purposes leading to variable end results.

Dendrimers have also been investigated for transplacental transfer abilities. One study investigated the placental uptake of PAMAM dendrimers in comparison with antipyrine, a freely diffusible molecule, and showed that the former exhibited a significantly lower transfer from maternal to the fetal side across the perfused human placenta, demonstrating the possibility of delivering drugs to the mother but not the fetus (Menjoge et al., 2011). Another group used PAMAM dendrimers to stabilize and deliver siRNA to the placenta of preeclamptic rat model in order to reduce the secretion of sFlt1, an antiangiogenic factor that is excessively secreted from the placenta, causing preeclamptic symptoms. Results showed that employing PAMAM dendrimer significantly reduced the secretion of the sFlt1 and led to improved pregnancy outcomes in the preeclamptic rats (Yu et al., 2017).

More recently, modification of nanocarriers with moieties capable of targeting the placenta has been in a timed pregnant mouse model. Liposomes encapsulated with carboxyfluorescein or insulin-like growth factor 2 were

incubated with tumor-homing peptides after liposome preparation were administered to timed-pregnant mice on GD 11.5, 13.5, 15.5, and 17.5 and compared to plain liposomes. Targeting liposomes significantly increased placental weight and improved fetal weight (King et al., 2016b); however, with studies involving nanocarriers, more specifically liposomes, it is imperative to show the release profiles of the encapsulated materials to eliminate bias that can be introduced via different release profiles between the targeting and control liposomes. Moreover, the study shows quantification only based on fluorescence localization of the carboxyfluorescein within the placental tissue. Furthermore, targeted liposomes to the uterus have been employed to reduce preterm birth in an in vivo (mouse) model of pregnancy. Indomethacin, a tocolytic agent that can reduce uterine contractions but can cross the placenta and cause fetal complications, was encapsulated in liposomes that were decorated with oxytocin receptor antagonist to reduce placental passage and target the uterus. Results showed inhibition of uterus contractility in ex vivo model and increasing drug concentration in the uterus in vivo (pregnant mice), maintaining the preterm birth rate (Refuerzo et al., 2016). Another study also designed liposomes with conjugated antibodies that bind the extracellular domain of the oxytocin and encapsulated with contraction-blocking or contraction-enhancing agents and tested them in an in vitro model as well as timed-pregnant mice. In vitro results showed the blocking and enhancing activities while in vivo results showed significant accumulation of the targeted liposomes within the uterus of the pregnant mice (Paul et al., 2017).

More recent applications of targeted nanocarriers using lipid-PLGA nanoparticles incubated with targeting peptides have also shown positive results in terms of placental targeting (Zhang et al., 2018). Such nanoparticles were modified with synthetic placental CSA-binding peptide (pICSA-BP) that can bind to chondroitin sulfate A (CSA), a sulfated polysaccharide expressed on the trophoblast layer. In vivo results show significant accumulation within the placental tissue. The study also reported that (pICSA-BP) caused dramatic placental and fetal developmental impairment. While targeted drug delivery to the placenta can be beneficial, it is essential to consider the fate of the nanocarrier and the safety of the fetus as well as the mother. This is illustrated in several other studies that use nanocarriers that can impose toxicity to the fetus as well as some maternal tissues.

1.4 Hypothesis and Objectives

We hypothesize that GM conjugation to lipid and dendrimer nanocarriers will promote their uptake in the SynT layer of in vitro and in vivo placental models. The rationale for this work is that GM is a substrate for megalin, a surface receptor in the SynT involved in clathrin-mediated processes, and thus its presence (and presentation) on the surface of the nanocarriers will lead to specific interactions with the SynT layer, and thus accumulation of the cargo encapsulated/conjugated by the nanocarriers. We propose to test our hypothesis by performing the work proposed in the following two aims:

Aim #01: Synthesize GM-modified lipid conjugates and investigate the uptake of corresponding liposomal formulations in an in vitro (BeWo polarized

monolayer) and *in vivo* (timed pregnant Balb/c) model of the SynT layer. We hypothesize that the conjugation of GM on the PEG modified lipids (instead of directly to the lipids) that will form the liposomes will be available to interact with the megalin receptors, and that an increase in the density of the targeting moiety on the liposomal surface will further promote its internalization. We further hypothesize that the presence of the low binding GM on the surface of PEGylated liposomes will lead to stable nanocarriers *in vivo*, and thus promote the targeting of the megalin receptors on the apical side of the SynT layer.

In Chapter 2, we report the details of this objective. Briefly, we report the chemical synthesis of the lipid to the targeting moiety, gentamicin. We also report the characterization using Matrix-Assisted Laser Desorption and Ionization (MALDI) and Nuclear Magnetic Resonance (^1H NMR) and the purification using extraction and dialysis. We describe the preparation and characterization of liposomes. Next is a detailed description of the *in vitro* and *in vivo* studies with explanation of the biodistribution analysis both quantitatively (tissue extract and semi-quantitatively (IVIS *in vivo* imaging system)).

Aim #02: Synthesize GM-modified PEGylated polyester dendrimers and investigate the uptake of corresponding dendrimer formulations in an *in vitro* (BeWo polarized monolayer) and *in vivo* (timed pregnant Balb/c) model of the SynT layer. For the *in vivo* study, we first investigate the pharmacokinetics (PK) of the PEGylated GM-dendrimers in order to determine the time point at which the biodistribution study is performed. Following that, the biodistribution is executed at the determined time point. Concentrations in maternal tissues

(placentas, kidneys, and liver) as well as fetuses are analyzed using both *In Vivo* Imaging System (IVIS) and tissue extract are reported.

In Chapter 3, we explain the details of this objective. Briefly, we discuss the chemical modification of the dendrimers, starting with partial conversion of the dendrimer terminal –OH groups to –NH₂, followed by the conjugation of Cyanine 5.5 (Cy5.5) and finally the conjugation of HO-PEG-OCH₃ (control) or PEG-GM (targeting modification- **in progress**). Throughout this process, purification and characterization using MALDI and ¹H NMR are reported for every step. Thereafter, we report the PK study with time points (0.25, 0.5, 1, 8, 24 and 48 h). Plasma concentration vs. time curves are plotted and evaluated for AUC, t_{1/2}, and K_{el}. Finally, biodistribution will be evaluated based on tissue extract and IVIS imaging (similar protocols to those in Chapter 2).

Different from liposomes, dendrimers have the disadvantage of not having a well-known toxicity profile in humans. However, they allow for the conjugation of the therapeutic cargo through designer bonds that allow for more detailed controlled of spatial and temporal release of the cargo and are thus also proposed here.

1.5 Relevance and Innovation

This work is innovative in several aspects. We are the first group to propose the use of AGs (in this case GM) as a targeting moiety to the placenta. In particular, this is the first time that GM- modified lipids are synthesized and the ability to target models of the placenta in vitro and in vivo demonstrated. Such novel methods of targeting the placenta for the delivery of drug and biologics are

significant as they provide for a nanotherapy platform for the potential treatment of diseases of the pregnancy.

CHAPTER 2

Megalín-targeting Liposomes for Placental Drug Delivery

Ali Alfaifi^{1,2,3}, Rodrigo S. Heyder^{2,3}, Elizabeth Bielski^{2,3,#}, Rashed Almuqbil^{2,3}, Mahendra Kavdia¹, Phillip M. Gerk² and Sandro R. P. da Rocha^{*2,3}

¹Department of Biomedical Engineering, Wayne State University, Detroit, MI

²Department of Pharmaceutics and ³Center for Pharmaceutical Engineering and Sciences – School of Pharmacy, Virginia Commonwealth University, Richmond, VA

* To whom correspondence should be addressed:

Professor and Director of Pharmaceutical Engineering - School of Pharmacy
Department of Pharmaceutics, Virginia Commonwealth University
Chemical and Life Science Engineering and Massey Cancer Center
Smith Building, 4th Floor, Room 450A
410 North 12th Street
P.O.Box 980533
Richmond, Virginia 23298-0533
Phone: (804) 828-0985 / Fax: (804) 828-8359
E-mail: srdarocha@vcu.edu

current position: ORISE Fellow at FDA in Division of Therapeutic Performance (DTP), OGD, ORS, CDER

ABSTRACT

Every year, complications during pregnancy affect more than 26 million women. Some of those diseases are associated with significant morbidity and mortality, as is the case of preeclampsia, the main cause of maternal deaths globally. The ability to improve the delivery of drugs to the placenta upon administration to the mother may offer new opportunities in the treatment of diseases of the pregnancy. The objective of this study was to develop megalin-targeting liposome nanocarriers for placental drug delivery. Megalin is a transmembrane protein involved in clathrin-mediated endocytic processes, and is expressed in the syncytiotrophoblast (SynT), an epithelial layer at maternal-fetal interface. Targeting megalin thus offers an opportunity for the liposomes to hitchhike into the SynT, thus enriching the concentration of any associated therapeutic cargo in the placental tissue. PEGylated (2 KDa) lipids were further modified with gentamicin (GM), a substrate to megalin receptors, and used to prepare placental-targeting liposomes. The rate and extent of uptake of a fluorescent probe encapsulated within the liposomes into an *in vitro* model of the SynT (polarized BeWo monolayers) was assessed by flow cytometry. Targeting liposomes containing 5 mol% GM-modified lipids enhanced the uptake of the probe by 1.5 fold compared to the non-targeting control. An increase in mol% of the modified lipid resulted in further enhancement in uptake 2 fold compared to the control. In a competition assay, inhibition of the megalin receptors resulted in a significant reduction in uptake of the fluorescence probe encapsulated in GM-modified liposomes compared to the uptake without free inhibitor ($p < 0.0001$), indicating the involvement in the receptor in the internalization of the liposomes. The ability of the targeting liposomes to enhance accumulation of a fluorescence probe

was also assessed in an *in vivo* placental model - timed-pregnant Balb/c mice at gestational day 18.5. The targeting liposomes increased the accumulation of a conjugated fluorescence probe in the placenta with a total accumulation of 2.8% of the initial dose, which corresponds to an increase of 94 fold compared to the free probe ($p < 0.0001$), and 2-4 fold compared to the non-targeting control liposomes (< 0.0001), as measured by both tissue extraction and *ex vivo* imaging. Taken together, these results demonstrate that megalin-targeted liposomes may offer an opportunity to enhance the delivery of therapeutics to the placenta for the treatment of diseases of the pregnancy.

2.1 INTRODUCTION

More than 130 million newborns are delivered every year all over the world.(Keelan et al., 2015a) Over 20% of those pregnancies experience at least one complication (Duley, 2009). Some pregnancy-related complications lead to high maternal and fetal morbidity and mortality, including cases of preeclampsia (Roberts and Gammill, 2005), intrauterine growth restriction (IUGR),(Romo et al., 2009) and bacterial (McDonagh et al., 2004) and viral(Racicot and Mor, 2017; Silasi et al., 2015) infections. Preeclampsia affects about 8% of all pregnancies and accounts for 10-15% of all maternal deaths globally(Duley, 2009). IUGR, affects approximately 7-15% of all pregnancies(Yamashita et al., 2011) and is commonly associated with premature delivery (Garite et al., 2004; Goldenberg et al., 2008). Many pregnancy-related complications originate due to a compromised placenta, which is, therefore, a valuable target for the delivery of small molecule drugs and biologics (Al-Enazy et al., 2017; Audus, 1999).

The placenta is the tissue that governs the exchange of nutrients and waste between the mother and the fetus (Griffiths and Campbell, 2014). It contains independent functional vascular units called cotyledons. The villous trees located within the cotyledons separate maternal circulation from fetal circulation. The syncytiotrophoblast (SynT) is a multinucleated epithelial layer in the villous trees that is in direct contact with the maternal blood and is covered on the apical (maternal) side with branched microvilli that maximizes the surface area for gas and nutrient/waste exchange. The maternal side of the SynT layer has been shown to express megalin receptors (Akour et al., 2015a; Akour et al., 2013), which are involved in clathrin-mediated endocytic processes (Orlando et al., 1998; Saito et al., 1994). Megalin is thus a potential target for ligand-modified drug nanocarriers for the active targeting and delivery of therapeutic molecules to the placenta.

Our team has previously shown that the uptake of gentamicin (GM) by polarized human choriocarcinoma (BeWo) cells, an *in vitro* model of the SynT (Li et al., 2013; Poulsen et al., 2009), is mediated by megalin receptors (Akour et al., 2015b). These natural aminoglycosides (Clarot et al., 2004) have low plasma protein binding affinity (Mehrotra et al., 2004) and have been extensively used in the clinic to treat infections in both the expecting mother and fetus (Dashe and Gilstrap III, 1997), and thus have known cytotoxic profiles. Such characteristics make GM stand out as candidate targeting ligands to megalin.

Liposomes have been extensively employed in the clinic as nanocarriers in drug products containing nanomedicines (Pattni et al., 2015) for the treatment

of various diseases including malaria, influenza and different types of cancers.(Bozzuto and Molinari, 2015b) Targeted delivery with liposomes can be active or passive. While passive delivery depends on the unique physiology of the targeted tissue (Šentjurc et al., 1999), active delivery involves surface modification with a ligand, which can be a small molecule or a biomacromolecule (Forssen and Willis, 1998; Tagalakis et al., 2011). Several ligands have been conjugated to liposomes for active delivery such as folic acid, transferrin and mannose.(Pattni et al., 2015) Such surface-modified liposomes have been shown to enhance tissue specificity of the nanomedicine (Derycke et al., 2004; Gabizon et al., 2004; Lee and Low, 1995; Pattni et al., 2015; Song et al., 2008; Zong et al., 2014) and consequently the therapeutic index of the encapsulated cargo.

Liposomes have also been studied pre-clinically in *in vivo* models of pregnancy to evaluate their potential for the delivery of drugs to the placenta (Bajoria et al., 1997b) and are of particular importance for diseases of the pregnancy given their known toxicity profiles (Parnham and Wetzig, 1993). Physicochemical properties of liposomes have been exploited in order to manipulate placental uptake. Small unilamellar liposomes were shown to increase placental uptake (Tuzel-Kox et al., 1995) while multilamellar liposomes decreased placental uptake (Refuerzo et al., 2015). Anionic liposomes also exhibited increased placental uptake compared to a cationic counterpart (Tuzel-Kox et al., 1995). Recently, a tumor-homing peptide was shown to accumulate in the placenta of a mouse model of pregnancy (King et al., 2016a)

Carboxyfluorescein encapsulated in PEGylated liposomes accumulated in the placenta of pregnant mice and at a higher extent (as qualitatively assessed by confocal microscopy) when the liposomes were pre-incubated with the tumor-homing peptides (King et al., 2016a).

Given the challenges and opportunities described above, the objective of this work was to develop a megalin-targeting liposome that may serve as a platform for active delivery of therapeutics to the placenta. We synthesized GM-modified lipids and prepared and characterized targeting liposomes with such lipids. We assessed their interaction with both *in vitro* and *in vivo* models of the placenta. Targeting liposomes were shown to enhance the uptake of an encapsulated fluorescence probe in polarized BeWo cells (*in vitro* model of the placenta) in a megalin dependent way. These liposomes were also seen to accumulate in the placental tissue in an *in vivo* pregnancy model (timed pregnant Balb/c mice) at significantly greater concentrations than controls.

2.2 MATERIALS AND METHODS

2.2.1 Materials. Hydrogenated Soy Phosphatidylcholine (HSPC) and N-(Carbonyl-methoxypolyethyleneglycol 2000)-1,2-distearoyl-sn-glycero-3-phosphoethanolamine, sodium salt (DSPE-PEG2K) were purchased from NOF America (White Plains, NY). 1,2-distearoyl-sn-glycero-3-phosphoethanolamine-N-[amino(polyethylene glycol)-2000] (DSPE-PEG2K-NH₂) was purchased from Laysan Bio Inc. (Arab, AL). Gentamicin (GM), cholesterol (CHOL), chloroform and ethanol were purchased from VWR Analytical. Fluorescein isothiocyanate (FITC) was purchased from Thermo Fisher Scientific. Cyanine 5.5 was

purchased from Lumiprobe (Hunt Valley, MD). Eagle's Minimum Essential Medium (EMEM) and Trypsin-EDTA (1X) were purchased from Corning. DMEM/F12 was purchased from Thermo Fisher and fetal bovine serum (FBS, USDA Origin) was purchased from Serum Source International (Charlotte, NC). Tissue culture flasks, non-essential amino acids (NEAA, 100X), Transwell inserts (polyester membrane, 0.33 cm², 1 μm pore size) were purchased from VWR International. Phosphate buffer saline (PBS, 1X, pH=7.4), Hank's Balanced Salt Solution (HBSS, 1X, pH=7.4), citrate buffer (pH=4.5) and tissue digesting buffer were prepared in our laboratories. Di-*tert*-butyl dicarbonate (BOC), (dimethylamino) pyridine, 4- [4-(dimethylamino)pyridine, 99%] (DMAP), cesium fluoride (CsF) (N,N-dimethylformamide), anhydrous, 99.8+% (DMF) and hydrogen chloride, 4M in 1,4-dioxane, 99% were purchased from Alfa Aesar. Succinic anhydride (SA), [N-Hydroxysuccinimide (NHS) and (N-(3-dimethylaminopropyl)-N'-ethylcarbodiimide hydrochloride) (EDC) were purchased from Sigma Aldrich.

2.2.2 Synthesis and Characterization of Targeting Lipids.

The synthesis of the targeting lipid DSPE-PEG2K-GM was performed by conjugating GM to the DSPE-PEG2K-NH₂ as shown in Scheme 1. First, the amine groups of GM were protected by addition of di-*tert*-butyl dicarbonate (BOC) – Scheme 1a. Briefly, GM (0.0795 mmol) and sodium carbonate (0.7726 mmol) were dissolved in DI H₂O. BOC (0.5023 mmol) was dissolved in 1 mL acetonitrile and added drop-wise and the reaction was stirred for 24 h. The reaction mixture was diluted with 10 mL DI H₂O and then extracted with ethyl

acetate (3 × 10 mL). The organic layers were combined and then dried over anhydrous sodium sulfate for 30 min. The sodium sulfate was filtered off and the organic solvent was removed by rotary evaporation and further dried under high vacuum for 6 h to obtain BOC-protected GM product (GM-BOC). The GM-BOC (0.075 mmol) was then dissolved in a 6 mL anhydrous ethyl acetate and reacted with succinic anhydride (SA, 0.15 mmol) in the presence of 4-dimethylaminopyridine (DMAP, 0.15 mmol) and cesium fluoride (CsF, 0.03 mmol) for 24 h to yield BOC-protected gentamicin terminated with a carboxyl group (-COOH), GM-BOC-SA. The reaction mixture was diluted with 5 mL ethyl acetate and purified by extraction against DI H₂O (3 × 7 mL) and dried as explained above. The product (0.037 mmol) was then dissolved in 10 mL anhydrous DMF and reacted with EDC and NHS to activate the -COOH followed by the addition of DSPE-PEG2K-NH₂ (0.026 mmol) for 24 h to form DSPE-PEG2K-GM-BOC – Scheme 1b. After the completion of the reaction, the DMF was removed by vacuum for 6 h. The deprotection of BOC from the DSPE-PEG-GM-BOC product was performed by dissolving it in 5 mL 4.0 M HCl in dioxane for 30 min followed by removal of the solvent by a flow of nitrogen to yield the gentamicin-terminated, PEGylated lipid DSPE-PEG2K-GM. Lastly, the final product was purified by dissolving DSPE-PEG2K-GM in DMSO, adding it to a dialysis tube (MWCO 1000 Da) and dialyzing against DMSO for 24 h followed by dialysis against deionized water for 24 h, with periodical exchange of the solvents. The final product was lyophilized and obtained as powder. The DSPE-PEG2K-GM was characterized by matrix-assisted laser desorption/ionization Time-of-Flight spectroscopy

(MALDI-TOF, Voyager-DE PRO, JBI SCIENTIFIC) and proton nuclear magnetic resonance spectroscopy (^1H NMR, Bruker avance iii 400 MHz).

2.2.3 *In vitro* Studies

2.2.3.1 Liposome preparation.

Liposomes were prepared following the thin-film hydration method (Akbarzadeh et al., 2013b; Laouini et al., 2012), and using sonication to produce small unilamellar liposomes (ULV). Different molar ratios of HSPC, CHOL, and DSPE-PEG2K or DSPE-PEG2K-GM were dissolved in chloroform in a round bottom flask. The mixture was then vortexed to ensure homogeneity. Chloroform was removed by rotary evaporation at 40 °C followed by high vacuum overnight to ensure the removal of the residual organic solvent. The lipid film was then hydrated with 3 mL of PBS to form liposomes. The liposome suspension was sonicated for 10 min over ice with 30% power intensity using the OmniRuptor 250 Ultrasonic Homogenizer to obtain the optimal size, followed by centrifugation at 141,000 rcf_{max} (Beckman Coulter XL-100K Optima Ultracentrifuge, SW41 Rotor) for 2 h at 4 °C to pelletize them.

2.2.3.2 FITC loading in Liposomes.

The liposome pellet was then reconstituted with 3 mL of citrate buffer (pH= 5.5) containing 0.1 mg/mL of FITC and incubated overnight at 4 °C to actively load FITC within the liposomes following a previously established method (Fritze et al., 2006). After overnight incubation, the liposomes were centrifuged again for 2 h at 4 °C. The supernatant was collected and FITC concentration was assessed, providing an indirect measure of the encapsulation efficiency (Indirect

EE). EE was also assessed directly (Direct EE) by reconstituting the liposomes in PBS, adding a fraction of that sample to ethanol (rupturing liposomes) and subsequently quantifying the amount of FITC (Ohnishi et al., 2013; Panwar et al., 2010).

$$\text{Direct EE} = \frac{|\text{Encapsulated FITC Concentration}|}{|\text{Total FITC Concentration}|}$$

$$\text{Indirect EE} = \frac{|\text{Total FITC Concentration}| - |\text{FITC Concentration in Supernatant}|}{|\text{Total FITC Concentration}|}$$

2.2.3.3 Liposome Characterization.

Three different formulations were investigated in the *in vitro* studies: GM-targeting liposomes containing HSPC:CHOL:DSPE-PEG2K-GM with molar ratios of (5.5:4:0.5) named **5PEG2K-5GM** and (5.5:3.5:1) named **10PEG2K-10GM**. The third group acting as the control lacking the GM-targeting moiety contained HSPC:CHOL:DSPE-PEG2K with molar ratio of (5.5:3.5:0.5) and was named **5PEG2K-0GM**. The hydrodynamic diameter (HD) and zeta potential (ζ), a measure of the surface charge of the liposomes, were characterized by light scattering (LS) using a Malvern Zetasizer Nano-ZS (Malvern, UK).

2.2.3.4 *In vitro* FITC Release. After determining the Direct EE, FITC release from liposomes was evaluated under sink conditions. Briefly, a 3 mL aliquot of liposomes containing encapsulated FITC was sealed in a dialysis tube with 8,000 MWCO. The tube was then dialyzed against a 40 mL PBS (10 mM, pH 7.4) at 37 °C in the dark. The FITC released from the liposomes into surrounding PBS was

analyzed by taking 0.1 mL samples from the dialysate at intervals 0, 15 min 30 min, and every hour from 1-6 h, and measuring the fluorescence of FITC (Excitation: 490 nm, Emission: 525 nm) using Microplate Reader (BioTek Instruments, Inc. Winooski, VA, USA). The samples were taken in triplicate and returned to the dialysate buffer after the measurements were completed. The amount of FITC was calculated based on an established standard curve. Release profiles were obtained from three independent liposome formulations with consistent EE.

2.2.3.5 Preparation and characterization of the *in vitro* Placental Model

2.2.3.5.1 Cell Culture.

Human Choriocarcinoma (BeWo) cells (which express megalin) were cultured with DMEM/F12 medium supplemented with 10% fetal bovine serum (FBS) and 1% penicillin–streptomycin and incubated at 37 °C with 5% CO₂. Human hepatocellular carcinoma (HepG2) cells (used as a negative control as they do not express megalin) were cultured with EMEM supplemented with 10% (FBS) and 1% penicillin–streptomycin and incubated at 37 °C with 5% CO₂.

2.2.3.5.2 BeWo Monolayer Formation and Polarization.

The polarization of the BeWo cells was assessed indirectly by measuring the transepithelial electrical resistance (TEER) as a function of time. Briefly, BeWo cells were seeded into 24-transwell plate inserts with a pore size of 1 μm at a 150,000-cells/cm² density. Medium was changed in both apical and basolateral side every other day. TEER values were then recorded everyday for 9 days post-seeding using EvomX meter (World Precision Instruments Inc) and

reported as a function of time. Background resistance was determined in blank inserts.

2.2.3.5.3 Tight Junctions in the BeWo Monolayer.

The monolayer formation and polarization of the BeWo cells was also verified using immunocytochemistry (ICC) by assessing the formation of tight junctions between the cells. BeWo cells were seeded into 24-transwell plate inserts with a pore size of 1 μm at a 150,000-cells/cm² density and allowed to grow for 6 days post-seeding. Cell monolayers were fixed on Transwell insert membranes using 4% paraformaldehyde for 20 minutes. After fixation, nonspecific binding was blocked by 2% BSA in PBS. Monolayer membrane was then incubated with primary rabbit ZO-1/TJP1 antibody (Invitrogen) for one hour at room temperature followed by one hour incubation with donkey anti-rabbit antibodies (Life Technologies). Nuclei staining was accomplished by incubation with Hoechst 33342 (Thermo fisher Scientific) for 20 minutes. Monolayers were washed 3 times for 5 minutes after each of the previous steps. Lastly, the membrane was cut, mounted on a slide and visualized using confocal laser scanning microscope (Zeiss LSM 700)

2.2.3.5.4 BeWo Monolayer Cross-Section.

Cross-sections of the cell monolayers grown on inserts were processed at the VCU Microscopy Core Facility. Briefly, BeWo cells were grown on the inserts at the same conditions as mentioned above. On the sixth day post-seeding the BeWo cell monolayer was fixed with 2.5% glutaraldehyde in 0.1 M phosphate buffer (pH 7.4) overnight. Samples were then dehydrated using a series of

ethanol concentrations followed by Toluidine Blue/Azure II/ methylene blue staining. Finally, samples were cut into 1- μm slices using an ultramicrotome and visualized using the light microscope.

2.2.3.5.5 Liposomal Targeting *in vitro*.

Internalization of FITC encapsulated in liposomes was determined by flow cytometry using Cytoflex Flow Cytometer (Beckman Coulter) following a method previously described by our laboratories.(Bielski et al., 2015; Zhong et al., 2016a) Briefly, BeWo cells were grown into confluent, polarized monolayers in a 96-transwell plate by seeding 150,000-cells/cm² and allowed to grow for 6 days as described earlier. On day 6, each well was washed twice and incubated in sterile Hank's Balanced Salt Solution HBSS buffer for 30 minutes followed by the addition of the non-targeting and targeting liposomal formulations (**5PEG2k-0GM**, **5PEG2k-5GM**, **10PEG2k-10GM**) each containing 250 ng of encapsulated FITC. At time points 0.25, 0.5, 1, 2, 3, 4, 5, 6 h, after contacting with the liposomes, the cell monolayers were washed thrice with cold sterile HBSS (1X, pH 7.4), incubated with trypsin-EDTA, and resuspended in 0.5 mL HBSS. Samples were run in the flow cytometer where the median fluorescence intensity (MFI) of FITC was recorded to analyze the rate and extent of cellular internalization of the FITC encapsulated in the liposome systems as a function of GM density and time. Similar experiments were performed in HepG2 cell monolayers, which serve as a control cell line that does not express megalin receptors. Finally, Competition studies were performed in BeWo monolayers using similar procedure as described above, and comparing FITC internalization in the presence and

absence of (2 mM) free GM, which was incubated with the cell monolayers 20 minutes prior to the liposomal treatments. The GM concentration of 2 mM was chosen based on cell viability assay – BeWo cells are 100% viable at that concentration, as shown in **Figure S2.3**.

2.2.4 *In Vivo* Experiments.

2.2.4.1 Synthesis of Cy5.5-modified PEGylated Lipids: DSPE-PEG2K-CY.

Cyanine5.5 (Cy5.5-COOH) was conjugated to DSPE-PEG2K-NH₂ for the preparation of liposomes used for the *in vivo* studies - **Scheme S1**. Briefly, the Cy5.5-COOH was activated by reacting with NHS and EDC (both 1.5 molar eq.) in dry DMSO. The activated Cy5.5 was then reacted with DSPE-PEG2K-NH₂ at 0.8 molar eq., followed by addition of the products to a dialysis tube (MWCO 1000 Da) and dialyzing against DMSO for 24 h followed by dialysis against deionized water for 24 h. The final product, DSPE-PEG2K-CY, was lyophilized and obtained as powder and characterized by (MALDI-TOF) - **Figure S2.1**.

2.2.4.2 Preparation of Targeting Liposomes for *in vivo* studies.

For the *in vivo* studies, lipid-conjugated Cy5.5 (DSPE-PEG2K-CY) was used as a tracer instead of encapsulated FITC, thus allowing us to overcome issues associated with tissue auto-fluorescence that prevents accurate biodistribution assays with FITC. The same liposomal preparation method mentioned earlier was used in this case, except for the FITC encapsulation steps. Briefly, HSPC, CHOL, DSPE-PEG2K or DSPE-PEG2K-GM and DSPE-PEG2K-CY were mixed in chloroform in the following molar ratio: 5.33:4:0.5:0.17, respectively. Chloroform was removed and the lipid film was hydrated and

sonicated. The HD and ζ of the liposomes were determined as described earlier. Non-targeting (control) **10PEG2K-0GM-CY** and targeting liposomes **10PEG2K-10GM-CY**, both with 10mol% PEGylated lipids were investigated *in vivo*.

2.2.4.3 Timed pregnancy.

All animal experiments were performed in accordance with the guidelines of the Institutional Animal Care and Use Committee at Virginia Commonwealth University (IACUC approved protocol # AD10001841). Eight-week-old female Balb/c mice (20-22 g) were housed under a 12 h light/dark cycle and allowed food and water ad libitum. After mating, female mice were inspected daily to observe the presence of a mating plug. Upon detection of the mating plug, gestational day 0.5 (GD 0.5) was assigned. Due to Balb/c strain having higher chance of false positive mating plugs, we further assessed pregnancy by tracking weights of the pregnant females, as discussed previously (Heyne et al., 2015). Biodistribution / targeting experiments were carried out at GD18.5, at which placental barrier is analogous to human third trimester placenta (Georgiades et al., 2002). Female mice were divided in 4 treatment groups as follows: Group 1: PBS; Group 2: free Cy5.5; Group 3: non-targeting liposomes (**10PEG2K-0GM-CY**); and Group 4: targeting liposomes (**10PEG2K-10GM-CY**). On GD 18.5, mice were administered the formulations retro-orbitally with 0.70 mg/Kg Cy5.5 equivalent. Four hours post treatment, mice were euthanized, followed by laparotomy; fetuses and maternal tissues (placentas and kidneys) were collected for analysis. We chose 4 h exposure time based on previous liposomal studies. (Refuerzo et al., 2015; Refuerzo et al., 2016; Tuzel-Kox et al., 1995)

2.2.4.4 Biodistribution: ex vivo imaging and tissue quantification.

The ability of the liposomes to target the placenta was indirectly assessed by measuring the concentration of Cy5.5 in tissue. *Ex vivo* Cy5.5 fluorescence intensity of each tissue was measured using IVIS Imaging. After tissue excision, they were washed in PBS (pH. 7.4) and placed in the IVIS chamber for measurement at 680/710 nm. For each mouse, the average intensity of five placentas, five fetuses, and two kidneys were assessed, and this was repeated for n=4 pregnant mice. For the tissue extraction studies, the total dose of Cy5.5 was also directly determined in relevant tissues, for a total of n = 4 pregnant mice for each group. In this case, calibration curves were constructed by spiking known amounts of Cy5.5 in placenta (3 placentas pooled together) and fetus (1 fetus), and Cy5.5 assessed per gram tissue. Similar placental pooling was done when assessing biodistribution. Each tissue (or pooled tissue) was washed in PBS (pH.7.4), placed in known volume of digesting buffer (0.5 M phosphate buffer) and mechanically broken down using tissue homogenizer to create a uniform suspension. Tissue suspension was allowed to shake/rotate for 72h at 4°C. Subsequently, each tissue homogenate was centrifuged for 10 min at 14000 g at 4°C. Supernatant was collected and fluorescence intensity was measured (excitation/emission 680/710 nm) using microplate reader (BioTek Synergy HT). Cy5.5 concentration was measured based on established calibration and expressed as % of initial dose (% ID) per gram tissue. Absolute concentrations are reported in *Supporting Information*. This procedure follows previously

established methods in our laboratories for tissue quantification of fluorescent probes (Zhong et al., 2016b).

2.2.5 Statistical Analysis.

All data are presented as mean \pm standard deviation (SD). Each measurement had a minimum of four independent repeats ($n \geq 4$) in which the mean and SD were subsequently calculated. GraphPad Prism 7 software was utilized to perform two-way analysis of variance (ANOVA) followed by Tukey's Multiple Comparison Test. Means were considered statistically significant if $p < 0.05$. P-values were categorized as * $p < 0.05$, ** $p < 0.01$, *** $p < 0.001$ and **** $p < 0.0005$.

2.3 RESULTS AND DISCUSSION

2.3.1 Ligand Design and Synthesis of the Targeting Lipid.

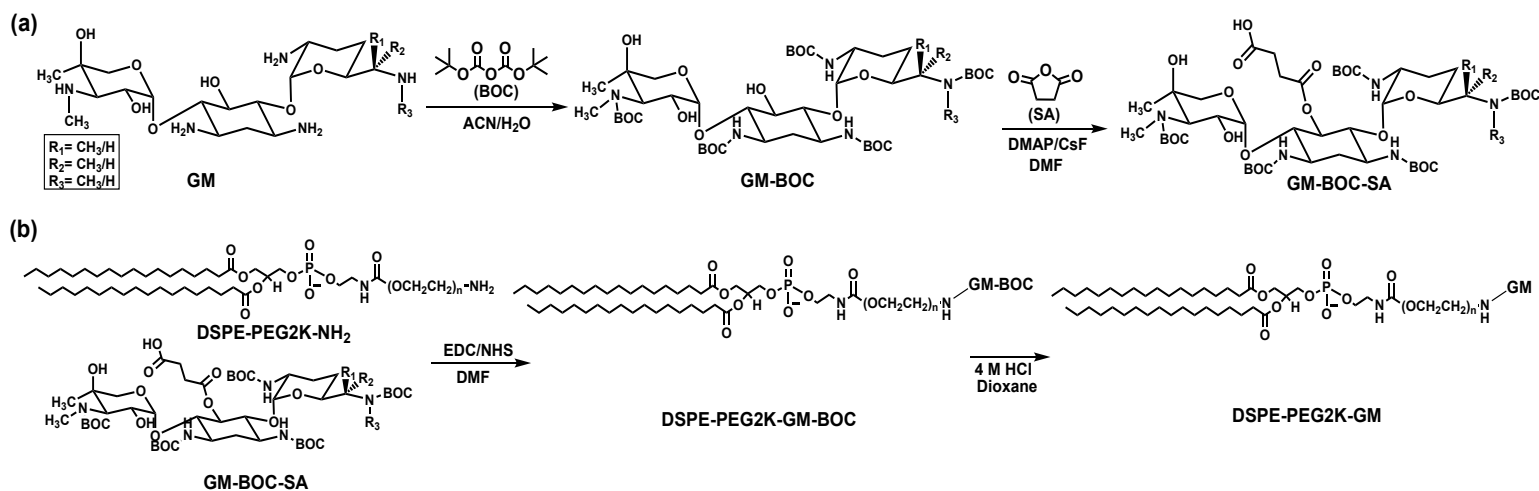
2.3.1.1 Ligand Design.

There are several reasons for selecting gentamicin (GM) as the ligand to develop placental-targeting liposomes. First, GM is a substrate of megalin, which is a surface receptor in the apical (maternal) side of the SynT layer (Akour et al., 2013). This is relevant as megalin is known to be involved in clathrin-mediated endocytosis processes in the human placenta (Orlando et al., 1998; Saito et al., 1994), and is also expressed in the *in vivo* (mouse) and *in vitro* (polarized BeWo cell monolayers) models of pregnancy used in this work (Akour et al., 2015b; Saito et al., 1994). GM also has unique physicochemical properties as a targeting agent (Oroojalian et al., 2017) as it has low plasma protein binding affinity (Nagai and Takano, 2004; Pechere and Dugal, 1979) and is expected, therefore, to

confer enhanced stability to liposomes when in systemic circulation, thus further promoting their placental targeting ability. Moreover, GM is currently used in the clinic to treat maternal and fetal infections during pregnancy (Ward and Theiler, 2008) and thus has a known toxicity profile.

2.3.1.2 Synthesis of the Targeting Lipids.

The DPSE-PEG2K-GM targeting lipids were conjugated as illustrated in Scheme 1. GM is composed of three major components known as C1, C1a and C2 (Gberindyer et al., 2017; Seidl and Nerad, 1988; Sun and Liu). These major components have slightly different molecular weights: 472, 486, 500 Da, respectively – see Scheme 1a. GM has 5 amine groups, which we believe are involved in its uptake into the SynT by megalin. Therefore, we conjugated GM to the lipid using a hydroxyl (-OH) group instead.



GM=Gentamicin
 BOC=Di-tert-butyl dicarbonate
 SA= Succinic Anhydride
 DSPE-PEG2K-NH₂= 1,2-distearoyl-sn-glycero-3-phosphoethanolamine-N-[amino(polyethylene glycol)-2000]

Scheme 2.1: Schematic of the chemical synthesis of the targeting lipid DSPE-PEG2K GM.

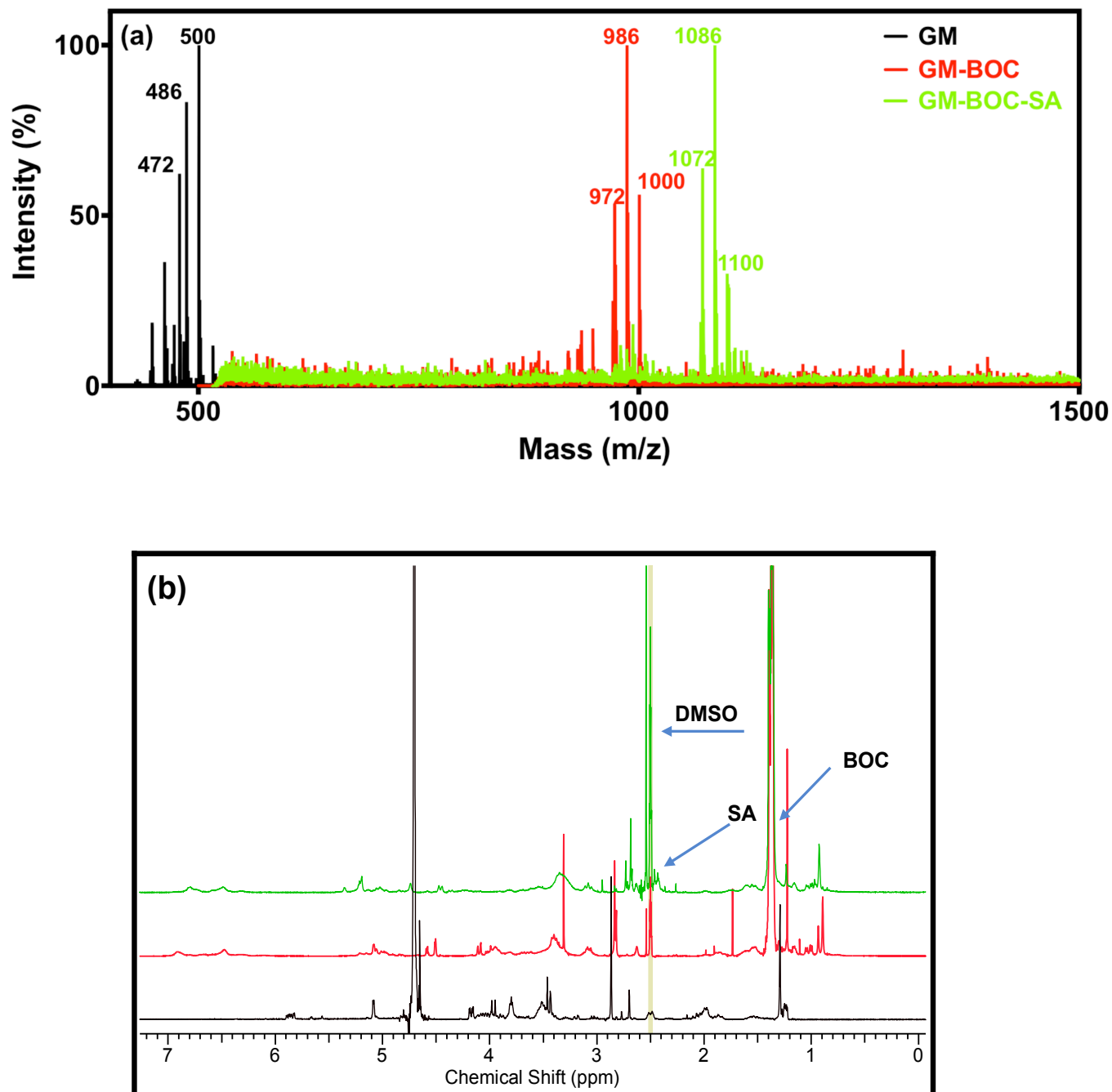


Figure 2.1 (a) MALDI-ToF spectra showing the main three peaks of gentamicin (GM, 478, 486, 500Da), BOC-protected gentamicin (GM-BOC, 972, 986, 1000Da) and the succinic anhydride (SA) modified protected gentamicin (GM-BOC-SA, 1072, 1086, 1100Da). (b) ^1H NMR spectra showing the successful modification of gentamicin (GM, black) with BOC (GM-BOC, in red) and SA (GM-BOC-SA, green).

The NH₂ groups of GM were first protected with BOC (MW: 101 Da) leading to GM-BOC products of mass corresponding to 972, 986, 1000 Da, respectively. After protection, a carboxyl functionality (-COOH) was added to GM-BOC via conjugation of succinic acid to the more reactive -OH, to form GM-BOC-SA, with expected masses of 1072, 1086, 1100 Da, respectively. MALDI-ToF spectra for the various GM conjugates are shown in **Figure 2.1a**.

These chemical modifications were followed, as well, using ¹H NMR (**Figure 2.1b**). When compared to the spectrum of the free drug, it is possible to observe the appearance of new peaks due to the chemical modifications discussed. Firstly, the introduction of BOC groups resulted in the appearance of a strong peak in the range 1.37-1.40 ppm (-CH₃). Additionally, the new peaks in the region 6.33-6.92 ppm correspond to the hydrogens present in the -NH-Boc group, confirming the protection of all amine groups. The reaction with succinic anhydride lead to new peaks in the range of 2.43-2.47 ppm (very close to the residual solvent peak), which correspond to the new -CH₂ groups conjugated to the molecule. Besides those, a broad peak is present at 12.18 ppm, corresponding to the -COOH group. GM-BOC-SA was subsequently conjugated to DSPE-PEG2K-NH₂ forming an amide bond as shown in Scheme 1b. The DSPE-PEG2K-GM-BOC (MW: ~3861 Da), was lastly deprotected (BOC groups removed), yielding the targeting lipid DSPE-PEG2K-GM, with an m/z of ca. 3500Da. MALDI-ToF spectra are shown in **Figure 2.2**.

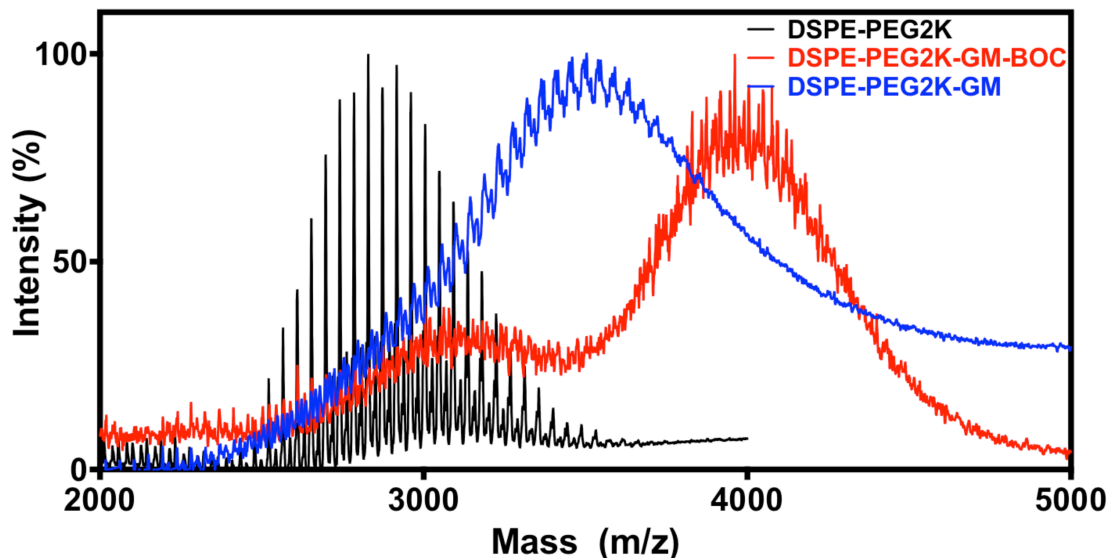


Figure 2.2 MALDI-ToF results showing DSPE-PEG2K (2792Da, black), conjugated DSPE-PEG2K to SA-modified, protected gentamicin (DSPE-PEG2K-GM-BOC, 3961Da, red) and the deprotected final product, the targeting lipid DSPE-PEG2K-GM (3500Da, blue).

2.3.2 *In vitro* studies.

2.3.2.1 FITC-loaded Liposome Preparation and Characterization.

Three different liposomes were prepared for the *in vitro* studies: PEGylated liposome with 5 mol% PEGylated lipid (i) without GM modification (without targeting ligands) (**5PEG2K-0GM**) and (ii) with targeting ligands (**5PEG2K-5GM**), and PEGylated liposome with a higher mole fraction of PEGylated lipids (10 mol%) that were modified with the targeting ligands (**5PEG2k-10GM**). The size (hydrodynamic diameter, HD in nm) and surface charge (zeta potential, ζ in mV) of the various formulations are summarized in **Table 2.1**.

Table 2.1: Hydrodynamic Diameter (HD), Zeta Potential (ζ), FITC Encapsulation Efficiency (EE) and percent release at 6h (pH 7.4) for the three different liposomal formulations used in the *in vitro* studies. SD = standard deviation, n = 4.

Liposome	HD \pm SD (nm)	ζ (mV)	EE (%)	% Release at 6h (pH 7.4)
5PEG2K-0GM	105 \pm 12	- 4.4 \pm 2.3	86.5 \pm 7.2%	28.7 \pm 1.5%
5PEG2K-5GM	112 \pm 18	- 4.3 \pm 2.5	84.4 \pm 3.3%	28.2 \pm 1.6%
10PEG2K-10GM	117 \pm 19	- 3.7 \pm 3.3	85.2 \pm 8.3%	27.0 \pm 1.6%

5PEG2K-0GM = liposomes prepared with 5mol% of DSPE-PEG2K lipid.

5PEG2K-5GM = liposomes prepared with 5mol% of DSPE-PEG2K-GM lipid.

10PEG2K-10GM = liposomes prepared with 10mol% of DSPE-PEG2K-GM lipid.

Non-targeting liposome controls **5PEG2K-0GM** showed an average HD of 105 \pm 12 nm, with the targeting liposomes **5PEG2K-5GM** and **5PEG2k-10GM** having a similar (not statistically different from the non-targeting control) HD of 112 \pm 18 and 117 \pm 19 nm, respectively. The size of liposomes is a critical attribute (Juliano and Stamp, 1975) and impacts their behavior including cellular uptake. (Bajoria and Contractor, 1997) The preparation of liposomes with similar sizes thus helps remove confounding effects that may arise due to size differences.

The zeta potential (ζ) of all liposomes is slightly negative and very close (no statistically significant difference) among the three formulations with **5PEG2k-0GM** -4.4 \pm 2.3 mV, **5PEG2K-5GM** -4.3 \pm 2.5 mV and **10PEG2K-10GM** -3.7 \pm 3.3 mV, as measured in PBS. These negative ζ happen in spite of the

presence of GM that has 5 protonatable amines each. This is important as cationic liposomes have been shown to significantly reduce placental uptake of liposomes when compared to anionic counterparts (Bajoria et al., 2013).

The encapsulation efficiency (EE %), drug loading and release profiles were also consistent among the three systems. The encapsulation of FITC was $86.5 \pm 7.2\%$, $84.4 \pm 3.3\%$ and $85.2 \pm 8.3\%$ of the starting FITC amount for **5PEG2K-0GM**, **5PEG2K-5GM** and **10PEG2K-10GM**, respectively, as summarized in **Table 2.1**. The loading efficiency of FITC was ca. 7 wt./wt.% drug-to-lipid ratio. Although it was possible to achieve higher loading efficiencies, this amount was sufficient to work with in terms of fluorometric analysis.

The release profiles are shown in **Figure 2.3** and were seen to be consistent among the different formulations throughout the first 6 hours with 28.7%, 28.2% and 27.0% being released at the end of 6h incubation at pH 7.4. The fact that the three systems follow the same release profile helps remove any confounding effect that may arise regarding rate and extent of uptake of FITC in the monolayers due to liposomal (encapsulated FITC) vs. free FITC (released FITC) in the medium as will be discussed next. Overall, the characteristics of the three systems were not impacted by the presence of GM on the liposomes, or by the different mol % of the targeting lipid containing PEG 2000Da. In fact, the small ratios of GM used to prepare the liposomes may explain the consistency in profiles for size, zeta potential, drug loading, encapsulation and release among the three formulations.

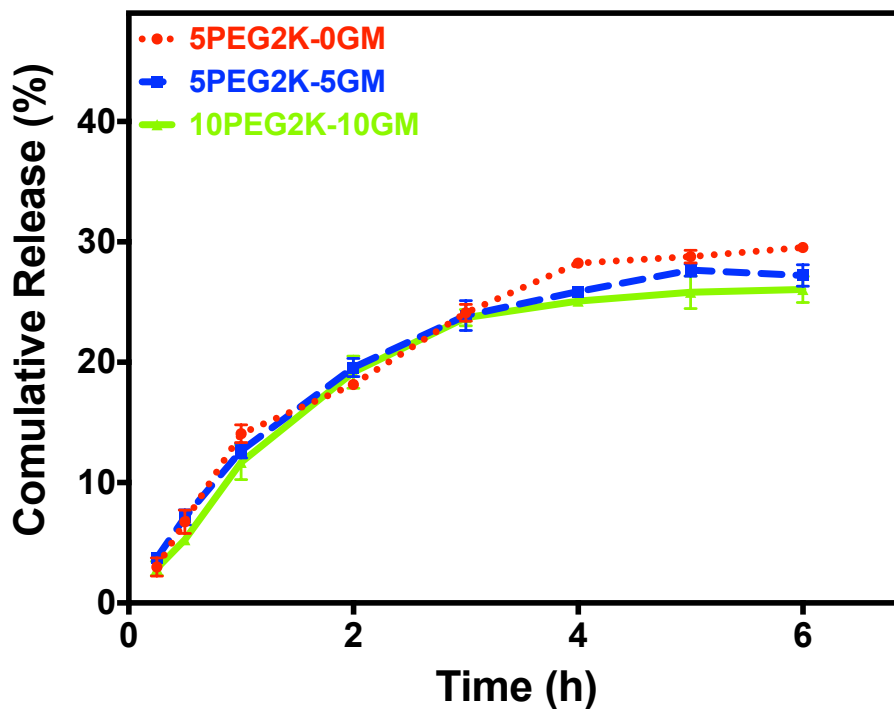


Figure 2.3 Cumulative amount of FITC released from actively-loaded, non-targeting (5PEG2K-0GM, red dotted line) and targeting (5PEG2K-5GM – blue dashed line, and 10PEG2K-10GM green line), liposomes at pH 7.4 over 6 hours - incubated at 37 °C. Data represents mean \pm SD (n = 4). 5PEG2K-0GM = liposomes with 5 mol% DSPE-PEG2K lipid; 5PEG2K-5GM = liposomes with 5 mol% DSPE-PEG2K-GM lipid; 10PEG2K-10GM = liposomes with 10 mol% DSPE-PEG2K-GM lipid

2.3.2.2 The *in vitro* Placental Model.

BeWo cells have been shown to express megalin receptors, and when polarized monolayers are formed, BeWo cells have been shown to be involved in the uptake of gentamicin in a megalin-mediated manner (Akour et al., 2015b). Establishing polarized monolayer was thus essential for this cell line in order to be used as a model for the syncytiotrophoblast (SynT) layer. TEER was recorded to assess the integrity of the monolayer. **Figure 2.4a** shows the increase in TEER values over a period of nine days post cell seeding. TEER values plateau at 40-50 $\Omega \cdot \text{cm}^2$ around days 5-6. Optimal micrographs of tin sections of

prepared system (**Figure 2.4b**) show the formation of monolayers, compared to multilayers formed on day 7 and beyond - **Figure S2.2b**. BeWo monolayer polarization was confirmed by staining of the tight junction ZO1 proteins - **Figure 2.4c**. Monolayers were initially characterized on days 5, 6, 7 and 8. Day 6 was chosen to carry out the FITC internalization studies based on the plateauing of TEER values, formation of tight junctions and the presence of a monolayer (vs. multilayer on later days).

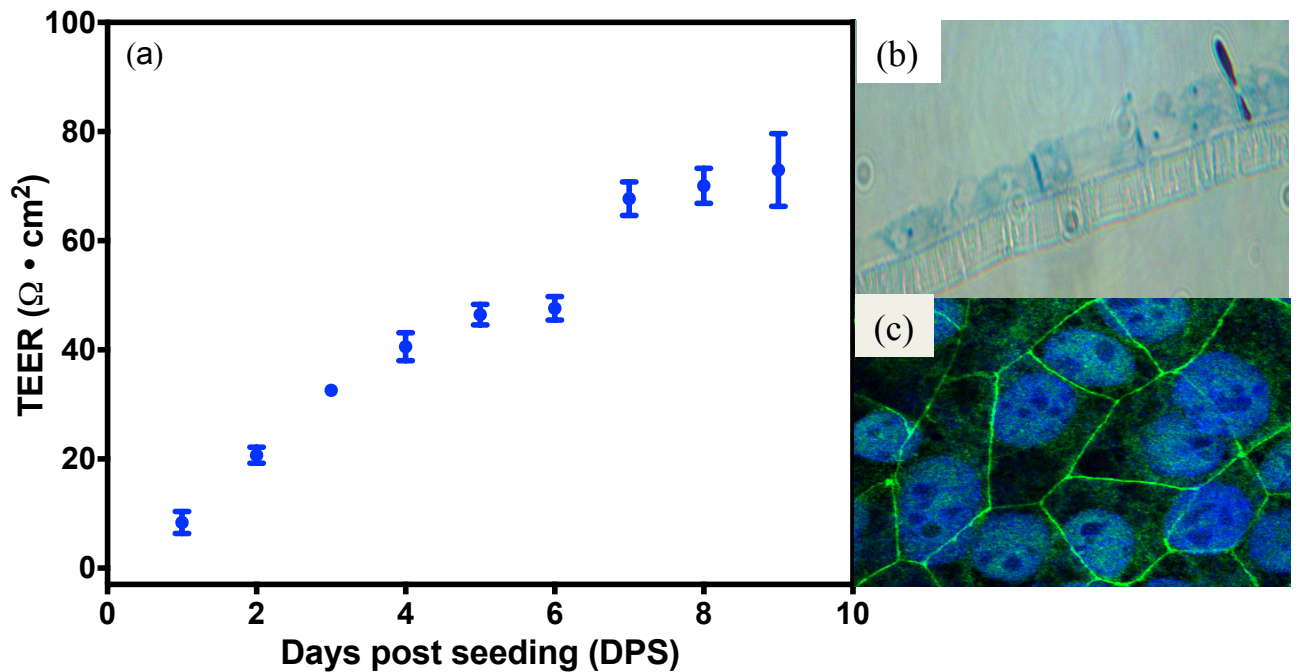


Figure 2.4: (a) Transepithelial electrical resistance (TEER) of BeWo monolayers cultured on 0.33 cm^2 Transwell® inserts as a function of time. Data represents mean \pm SD (n = 4). (b) 40X optical image showing a cross-section of the BeWo monolayer on the 6th day post seeding (DPS). (c) ZO-1 staining of a confluent BeWo monolayer obtained on the 6th DPS, indicating tight junction formation.

2.3.2.3 Targeting the *in vitro* placental model.

2.3.2.3.1 Uptake in BoWo Monolayers.

The uptake of FITC encapsulated in the different liposomal formulations by

BeWo polarized monolayers and a control monolayer (HepG2, which does not express megalin) was evaluated as a function of time using flow cytometry. Formulations containing two levels of GM at **5PEG2K-5GM** and **10PEG2K-10GM**, and the negative control (**5PEG2K-0GM**) were studied.

As shown in **Figure 2.5**, the extent and rate of internalization of liposomes were significantly enhanced upon the addition of the targeting agent - **5PEG2K-5GM** ($p < 0.0001$) and **10PEG2K-10GM** ($p < 0.0001$) at 6 h, compared to the control **5PEG2K-0GM**. During the first time point (15 min), there was no significant increase of uptake among compared to the control. At time = 0.5 h, the formulation with 10mol% targeting lipid **10PEG2K-10GM** showed a significant increase ($p = 0.0362$) compared to control; however, the uptake profile for **5PEG2K-5GM** remained not significantly different compared to control. Such uptake profile is not uncommon for the early time points as previously shown for liposomal systems with different targeting moieties (Hong et al., 2009; Zidan and Aldawsari, 2015).

After 1 h, uptake of **5PEG2K-5GM** and **10PEG2K-10GM** liposomes was significantly enhanced ($p = 0.0357$ and $p < 0.0001$ respectively) compared to the control group. At time = 2 h and longer contact times, both systems sustained significantly enhanced FITC uptake ($p < 0.0001$). Increasing the mol% of targeting lipid (compared **10PEG2K-10GM** and **5PEG2K-5GM**) also led to enhancement in FITC uptake at all times, except 0.25h.

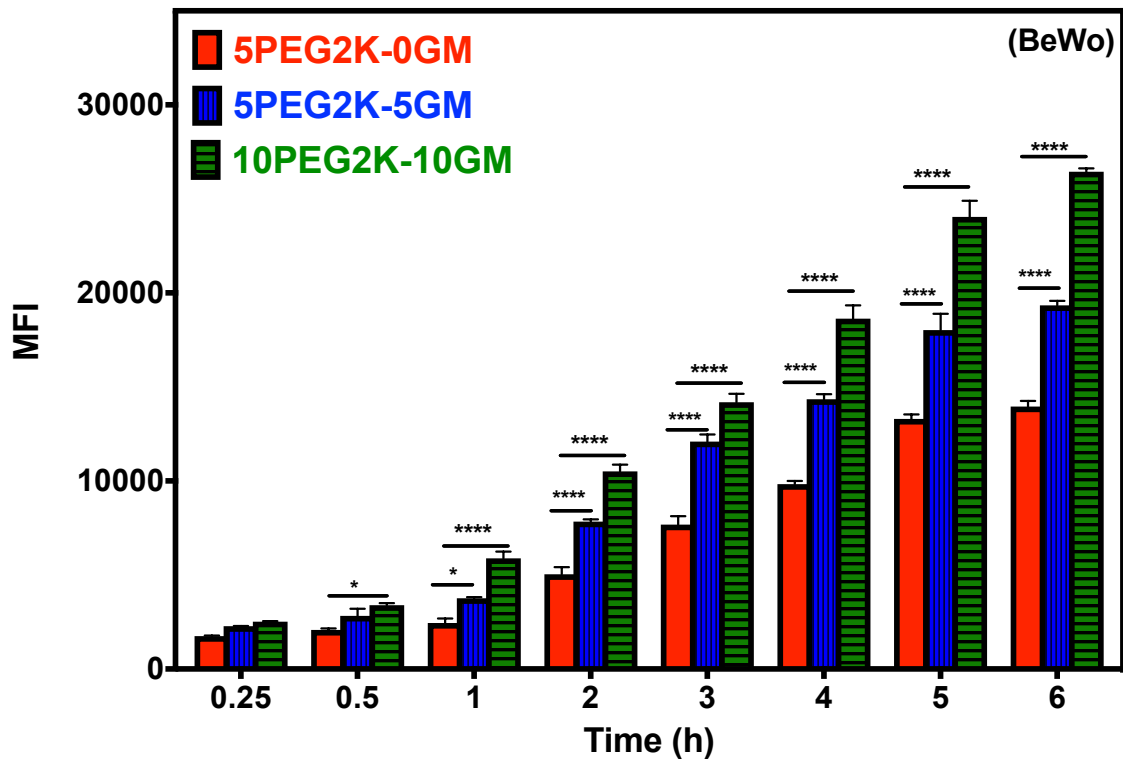


Figure 2.5: Cellular internalization of FITC on polarized BeWo cells (6th day post seeding) determined by flow cytometry, as a function of time post contacting the monolayer with FITC-encapsulated liposomes. The median fluorescence intensity (MFI) data represents mean \pm SD ($n = 4$), with at least 6,000 events (singlets). 5PEG2K-0GM = liposomes with 5 mol% DSPE-PEG2K lipid; 5PEG2K-5GM = liposomes with 5 mol% DSPE-PEG2K-GM lipid; 10PEG2K-10GM = liposomes with 10 mol% DSPE-PEG2K-GM lipid.

2.3.2.3.2 Uptake in Hepatocellular Carcinoma (HepG2) Monolayers.

Uptake of FITC encapsulated in *5PEG2k-0GM* and *5PEG2K-5GM* was also studied in hepatocellular carcinoma (HepG2) monolayers. HepG2 was used as negative control, as it does not express megalin receptors (Akour et al., 2015b). **Figure 2.6** shows the cellular uptake of FITC at 0.25, 3 and 6 h. There is no significant difference between the two systems at the three time points ($p > 0.999$, $p = 0.872$ and $p = 0.4528$ respectively). These results support the idea

that increases in uptake of FITC in BeWo cells seen for the liposomes with GM-modified lipids in **Figure 2.5** are due to specific interactions between GM and the megalin receptors, which we expect to lead to enhanced internalization of FITC via fluid phase endocytosis.

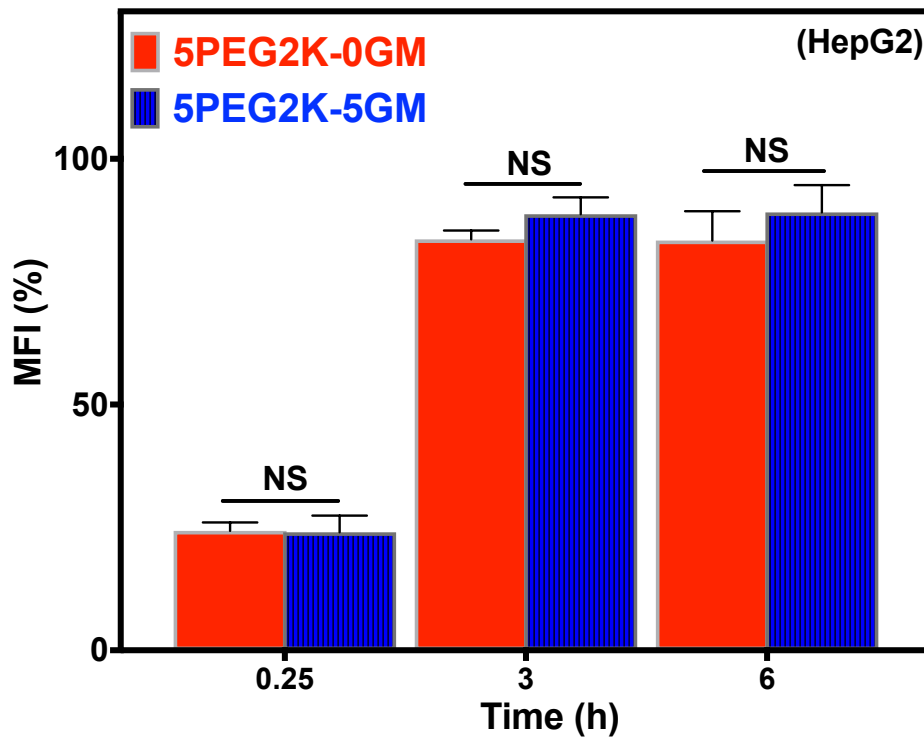


Figure 2.6: Normalized cellular Internalization of FITC on HepG2 cell monolayers determined by flow cytometry, as a function of time post contacting the monolayer with FITC-encapsulated liposomes. The median fluorescence intensity (MFI) data represents mean \pm SD ($n = 4$) with at least 6,000 events (singlets). 5PEG2K-0GM = liposomes with 5 mol% DSPE-PEG2K lipid; 5PEG2K-5GM = liposomes with 5 mol% DSPE-PEG2K-GM lipid.

Increases in FITC uptake with time for the targeting liposome systems (**Figure 2.6**) are expected even for monolayers that do not express megalin due to the fact that liposomes are known to be internalized via different endocytic mechanisms (Duzgune et al., 1999; Friend et al., 1996; Straubinger et al., 1983).

This includes those that are not receptor mediated as e.g. macropinocytosis (Swanson and King, 2018) and is also due to the internalization of free FITC that is being released from the liposomes as a function of time.

2.3.2.3.3 Competitive Inhibition of Megalin Receptors.

Competitive inhibition studies were carried out by saturating the megalin receptors with free GM before contacting the targeting and non-targeting liposome formulations with the polarized BeWo monolayers. Saturation was accomplished by adding 2 mM free GM in HBSS media 15 to the cell monolayer minutes prior to the addition of liposomal formulations. This molar concentration was selected based on the fact that BeWo cells retain 100% viability under such conditions – see Supporting Information - **Figure S2.3**. The uptake of **5PEG2K-5GM** was seen to be significantly higher than the control liposome ($p < 0.0001$) in the absence of free GM (GM -) as seen in **Figure 2.7** (as also shown in **Figure 2.5**); however, in the presence of 2 mM free GM (GM +), the uptake of **5PEG2K-5GM** was significantly reduced and seen not to be statistically different compared with non-targeting control **5PEG2k-0GM** ($p = 0.0599$).

Put together, the cellular internalization experiments described in this work support the idea that GM-modified liposomes are internalized in polarized BeWo monolayers via megalin-mediated endocytosis, and that the ability to target megalin leads to enhancement in the rate and extent of internalization of FITC, the encapsulated probe.

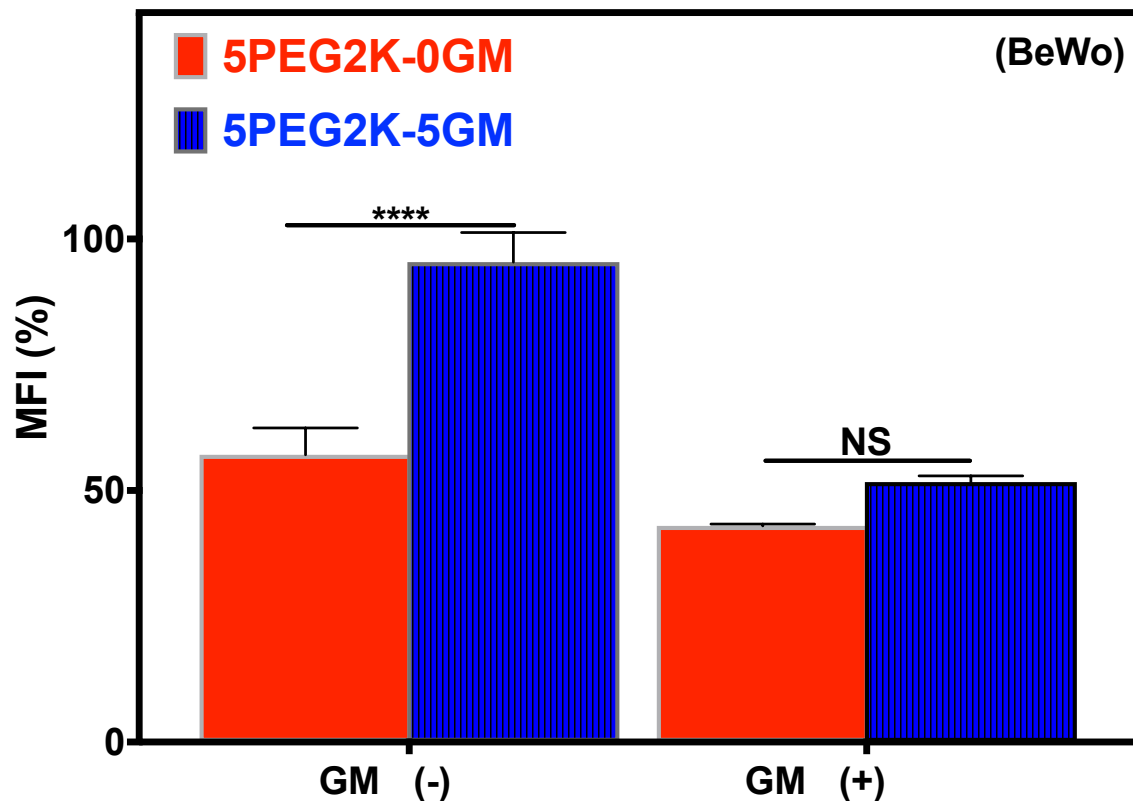


Figure 2.7 Normalized cellular Internalization of FITC on polarized BeWo cells (6th day post seeding) in the absence and presence of free gentamicin (Free GM; 2mM) determined by flow cytometry at 6 h post contacting the monolayer with FITC-encapsulated liposomes. The median fluorescence intensity (MFI) data represents mean \pm SD (n = 4) with at least 6,000 events (singlets). 5PEG2K-0GM = liposomes with 5 mol% DSPE-PEG2K lipid; 5PEG2K-5GM = liposomes with 5 mol% DSPE-PEG2K-GM lipid; 10PEG2K-10GM = liposomes with 10 mol% DSPE-PEG2K-GM lipid.

These results are of importance as they represent a novel strategy to potentially target the placenta and enhance the delivery of drugs and biologics to treat a variety of diseases of pregnancy. The liposomes with 10mol% targeting lipids (and the respective control) were thus selected to carry out the *in vivo* studies.

2.3.3 *In Vivo* Studies.

2.3.3.1 Synthesis and Characterization of Cy5.5-modified lipids (DSPE-PEG2K-CY).

Synthesis of the Cy5.5-conjugated lipid was achieved in a one-step reaction – Scheme S1. DSPE-PEG2K-NH₂ (MW ca. 2790 Da) was reacted with Cy5.5-COOH (MW 619 Da) via an amidation reaction to yield DSPE-PEG2K-CY (3400 Da), which was characterized by MALDI-ToF as shown in **Figure S2.1**.

2.3.3.2 Liposomal Formulations for *in vivo* Studies.

Liposomal formulations for *in vivo* studies were prepared with the Cy5.5 probe (DSPE-PEG2K-CY lipids) to avoid any potential sensitivity issues with FITC due to tissue background auto-fluorescence. The liposomal formulations for *in vivo* studies with the DSPE-PEG2K-CY lipid exhibited similar HD and ζ as the formulations with encapsulated FITC, as shown in Table S1, demonstrating that the presence of small amounts of the CY-lipid conjugate do not significantly impact the characteristics of the liposomes. The non-targeting liposomes (**10PEG2K-0GM-CY**) and the targeting (**10PEG2K-10GM-CY**) liposomes prepared with 1.7mol% of DSPE-PEG2K-CY and 10 mol% of PEGylated lipid (without or with GM targeting) had HDs of 103 nm and 114 nm, and ζ of -5.4 and -3.4 mV, respectively.

2.3.3.3 Targeting the *in vivo* placental model.

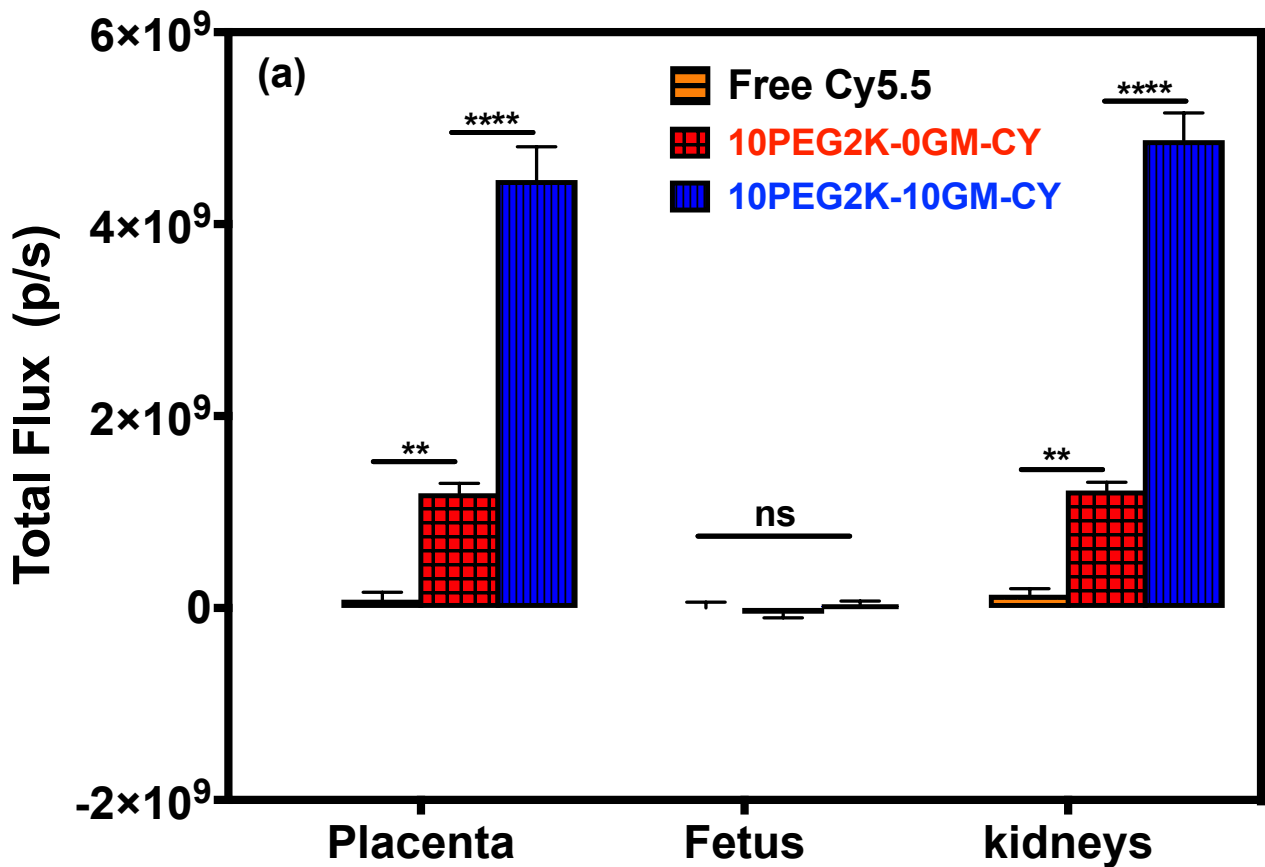
The *in vivo* biodistribution of Cy5.5 in pregnant mice was evaluated via an *in vivo* imaging system (Xenogen IVIS Spectrum), and also by tissue extraction and quantification of the fluorescence of Cy5.5. The total flux of Cy5.5 of the excised placental, fetal, and maternal kidney tissues for the treatment groups

including free Cy5.5, and the targeting and non-targeting liposomal formulations are shown in **Figure 2.8a**. Images of those tissues are shown in **Figure 2.8b**, including the PBS controls.

The results indicate that the total flux from the Cy5.5 probe in the placenta is significantly enhanced ($p=0.009$) by formulation of Cy5.5 in the PEGylated liposomes compared to free Cy5.5. It is likely that the prolonged circulation times of PEGylated liposomes (Kooijmans et al., 2016) combined with a SynT layer that has a high surface area and is highly irrigated by maternal blood (Georgiades et al., 2002) promotes the contact of the probe with the placenta when in liposome formulation, leading to its enhanced accumulation. Other studies have shown that physicochemical properties of PEGylated liposomes were manipulated to enhance delivery of placental limited-uptake drugs to the placenta (Bajoria and Contractor, 1997; Bajoria et al., 1997a; Bajoria et al., 2013; Valero et al., 2018). The presence of the targeting moiety in the **10PEG2K-10GM-CY** liposome formulations further promotes ($p<0.0001$) the accumulation of Cy5.5, leading to a 3.7 fold increase in flux in the placental tissue when compared to the non-targeting control liposomes. The results show that the presence of the targeting ligand GM not only leads to the preparation of liposomes with similar characteristics in terms of HD and ζ to the non-targeting PEGylated controls, but also seems to indicate that it does not negatively impact the *in vivo* stability of the formulation, as GM has low plasma protein binding (Pechere and Dugal, 1979).

For fetal tissues, IVIS imaging showed no significant accumulation of either free Cy5.5 ($p=0.3599$) or Cy5.5 formulated in the liposomes ($p=0.9917$ and

0.9149, for non-targeting and targeting, respectively) compared to the control fetal tissue (PBS administration) (n=6) or amongst each other. On the other hand, kidneys also show an increase in uptake of Cy5.5 formulated in liposome form compared to free Cy5.5, similar to placental tissues. Targeting further increased the uptake of Cy5.5 by 3.9 fold ($p < 0.0001$) as expected as this tissue also expressed megalin receptors.(Campeiro et al., 2019; Faber et al., 2006) Considering an average of 5 placentas, the flux ratio (all placentae to both kidneys) is ca. 2X, indicating a significantly higher placental accumulation for the targeting liposomes.



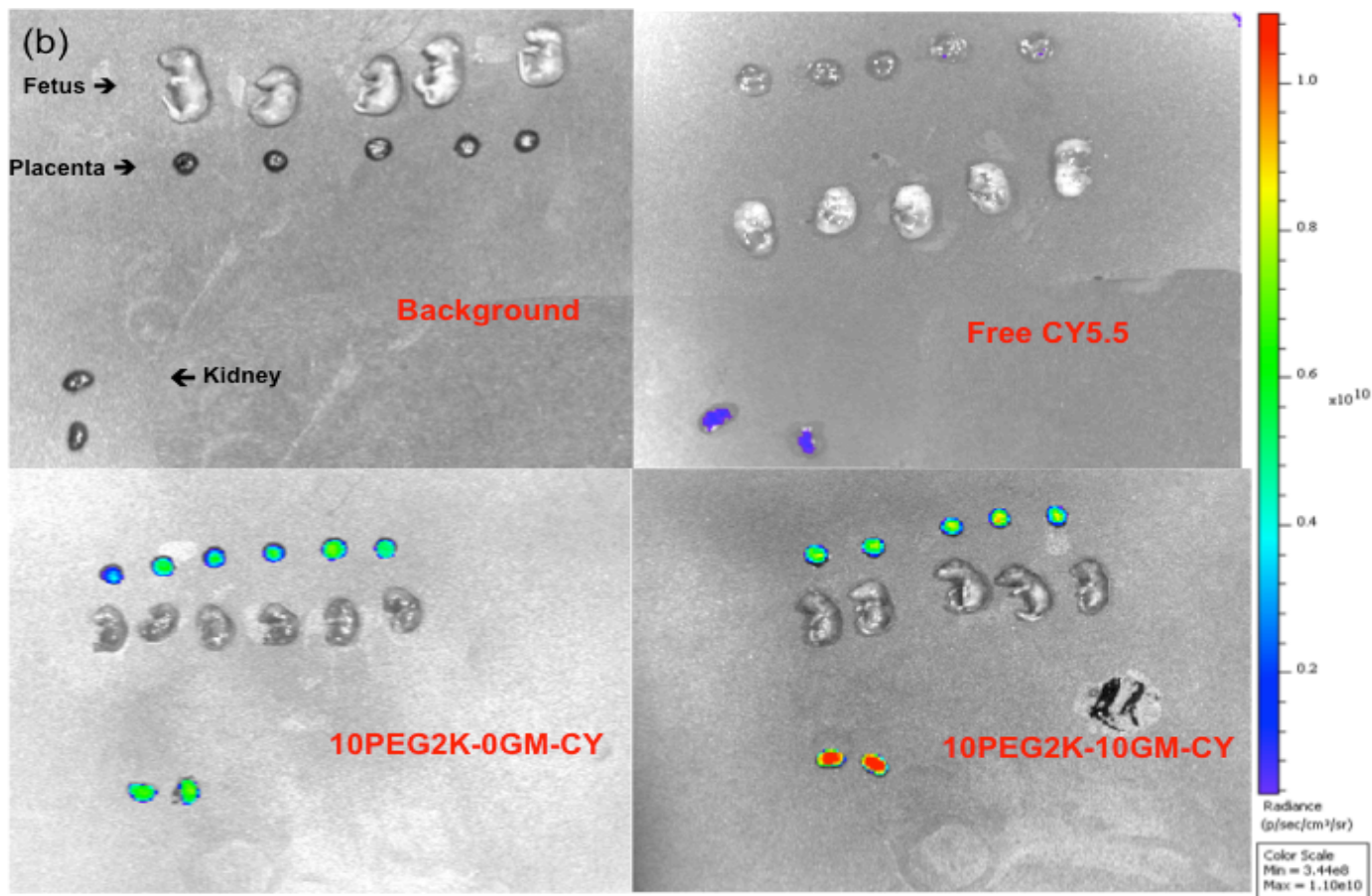


Figure 2.8: (a) Total flux of Cy5.5 for free Cy5.5, 10PEG2K-0GM-CY and 10PEG2K-10GM-CY liposomes measured ex vivo by IVIS imaging showing placentas, fetuses and kidneys 4 hr post treatment. Results shown have been subtracted from background which are fluxes of tissues exposed to PBS control only; (b) representative images of the placental and fetal tissues, as well as kidneys for the various treatment groups. 10PEG2K-0GM-CY = non-targeting liposomes with 10 mol% DSPE-PEG2K lipid and 1.7 mol % DSPE-PEG2K-CY lipid; 10PEG2K-10GM-CY = targeting liposomes with 10 mol% DSPE-PEG2K-GM lipid and 1.7 mol % DSPE-PEG2K-CY lipid.

The distribution of Cy5.5 in placental and fetal tissue was also assessed by tissue extraction (n=4). **Figure 2.9** shows the fluorometric analysis based on an established calibration curve, with the inset indicating the % accumulation in the placenta relative the initial dose of 25ug of Cy5.5.

Average concentration of Cy5.5 from **10PEG2K-10GM-CY** targeting liposomal formulations was ca. 88 fold greater than free Cy5.5. Mirroring the IVIS results, the targeting liposomes led to ca. 2 fold increase the accumulation of Cy5.5 compared to the non-targeting **10PEG2K-0GM-CY** liposomal formulation, with the following accumulated amounts in the placenta: **10PEG2K-10GM-CY**: 1405 ± 10 ng/g (2.81% total dose); **10PEG2K0GM-Cy**, 685 ± 5 ng/g (1.34% total dose); free Cy5.5, 128 ± 3 ng/g (0.03% total dose); $p < 0.0001$).

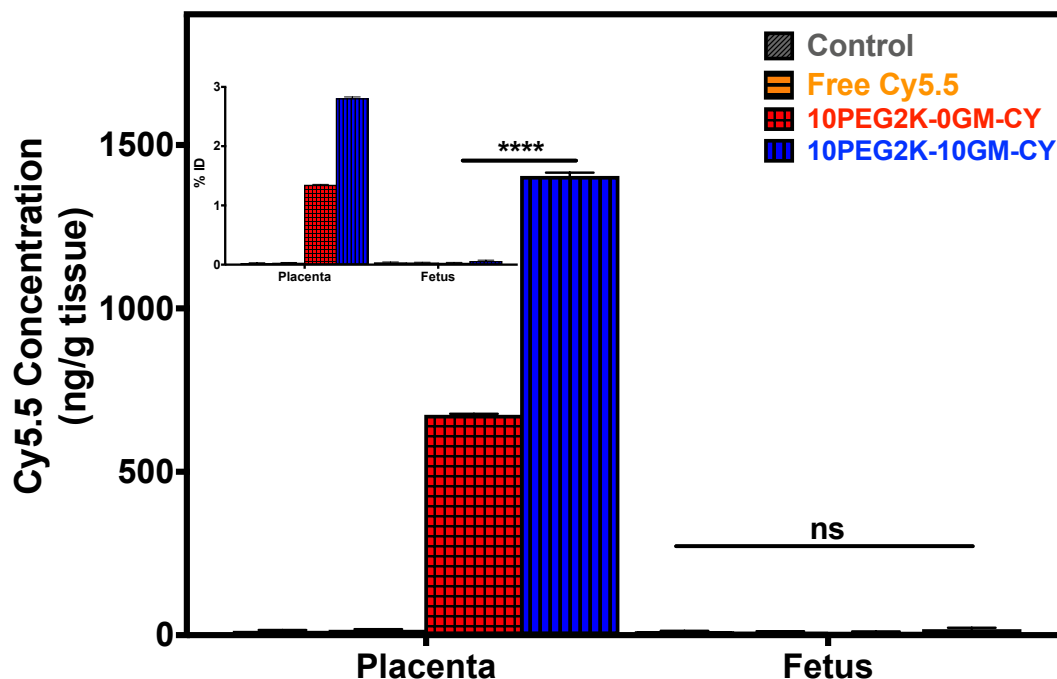


Figure 2.9: (a) Quantitative analysis (ng/g tissue) of Cy5.5 for control (no exposure to Cy5.5), free Cy5.5, 10PEG2K-0GM-Cy and 10PEG2K-10GM-Cy liposomes measured from homogenized tissues 4 hr post treatment; (b) same results plotted as % initial dose (%ID) – total of 25ug in tissue. Cy5.5 assessed fluorometrically by microplate reader and concentrations obtained based on established calibration curves on spiked tissues. 10PEG2K-10GM-CY = targeting liposomes with 10 mol% DSPE-PEG2K-GM lipid and 1.7 mol % DSPE-PEG2K-CY lipid.

Fetal analysis shows no significant accumulation of Cy5.5 (no statistical difference from PBS control) for any of the treatments groups (**10PEG2K-10GM-CY**, 14 ng/g; **10PEG2K-0GM-CY** 17 ng/g; free Cy5.5, 25 ng/g). While the current placental-targeting liposomal formulations do not show significant increases in the fetus in mice, it is important to reemphasize the anatomical differences between placenta of humans and rodents. Having three layers (two SynT layers and a third trophoblast layer)(Georgiades et al., 2002) at GD18.5, as opposed to one SynT layer in human third trimester placenta (Georgiades et al., 2002), mice placenta may represent a stricter barrier than that of humans, thus showing less transplacental transport of certain compounds (Kulvietis et al., 2011).

2.4 CONCLUSION

In this study we synthesized gentamicin (GM)-modified PEGylated lipids and demonstrated that the corresponding liposomal formulations prepared with these lipids promote the uptake of associated fluorescent probes in both *in vitro* (polarized BeWo monolayers) and *in vivo* (timed pregnant mice) placental models. GM is a substrate of megalin (Akour et al., 2013), a transmembrane protein in the apical side of the syncytiotrophoblast (SynT) layer of the maternal-fetal interface (human and murine placentae and BeWo cells), and the nanocarriers prepared here were designed to hitchhike those clathrin-mediated processes that megalin is involved in. Targeting liposomes promoted the uptake of the associated fluorescent probe in polarized BeWo monolayers to a significantly greater extent than the non-targeting PEGylated analogs, and the extent of uptake increased as the density of targeting lipids in the liposomes

increased. We also observed that competition for megalin receptors resulted in a decrease in uptake of the associated probe in targeting liposomes to the same level of non-targeting liposomes, further supporting the role of megalin endocytic processes in the uptake. In *in vivo* biodistribution experiments (IVIS and direct quantification by tissue extraction), formulation of the probe as conjugate to lipids resulted in significant enhancement in uptake in the placental tissue compared to the free probe. This is likely due to improved circulation of the conjugated probe, while no measureable amounts of the probe were found to transport into the fetal tissue. Addition of targeting lipids to the liposomal formulation further enhanced the uptake of the conjugated probe, leading to 2-4 fold higher uptake in the placenta compared to the non-targeting liposomes, while the probe is still not seen into fetal tissue. The proposed GM-targeting liposomal nanoformulations may serve as a platform for the delivery of small molecule therapeutics and biomacromolecules to support the treatment of diseases of pregnancy.

2.5 ACKNOWLEDGMENTS

SdR acknowledges partial financial support from the Center for Pharmaceutical Engineering and Sciences – School of Pharmacy, Virginia Commonwealth University (VCU), and VCU Presidential Research Quest Fund; RB acknowledges financial support from the School of Pharmacy at VCU for an undergraduate summer research experience in SdR's laboratories. AA acknowledges the Saudi Arabia Ministry of Education for the award of a full scholarship for the PhD degree. "Services and products in support of the research project were generated by the VCU Massey Cancer Center Microscopy

and Cancer Mouse Models Core Laboratory Shared Resources, supported, in part, with funding from NIH-NCI Cancer Center Support Grant P30 CA016059."

CHAPTER 3

Polyester Dendrimer for Placental Drug Delivery in Mice

Ali Alfaifi^{1,2,3}, Rodrigo S Heyder^{2,3}, Younan Ma^{2,3}, Joshua Zhang^{2,3}, Mahendra Kavdia¹, Phillip M. Gerk², Sandro da Rocha^{*2,3}

¹Department of Biomedical Engineering, Wayne State University, Detroit, MI, USA

²Department of Pharmaceutics and ³Center for Pharmaceutical Engineering and Sciences – School of Pharmacy, Virginia Commonwealth University, Richmond, VA

* To whom correspondence should be addressed.

Department of Pharmaceutics, School of Pharmacy &
Department of Chemical and Life Science Engineering, School of Engineering
Virginia Commonwealth University
Smith Building, 4th Floor, Room 450A
410 North 12th Street
P.O.Box 980533
Richmond, Virginia 23298-0533
Phone: (804) 828-0985 / Fax: (804) 828-8359
E-mail: srdarocha@vcu.edu

3.1 INTRODUCTION

There have been significant recent advances in the use of drug containing nanomedicines (Kesharwani and Iyer, 2015). There are several advantages in using nanotechnology for drug delivery including the ability to control the pharmacokinetics and biodistribution of the therapeutic cargo (Pattni et al., 2015), reduction of side effects (Lim et al., 2012), enhancing sustained release (Natarajan et al., 2014), and providing new strategies for the delivery of poorly soluble drugs (Gao et al., 2002). Several fields have benefited from nanomedicine such as oncology, ophthalmology, cardiology and microbiology (Doane and Burda, 2012; Shi et al., 2010). Moreover, numerous drug containing nanomedicines have been approved by the FDA, including Doxil®, a treatment of many different types of cancer. More recently, nanotechnology approaches have been proposed to tackle diseases of pregnancy (Refuerzo et al., 2016; Yu et al., 2017), which are very prominent and contribute to many maternal and fetal health problems with significant morbidity and mortality including preeclampsia (Roberts and Gammill, 2005). Some in vitro and in vivo model studies have shown promising results with regards to the delivery of therapeutics to the placenta in order to improve the health of the growing fetus (Refuerzo et al., 2016; Valero et al., 2018; Valero et al., 2017); however, there is still a long way to go in terms of developing drug containing nanomedicines for the treatment of diseases of pregnancy. There are many considerations when designing nanocarriers that can target the placenta to treat such disease including the potential toxicity that can be imposed to the mother or the fetus. Thus, it is

essential to consider the fate of such nanocarriers and whether there is a collateral damage associated with their use. In this chapter we discuss the potential of polyester dendrimers as a platform for the delivery of therapeutics to the placenta. While our end objective is to develop gentamicin (GM)-modified dendrimers for targeting megalin in the SynT, as we did for liposomes, here we report initial studies of PEGylated polyester dendrimers (their chemistry and characterization) and the design and initial steps in the preparation of GM-targeting dendrimers. We discuss PK results in non-pregnant animals to make preliminary determination of optimum times in which to study the biodistribution in the placenta and fetus of such carriers, which are our future experiments. We also have planned for the future in vitro uptake studies once the targeting dendrimer has been synthesized and characterized.

3.2 MATERIALS AND METHODS

3.2.1. Materials.

Gentamicin (GM), chloroform and ethanol (EtOH) were purchased from VWR Analytical. Cyanine 5.5 (Cy5.5) was purchased from Lumiprobe (Hunt Valley, MD). Eagle's Minimum Essential Medium (EMEM) and Trypsin-EDTA (1X) were purchased from Corning. DMEM/F12 was purchased from Thermo Fisher and fetal Phosphate buffer saline (PBS, 1X, pH=7.4), Hank's Balanced Salt Solution (HBSS, 1X, pH=7.4) were prepared in our laboratories. Di-*tert*-butyl dicarbonate (BOC), 4-(Dimethylamino)pyridine (DMAP, 99%), cesium fluoride (CsF), N,N-dimethylformamide anhydrous (DMF, 99.8+%) and hydrogen chloride, 4M in 1,4-dioxane (99%) were purchased from Alfa Aesar. Succinic anhydride

(SA), *n*-hydroxysuccinimide (NHS) and *N*-(3-Dimethylaminopropyl)-*N*'-ethylcarbodiimide hydrochloride (EDC) were purchased from Sigma Aldrich. BOC-6-aminohexanoic acid was purchased from Alfa Aesar.

3.2.2. Synthesis and Characterization of Gentamicin-PEG1000Da conjugated, Cy5.5-modified, generation 4, polyester dendrimers (G4OH-PEG1K-GM).

Previously we successfully synthesized 3 systems of non-PEGylated generation 4 polyester dendrimer (G4OH) by conjugating FITC (G4OH-FITC) and GM (G4OH-GM) directly on the surface of the dendrimer. MALDI-ToF and ¹H NMR characterization is shown in **Figure S 3.1**. Due to water solubility issues and potential issues related to the proximity of the targeting agent to the dendrimer surface, in the end we decided to change the route of the synthesis by including PEG as solubility enhancer, and also as a flexible spacer to conjugate the targeting GM to the dendrimer surface. In this new approach, we first conjugated a near infrared dye Cy5.5, which is commonly used in the *in vivo* studies and avoid tissue background issues as it happens with FITC.

In this new approach we used G4OH was obtained from previous synthesis in our laboratories (Heyder et al., 2017). A fraction of terminal –OH groups of the dendrimer were first modified to –NH₂. Briefly, G4OH dendrimer was reacted with BOC-6-aminohexanoic acid in the presence of DMAP and EDC followed by deprotection in 4M HCl in dioxane to yield partially –NH₂-terminated dendrimer, where 15 groups out of 48 terminal groups were converted. The

product was reacted with Cy5.5 in the presence of NHS and EDC to yield **G4OH-NH2-Cy5.5** (Intermediate product).

G4OH-NH2-Cy5.5 and HOOC-PEG1000 were reacted via an amidation reaction to give the final non-targeting control G4OH-NH2-CY5.5-PEG (named **CY-G4OH-PEG1K**). This product was purified by dialyzing against DMSO for 24 hrs followed and against water for 8 hrs with continuous replacement of the outer medium. Final product was lyophilized and stored as powder.

For the targeting dendrimer, the intermediate product **G4OH-NH2-Cy5.5** was reacted with bifunctional HOOC-PEG1000-NH2 with its amines protected giving **Cy5.5-G4OH-NH2-PEG-NH2-BOC** followed by deprotection in 4M HCl in dioxane. **Cy5.5-G4OH-NH2-PEG-NH2** was then reacted with the previously synthesized **GM-BOC-SA**, as described in Chapter 2. The final product (work in progress) will be deprotected to give the final product, the PEGylated targeting dendrimer **CY-G4OH-PEG1K-GM**.

Characterization of each step of the synthesis was performed using MALDI-TOF and ¹H-NMR. The hydrodynamic diameter (HD in nm) and surface charge (zeta potential – ζ in mV) of the dendrimer were characterized by Light Scattering using Malvern Zetasizer Nano-ZS (Malvern, UK).

3.2.3. In Vivo Experiments.

While our final goal is to measure the biodistribution of the targeting dendrimer and the control in the placenta (and fetal tissue), among other maternal tissues, because the targeting dendrimer was not finished yet, here we report only the pharmacokinetic studies performed in non-pregnant mice. These

PK results will help us understand the best time after administration of the dendrimers at which to collect initial biodistribution results. It will also help us determine the stability of the polyester dendrimer in the in vivo model.

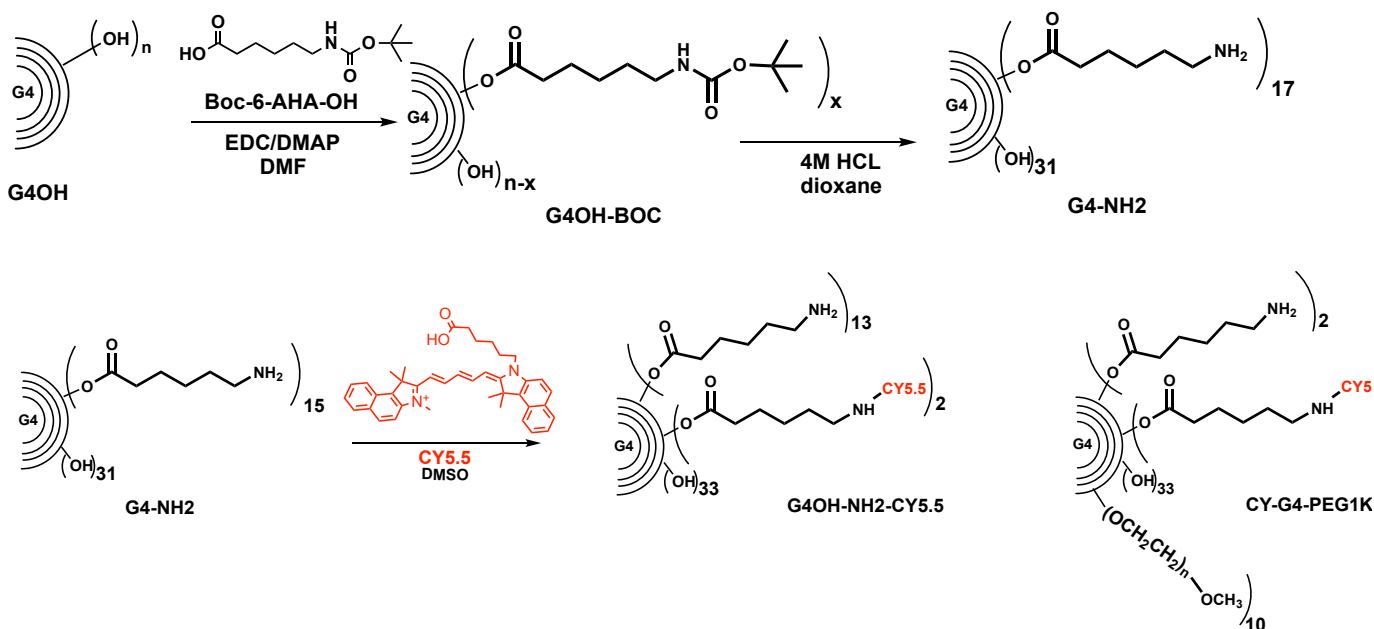
3.2.3.1 Pharmacokinetic Study in non-pregnant mice

The formulations were administered through a retro-orbital injection of 10 μg Cy5.5 eq. dose /mouse (20-22 g). Blood was collected at 0.25h, 0.5h, 1h, 8h, 24h and 48h via retro-orbital blood collection method for one time point followed by a terminal point for the following point. Blood was mixed with EDTA in ependorf tubes to prevent clotting. Blood samples were centrifuged for 15 minutes at 5000 RPM and plasma was collected. Plasma concentration of Cy5.5 was determined fluorometrically using a microplate reader (SynergyH1, Biotek), based on a pre-determined calibration curve in plasma. Plasma concentration vs. time curves were plotted and AUC, $t_{1/2}$, and K_{el} determined using GraphPad Prism 7.

3.2.4 Statistical Analysis. All data is presented as a mean \pm standard deviation. Each measurement had a minimum of three independent trials ($n \geq 3$) in which the mean and standard deviation were subsequently calculated. When necessary, GraphPad Prism 7 software was utilized to perform two-way analysis of variance (ANOVA) followed by Tukey's Multiple Comparison Test. Means were considered statistically significant if $p < 0.05$. P-values were categorized as * $p < 0.05$, ** $p < 0.01$, *** $p < 0.001$ and **** $p < 0.0005$

3.3 RESULTS AND DISCUSSION

3.3.1 Dendrimer Modification: hydroxyl terminated, generation 4, polyester dendrimers (G4OH) were synthesized in our laboratories as described earlier (Heyder et al., 2017). G4OH was modified with $-NH_2$ shown in the **Schematic 3.1**.



Scheme 3.1 Schematic overview of the partial conversion of $-OH$ to NH_2 , followed by conjugation of Cy5.5 then mPEG1K

MALDI-ToF (Voyager-DE/JBI SCIENTIFIC) and 1H -NMR results show – **Figure 3.1S and 3.2S** in Supplemental Information. Results show that 15 out of 48 terminal groups were successfully modified to $-NH_2$, as indicated by a shift in the mass of the G4OH from 5353 Da to 7412 Da (**Figure S3.2**), with each $-NH_2$ functional group representing a mass of 130 Da. 1H NMR results show that the reaction with boc-protected amino hexanoic acid, and subsequently deprotection, led to the appearance of new peaks related to the $-CH_2$ groups from the amino acid (1.31, 1.51, 1.57, 2.28, 2.74 ppm). Those peaks were used to assign the number of conjugated linkers, which is calculated as 15 (**Figure S 3.4 a, b**).

Cy5.5 (583 Da) was subsequently conjugated to the G4OH-NH₂ dendrimers via an amide bond. The successful addition of Cy5.5 was observed in the MALDI-ToF (**Figure S3.3** – Supplemental Information) through the appearance of a peak at 8698 Da. The conjugation of the dye was confirmed by ¹H NMR by the appearance of peaks in the 7.5-8.5 ppm range (related to the rings and double bonds of the structure) and the number of conjugates was determined through the integration of the peak at 6.35 ppm. This peak was selected due to the fact that it is very isolated from other peaks and no overlap was observed. The integration of it showed the conjugation of 1.8 molecules of dye per dendrimer (**Figure S3.4 c**).

Following the conjugation of Cy5.5, the product was divided to two batches for further reaction: control dendrimer (PEGylated and no GM), and targeting dendrimer (PEGylated with GM-modified PEG). For the control dendrimers, HOOC-PEG-OCH₃ (mPEG, 1160 Da) was conjugated via amidation reaction. MALDI-ToF shows an increase of the mass to 18500 indicating the addition of 8 PEG 1KDa (**Figure S3.5**). This was confirmed by ¹H NMR by the appearance of a very intense peak at 3.51 ppm, which is correspondent to the -CH₂ units of the polymeric chain. To quantify the number of polymer chains connected, we used the integration of the terminal methyl group (-CH₃) of mPEG at 3.24 ppm. It was determined that 10.2 PEG chains were conjugated per dendrimer (**Figure S3.4 d**). Additionally, in the spectrum of this final structure it is possible to observe the peaks of Cy5.5 showcasing that the dye was not affected by the reaction between dendrimer and mPEG.

For the targeting dendrimer, after HOOC-PEG-NH₂-BOC was conjugated to the dendrimer, MALDI-ToF results show a shift in peaks from 8698 to 20000 Da (**Figure S3.6**). Deprotection and conjugation of GM is in progress.

A summary of the characteristics for the various dendrimer cognates intermediates and the final targeting and control dendrimers is shown in **Table 3.1**. The characteristics include number of –NH₂ surface groups, number PEG1K and PEG1K-GM, and number of Cy5.5, as measured by MALDI-ToF (M) and ¹H-NMR (N).

Table 3.1 Molecular weight, number of Cy5.5, mPEG, and GM-PEG as shown by MALDI-ToF (M) and 1h NMR (N), the hydrodynamic diameter (HD) and surface charge (zeta potential, ζ) of the G4 polyester dendrimer conjugates.

G4OH	MW (Da)	#CY 5.5		mPEG		PEG-GM		HD (nm)	ζ (mV)
		<u>M</u>	<u>N</u>	<u>M</u>	<u>N</u>	<u>M</u>	<u>N</u>		
CY-G4OH-PEG1K	170900	2	1.8	8	10	0	0	7 ± 3	-15.4
CY-G4OH-PEG1K-GM		2	1.8	0	0	TBD		TBD	TBD

3.3.2 Pharmacokinetics (PK)

The plot of plasma concentration of Cy 5.5 as a function of time is shown in **Figure 3.1**. PK analysis for the PEGylated polyester dendrimer CY-G4OH-PEG1K shows ($t_{1/2}$) at 4.1 h, with elimination rate constant (K_e) of 0.169 h⁻¹.

Mean residence time was 4.8 h while total systemic clearance (Cl_{tot}) was 0.0059 ml/min. Area under the curve (AUC) was 17066305.04 ng/ml*min.

Based on this analysis, we will perform the biodistribution study at that time point 4 h. At this time point, we will perform our biodistribution study as 50% of the dendrimer has been distributed/eliminated. Similar studies will be performed for the targeting dendrimer. Once those experiments have been performed, we will measure biodistribution in pregnant animals.

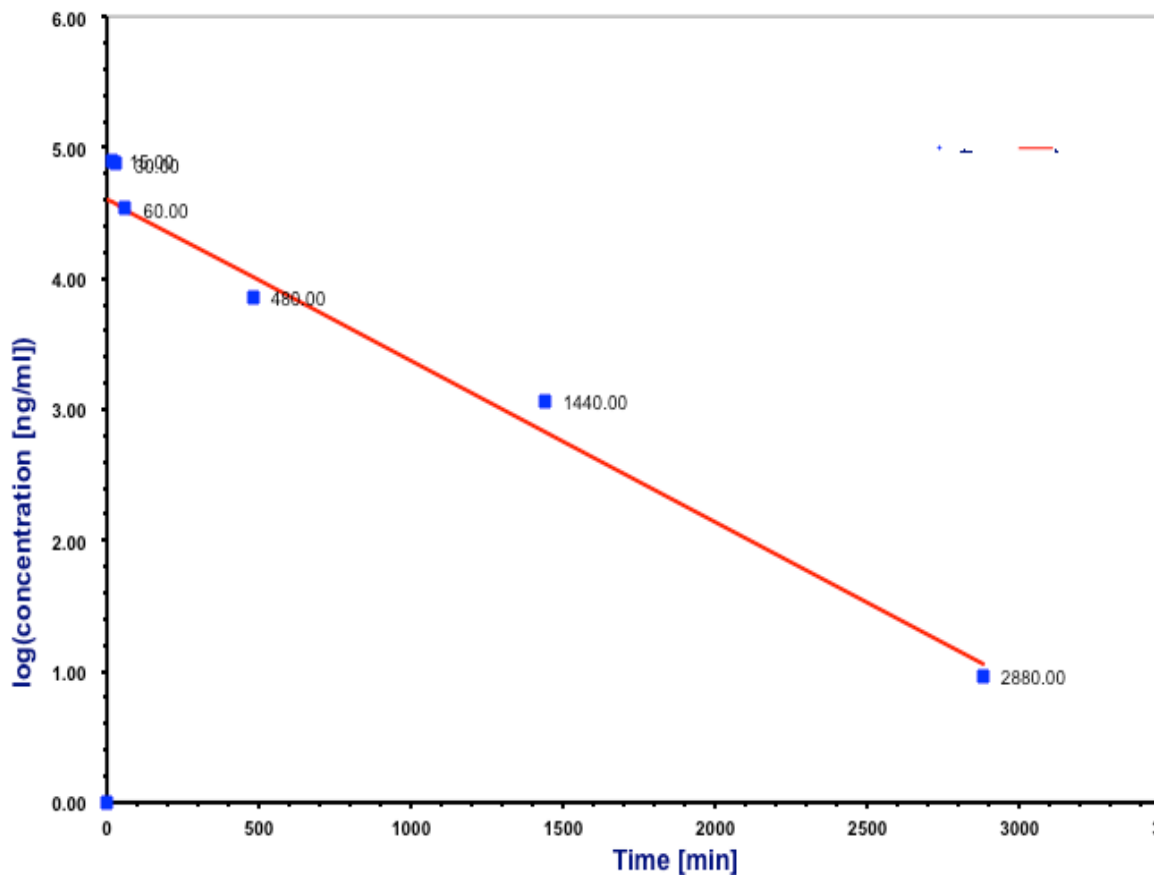


Figure 3.1 Plasma concentration (C_p) analysis as a function of time after retro-orbital administration of CY-G4OH-PEG1K. Concentrations are reported in log values (ng/ml)

3.4 CONCLUSION

Polyester dendrimers offer a great potential nanoplatform for the controlled delivery of therapeutics to the placenta. While their toxicity profile has not been studied in nearly as much detail as liposomes (at this time less translational potential), it offers an opportunity to control the release in a more predictable way, potential way to target fetal circulation and thus treat diseases of the fetus, and it is yet biodegradable and can also be excreted. In this Chapter we discuss the design, synthesis and modification of control polyester dendrimer conjugates and most of the steps towards the preparation of the targeting dendrimers. We also report some preliminary data on the pharmacokinetics of the non-targeting PEGylated polyester dendrimer. Their half-life were determined to be 4.1h, which compares with PAMAM with no PEG or low PEG density, as expected, as the density of PEG in this case is limited. These dendrimers are also almost completely eliminated after 24 hrs, which may be beneficial in terms of eliminating long-term toxicity issues.

This work is in progress and we are in the process of synthesizing the targeting dendrimer and assessing their pharmacokinetics. Subsequently, similar methods of *in vitro* uptake study and *in vivo* biodistribution will be executed based on what was reported in Chapter 2. We expect to finish these experiments shortly, as the timed pregnant mice reach the GD 18 within the coming weeks.

CHAPTER 4

CONCLUSIONS AND FUTURE WORK

Pregnancy-related complications are the major threat for the expecting mother and/or fetus because of the wide range of consequences that are associated with them. Preeclampsia, for instance, can lead to severe consequences for both the mother and fetus especially if not managed. It can lead to maternal and fetal morbidity and mortality (Jim and Karumanchi, 2017; Roberts and Gammill, 2005). IUGR is also another common disease of pregnancy that affects the growing fetus and is associated with preterm birth, which is also a major problem associated with pregnancy, contributing to approximately one million deaths annually (Goldenberg et al., 2008; Simmons et al., 2010). Unfortunately, there are no prescribed treatments to any of such complications; however, in some cases, a few medications are given to control the symptoms associated with those diseases. For example while preeclampsia does not have a treatment (besides delivering the baby), the high blood pressure associated with it is controlled by hypertension medications. Preterm birth may also be controlled using agents that can stop the uterine muscle contractions leading to delayed labor; however, preventing premature birth by simply stopping the uterine muscle contractions may not necessarily provide neonatal positive outcomes. Therefore, serious efforts with regards to developing treatments in obstetrics and gynecology are needed. Along with that, the development of formulations that can safely and efficaciously deliver the cargo is

critical so that the health of the mother and fetus is minimally affected by the treatment (Keelan et al., 2015b).

Our efforts to establish a nanoplatform that can be utilized to deliver therapeutic molecules in a targeted manner to the placenta, which is a major organ whose dysfunctions lead to many of the mentioned complications, are expected to support the development of such safe and effective formulations for treating diseases of the pregnancy. More specifically, we designed targeting nanocarriers that can bind megalin receptors expressed on the maternal side of the placental-fetal interface, the SynT later. We explored our strategies using existing well-established in vitro and in vivo models where megalin is also expressed.

In this work, we established a 2D in vitro placental model consisting of polarized monolayers of BeWo cells by culturing them and allowing them to grow as a function of time to confluent monolayers that form tight junctions. Because the SynT layer expresses certain receptors on the maternal side (apical side), the polarization of the BeWo monolayers was essential in order to mimic such conditions. We executed that by first seeding BeWo cells to porous membranes and culturing them for 9 days. Throughout the cell growth, we assessed the TEER values everyday. TEER values plateaued around 5-6 days, which is a surrogate for the monolayer polarization. We also confirmed the monolayer formation on day 6 by constructing cross-sections that show monolayers, and polarization by staining the tight junctions to confirm the barrier properties of the monolayers. Those results compared well / better then existing literature.

Future work regarding this model is to establish a more complex 3D model that can include more parameters and therefore be more representative of the placental barrier. The 3D model can be developed with BeWo cells on one side of the porous membrane, and fetal endothelial cells on the other side, representing maternal to fetal circulation. Moreover, a microfluidic system would enhance the flow properties on the apical side representing the maternal blood. Such model would make it more relevant not only to evaluate placental uptake of targeting nanocarriers but also transplacental crossing of agents from the maternal to the fetal circulations. It may also improve phenotype of the *in vitro* model.

On the other side, we successfully designed liposomes that can target the megalin receptors expressed on the apical side of the *in vitro* model of the SynT and enhance the uptake. DSPE-PEG-NH₂ was linked with the GM without modification of its amine groups. Using different molar ratios of this targeting lipid (5% or 10%), we were able to prepare different liposomal formulations and encapsulate FITC. We used 5% molar ratio of DSPE-PEG without the GM as a control. All the three systems showed consistency in terms of hydrodynamic size, surface charge, and encapsulation and release profiles, which were carefully assessed and were critical to the ability to measure the targeting potential of the nanocarriers. Our results showed enhanced uptake for both targeting systems compared to the control. We also concluded that higher density of DSPE-PEG-GM further enhances the uptake compared to the (5%) confirming that the uptake is megalin-mediated endocytosis. Furthermore, we tested the 5%

targeting liposomes with the non-targeting liposomes under different conditions. First, we tested the liposomal uptake in the presence and absence of 2 mM free GM as a method to saturate megalin receptors. Our results showed significant uptake reduction of the targeting liposomes in the presence of the free GM, further confirming liposomes are taken up via receptor-mediated endocytosis. Second, we tested the uptake of the same formulations on a different cell line (HepG2) that is known not to express megalin receptors. Results showed no significant difference between the two systems further confirming our hypothesis that modification nanocarriers with GM will result in enhanced uptake in megalin-expressing cells.

After concluding the positive results from the *in vitro* study, we successfully established an *in vivo* model using timed-pregnant female Balb/c mice. Liposomal formulations were altered to contain a near infrared dye. Cy5.5 was then conjugated to DSPE-PEG-NH₂ to replace FITC Encapsulation in order to establish a more robust strategy to assess the targeting / tissue biodistribution as the probe is not encapsulated but conjugated to the lipid, thus allowing us to directly assess the uptake of the nanocarrier/lipid instead of free probe that may be released in systemic circulation. We developed and implemented a new animal protocol for sourcing timed-pregnant mice. Targeting studies were performed on gestational day (GD) 18.5 as it represents the third trimester, as the placental barrier of mice and humans is functionally analogous at that time point of pregnancy (Georgiades et al., 2002). We performed biodistribution analysis at 4h post treatment based on previous studies performed with similar

PEGylated liposomes. Results showed enhanced targeting efficiency to the placental tissue for the GM liposomes compared to both the non-targeting liposomes and free drug model (Cy5.5) ($P < 0.0001$). Kidneys also showed enhanced uptake as was expected due to the presence of megalin receptors in that tissue. Finally, fetal concentration showed no significant uptake between the two liposomal systems and the free Cy5.5, which was a positive outcome as at this point we sought to avoid reaching fetal circulation. However, more studies are required to probe the kinetics of biodistribution of the nanocarriers. Also, there are different scenarios here. One may be interested in preventing the nanocarriers to reach the fetal circulation for safety reasons, but further consideration as to the potential of nanocarriers reaching the fetal circulation to treat specific fetal diseases should be considered as for example targeting neural inflammation. This work shows the capability of GM-modified nanocarriers to target megalin receptor expressing cells and deliver therapeutics to the placenta. Further investigation of the fetal and maternal concentrations of payloads (not only carrier) are needed, including small molecules and biologics to understand their true potential. Other areas to explore here including varying the PEG length, density (and targeting density), and the use of other targeting ligands that may further enhance uptake in the SynT.

In conclusion, this work has established a viable nanoplatform for the targeted delivery of therapeutics to the placenta for the treatment of placental-based pregnancy complications.

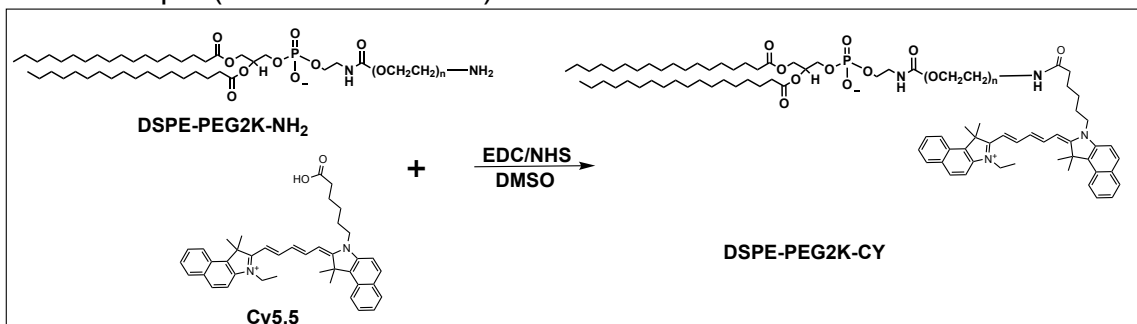
There are many other interesting future studies/ directions for this formulation. From my perspective, one of the most attractive would be encapsulating short interfering RNA (siRNA) for the treatment of preeclampsia. siRNA is unstable in blood and easily degraded, thus, its encapsulation would add several advantages including, stability, longer circulation, sustained release and targeted delivery.

Preeclampsia is a common disease of pregnancy and a leading cause of maternal deaths. In the recent years, it has been linked to an imbalance of angiogenic factors leading to less angiogenesis in the placenta and consequently preeclamptic symptoms including high blood pressure. More specifically, soluble fms-like tyrosine kinase-1 (sFlt-1 or sVEGFR-1) has been reported to be excessively expressed in placental tissue. Therefore, targeted delivery of siRNA to the placental tissue in order to knock down the expression of the corresponding genes would be a valuable direction to consider.

Extending this work to *ex vivo* studies of perfused human placenta and more relevant animal models, including non-human primates would be also helpful to test the approach in more relevant models. Some studies have used such model to assess the transplacental crossing of nanocarriers. PAMAM dendrimers, for instance showed a low rate of transfer from maternal to the fetal side across the perfused human placenta where others have used similar *ex vivo* model to show that the transplacental crossing of warfarin can be minimized when encapsulated in cationic liposomes (Bajoria et al., 2013).

Dendrimers nanocarriers (DNCs) were also used in the project in order to evaluate the GM targeting using a different platform than liposomes. We believe because of their size and stability, megalin-targeting dendrimers may be able to not only hitchhike through the megalin-mediated endocytosis, but also transport to the fetal circulation, and that would be a major breakthrough. Dendrimers are significantly smaller than liposomes and provide for the ability to carry a higher payload and implement triggered release mechanisms. While we are about to execute the experiments with the targeting dendrimers, we did not have time to report here the outcome of those experiments. We show, however, that we were able to modify polyester dendrimers with two Cy5.5 molecules. Cy5.5 is a near infrared dye that is important in tracking the distribution of the nanocarrier. We also show that the CY-Dendrimer was successfully conjugated with 10 PEG1000 molecules, and we are currently working on the conjugation of PEG with the GM targeting ligand. Here PK studies will help us decide optimum time to get the preliminary biodistribution studies. Besides that, the protocols for the in vitro and in vivo studies have already been established and we should be able to execute the studies as soon as the chemistry is done. In the mean time, we will start by measuring the biodistribution of the PEGylated dendrimers with Cy5.5. PEGylation alone is expected to improve partitioning to the placenta compared to free probe as we observed with the liposomes due to improved systemic circulation and extensive irrigation and surface area of the SynT.

APPENDIX

Scheme S2.1: Schematic of the chemical synthesis of Cy5.5-modified DSPE-2KPEG lipid (DSPE-PEG2K-CY).

Cy5.5 = Cyanine 5.5

DSPE-PEG2K-NH₂ = 1,2-distearoyl-sn-glycero-3-phosphoethanolamine-N-[amino(polyethylene glycol)-2000]

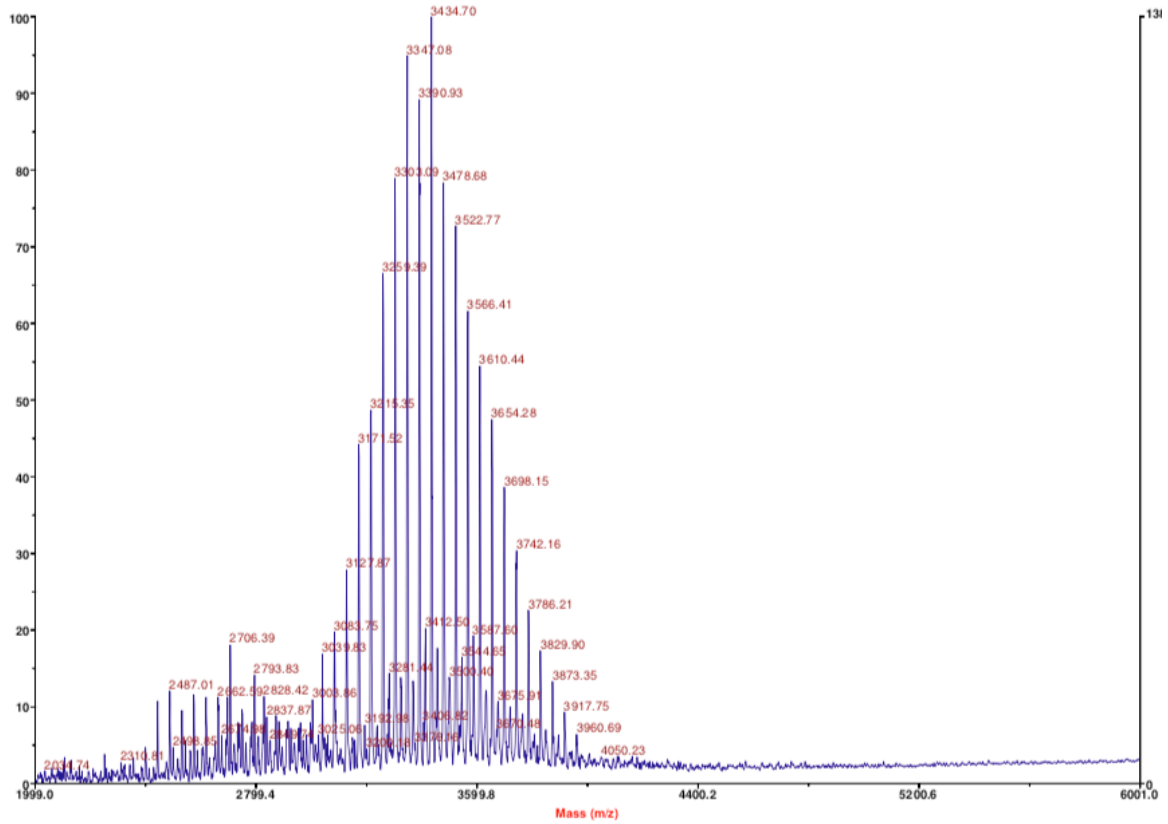


Figure S2.1: MALDI-ToF showing the peak shifts for DSPE-PEG2K-CY compared to DSPE-PEG2K (ca. 2790 Da, Figure 2). Cy5.5 with 619 Da.

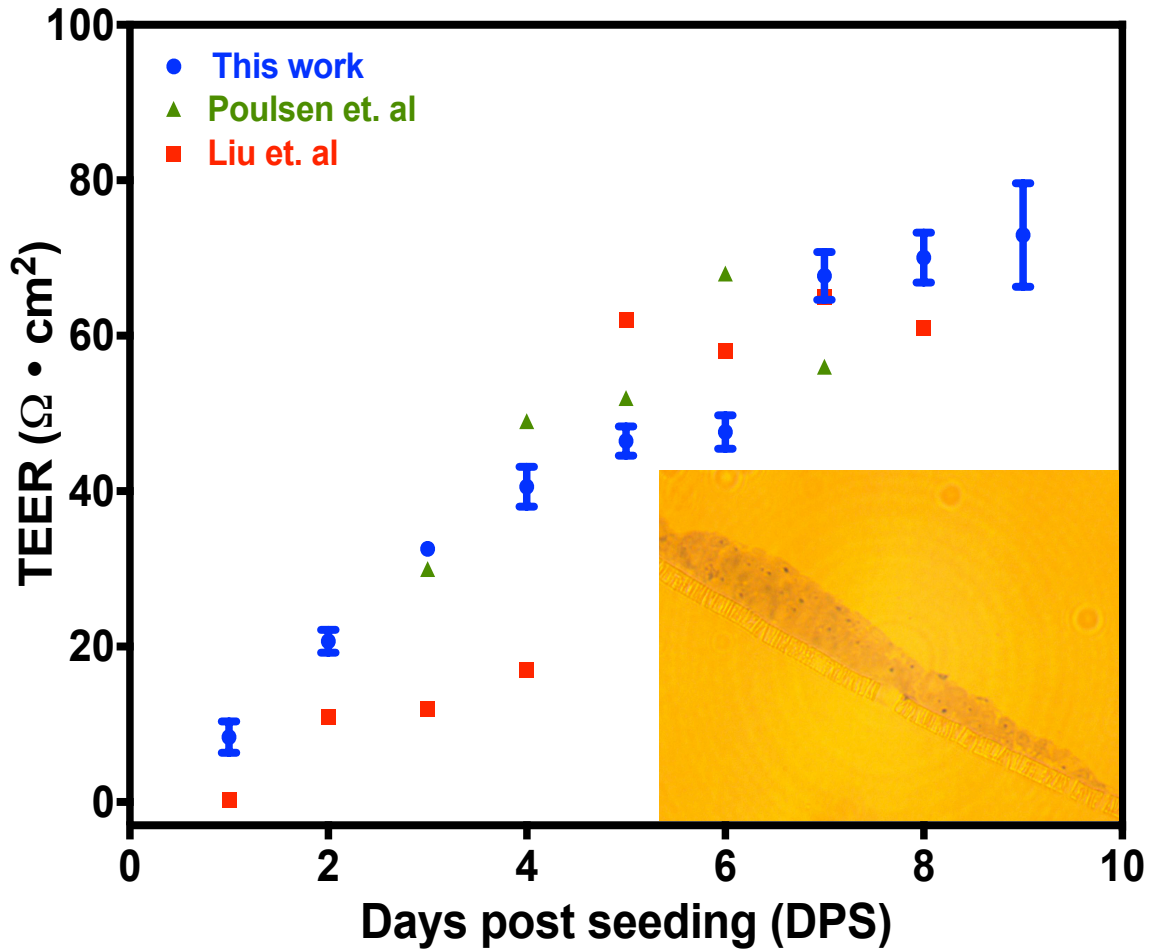


Figure S2.2. (a) Increase in transepithelial electrical resistance (TEER) of BeWo monolayers as a function of time. The figure shows the increasing TEER values of this study compared to other previously reported work (Hong et al., 2009; Poulsen et al., 2009). Note a shift in TEER at day 7. Based on cross section micrographs this corresponds to the formation of multilayers **(b)**. Our work is all at day 6 when BeWo is in monolayer form and polarized **(b)** as multilayer formation after day 6. Our work is performed when BeWo is polarized and in monolayer form – at day 6. .

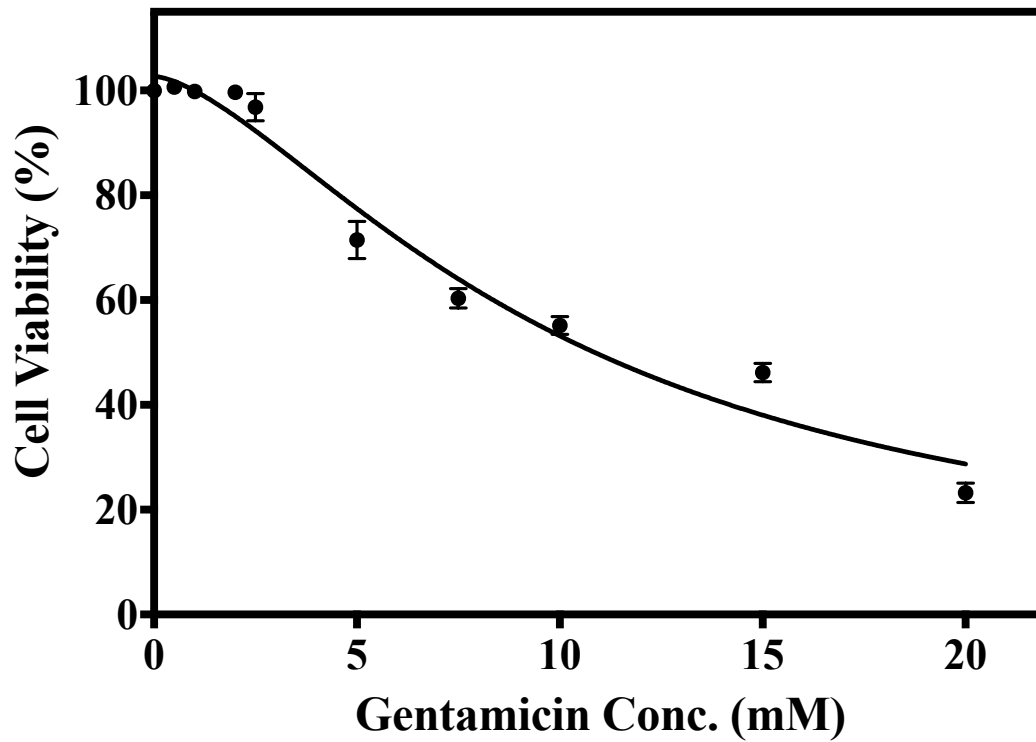
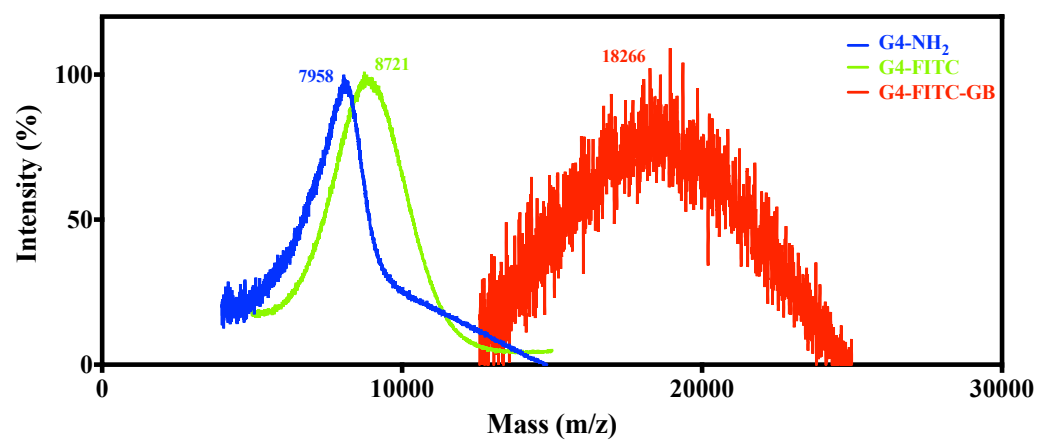


Figure S2.3. Cell Viability of BeWo Cell Monolayer after treatment with free gentamicin (n=3). IC₅₀ =10.09 mM.

Table S2.1. Hydrodynamic Diameter (HD) and Zeta Potential (ζ) of the *In Vivo* Liposomal Formulations. SD = standard deviation, n = 4.

Liposomes	HD \pm SD (nm)	ζ (mV)
10PEG2K-0GM-CY	103 \pm 3	- 5.4 \pm 2.3
10PEG2K-10GM-CY	114 \pm 4	- 3.4 \pm 1.3



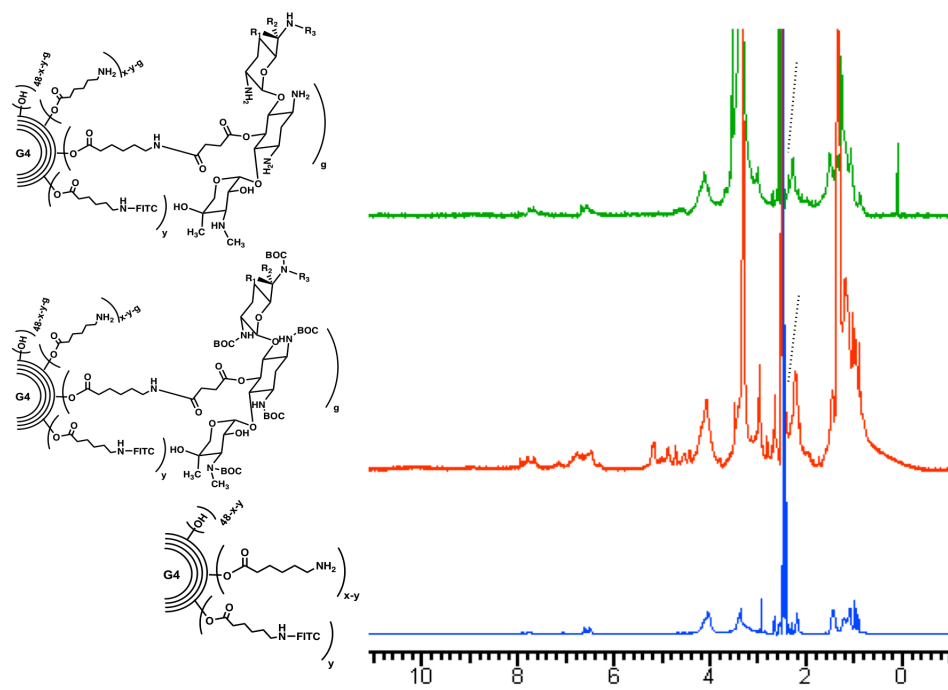


Figure S3.1 MALDI ToF and ^1H NMR showing successful modification of polyester dendrimer with FITC and GM.

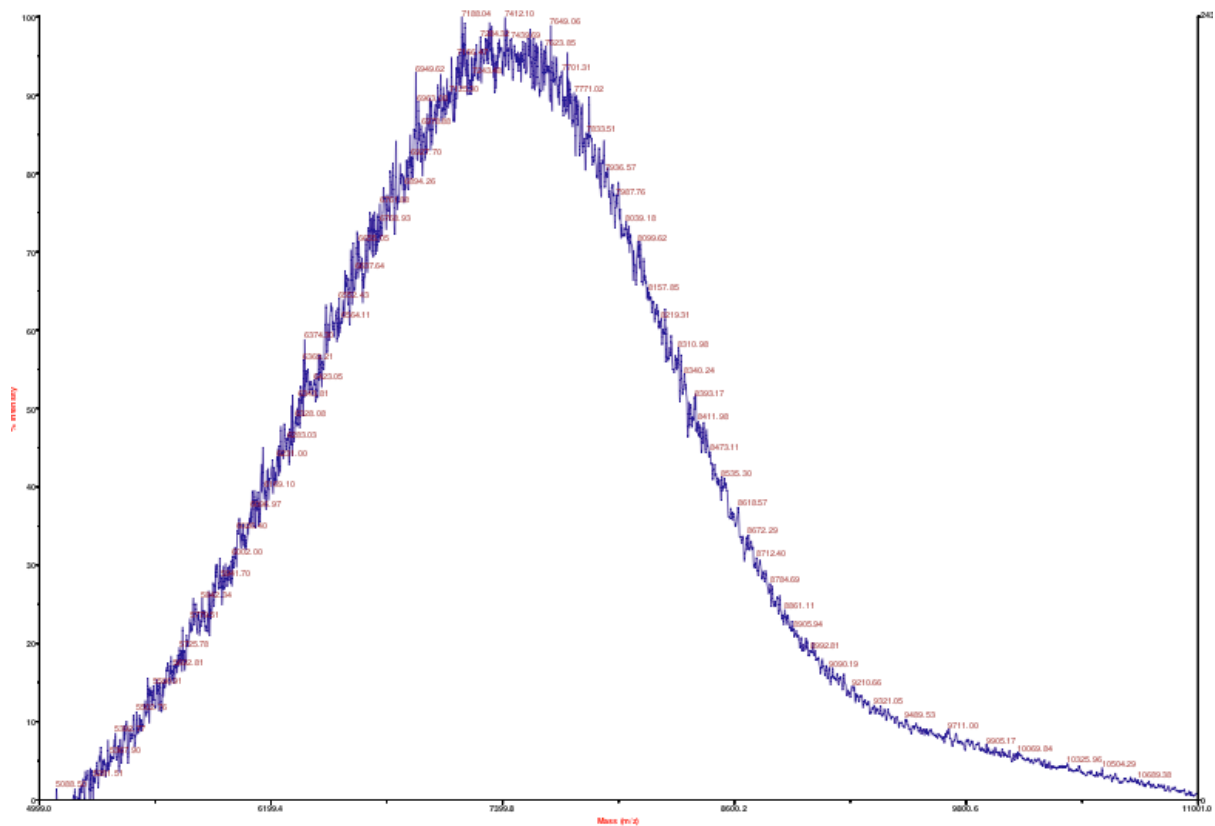


Figure S3.2 MALDI-ToF peak showing the successful partial conversion of **-OH** to **-NH₂** (15), **7498 Da**

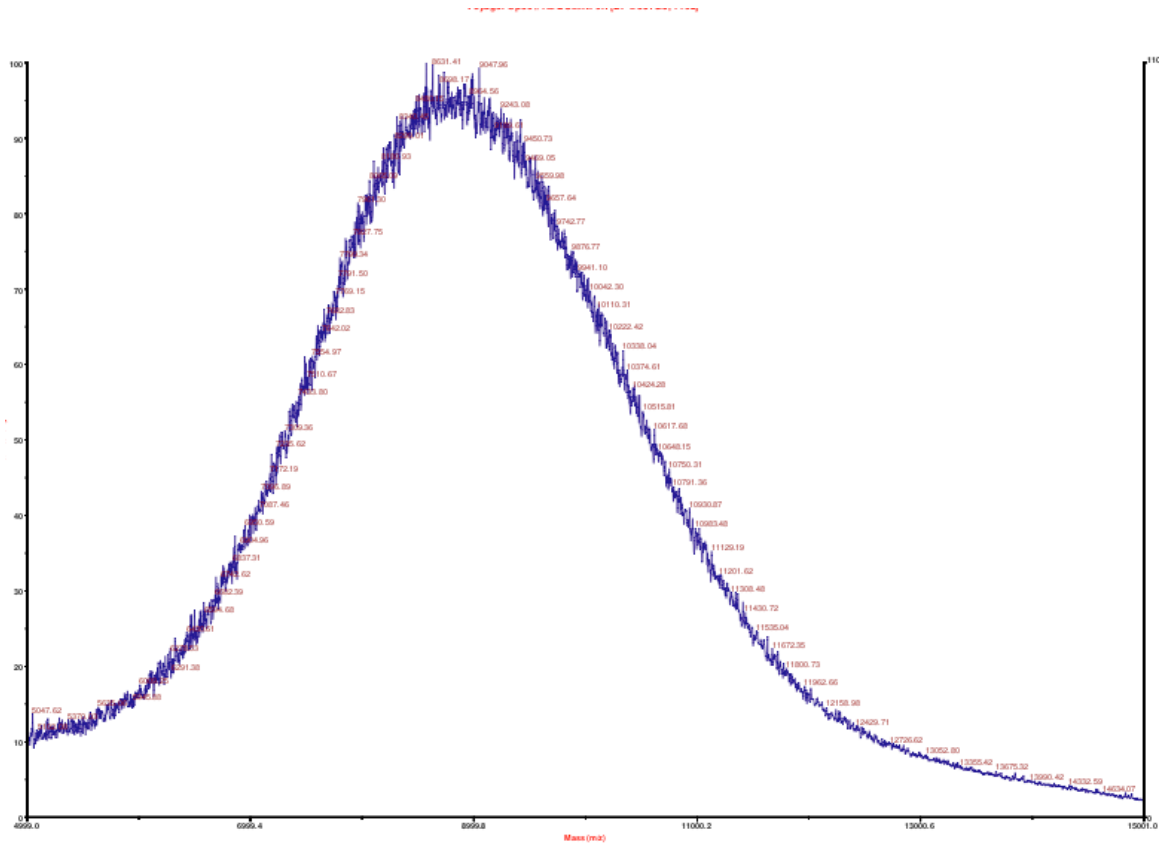


Figure S3.3 MADLI-ToF results showing the peak of G4OH-CY at 8600 Da

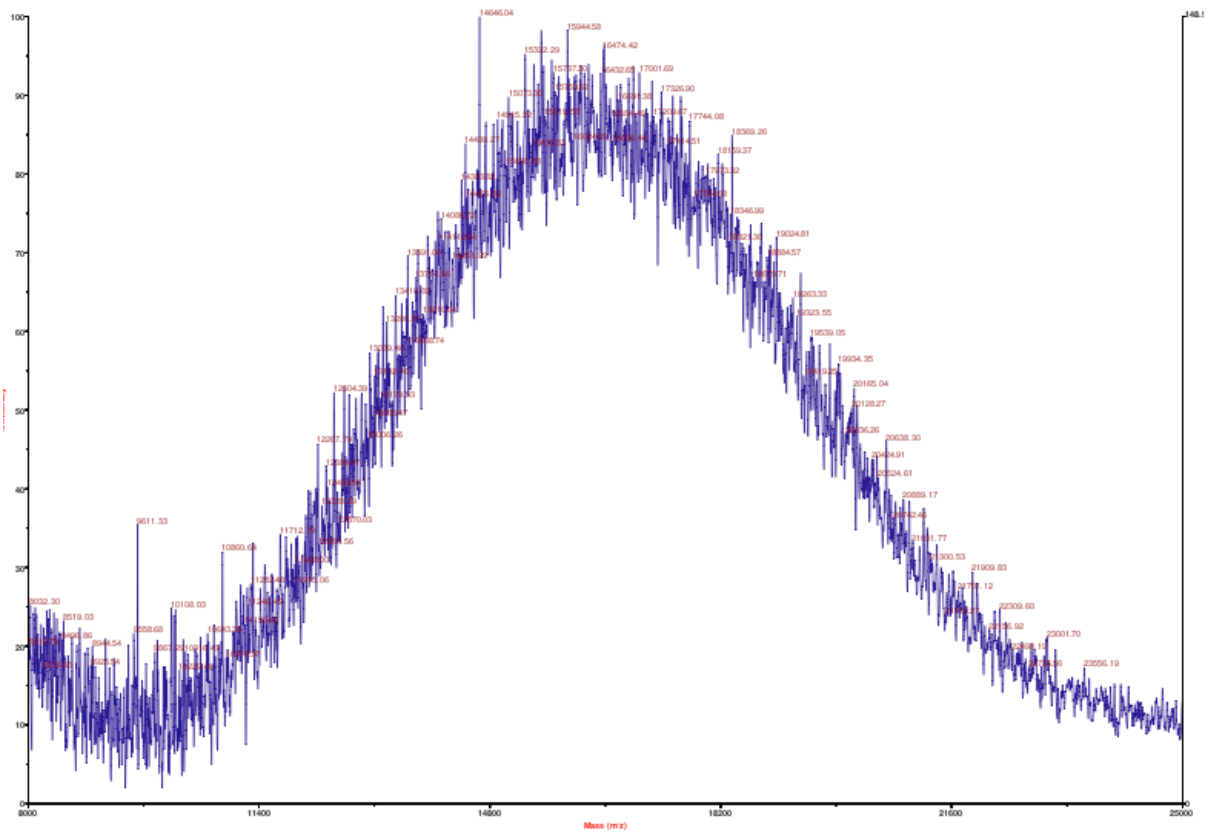
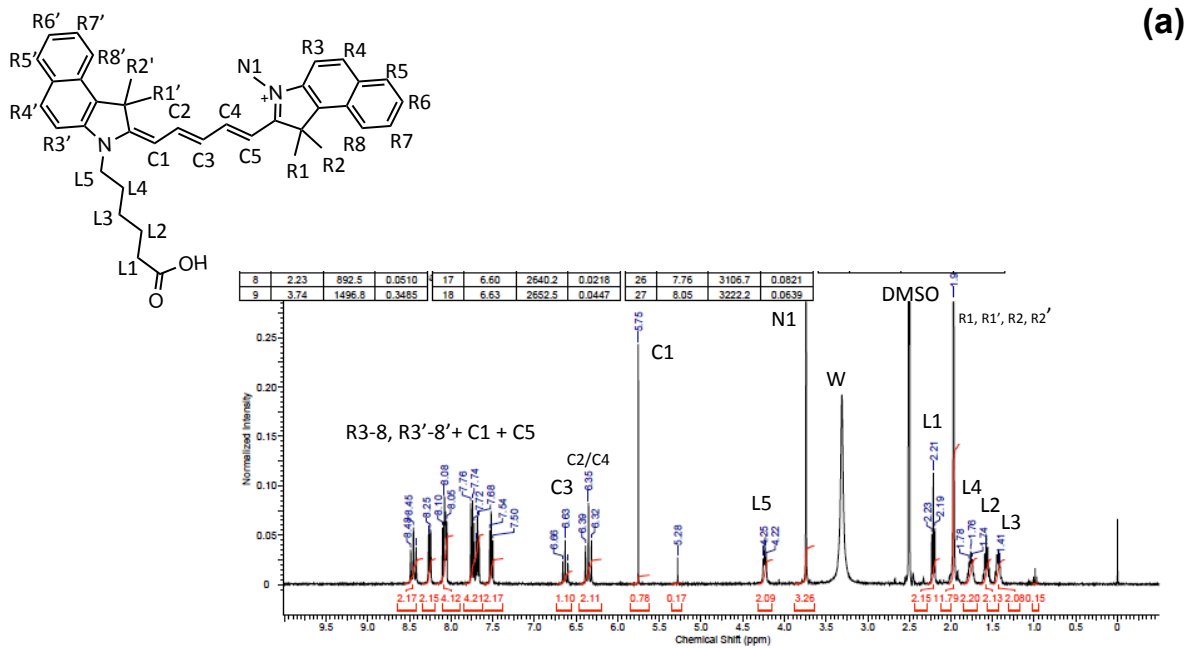
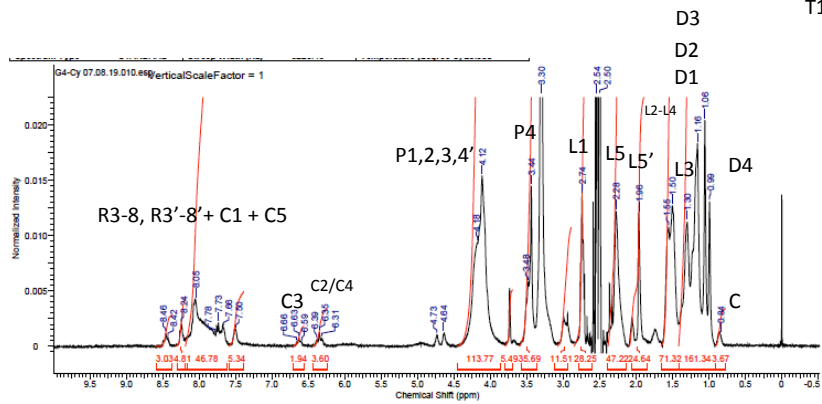
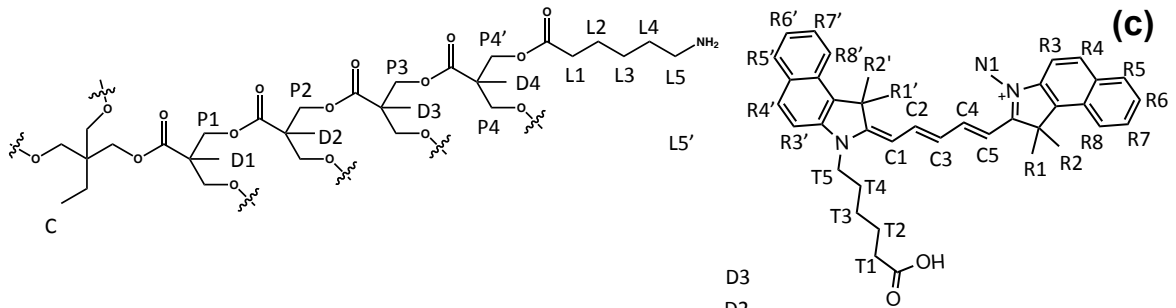
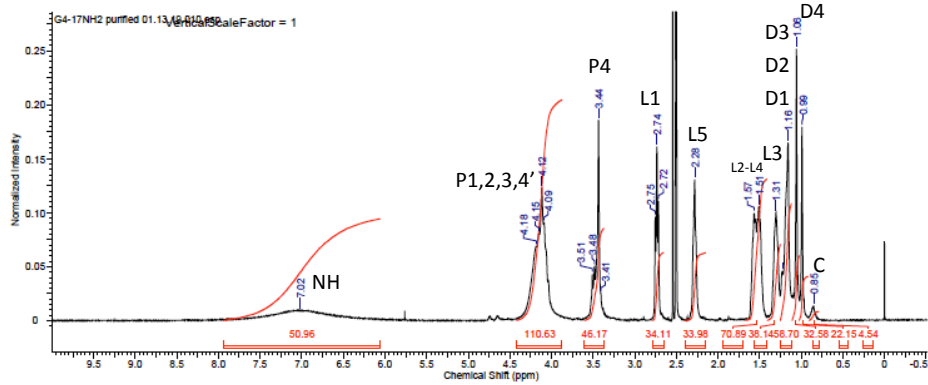
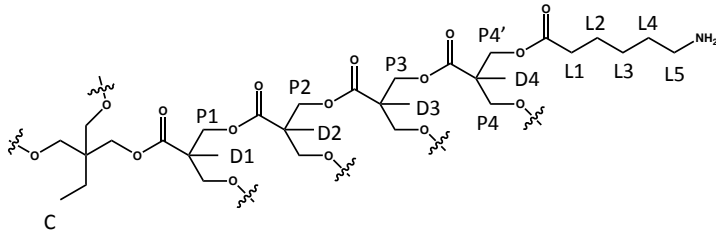


Figure S3.4 MADLI-ToF results showing the peak of G4OH-CY conjugation of mPEG1K at 17000 Da



(b)



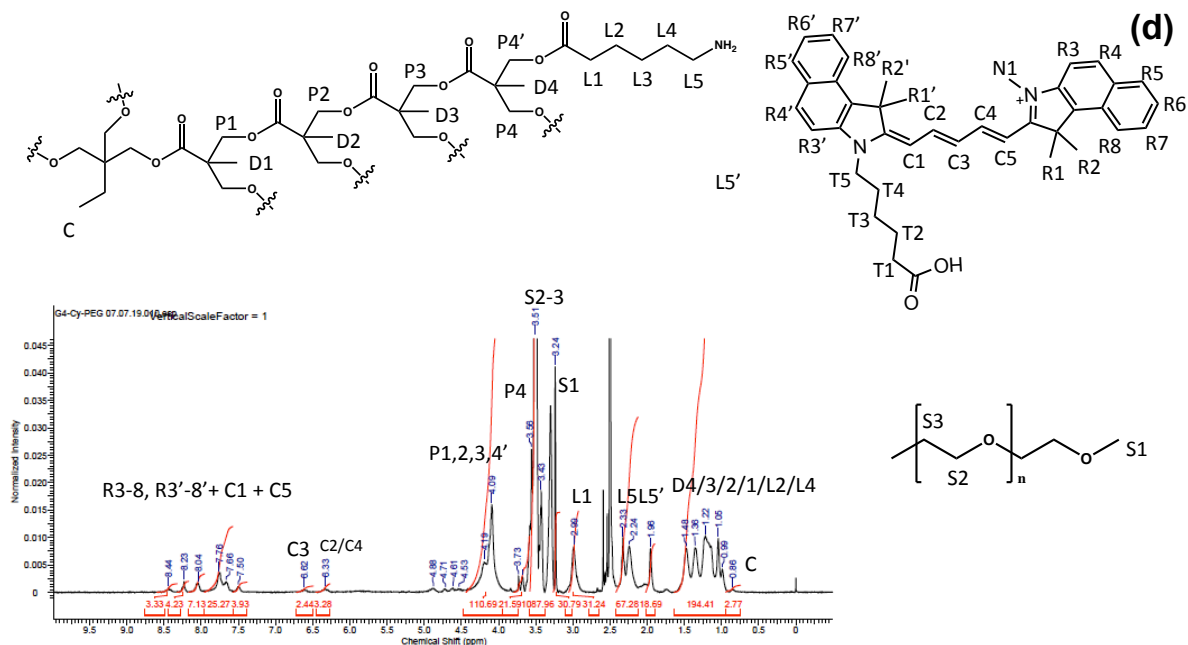


Figure S3.5 Detailed ^1H NMR spectra of (a) Cy5.5, (b) dendrimer, (c) G4OH-CY, and (d) G4OH-CY-mPEG1000.

^1H NMR Explanation

A fourth generation polyester dendrimer was first modified with a protected amino acid (linker) in order to add terminal amino groups to the dendrimer. This amino groups would have a higher nucleophilicity and would increase the efficiency of the reaction between the dendrimer and the dye (Cy5.5). The reaction with boc-protected amino hexanoic acid, and subsequently deprotection, led to the appearance of new peaks related to the $-\text{CH}_2$ groups from the amino acid (1.31, 1.51, 1.57, 2.28, 2.74 ppm). Those peaks were used to assign the number of conjugated linkers, what as calculated as 17. After this first modification, the macromolecule was reacted with Cy5.5

forming an amide bond between the linker and the dye. The conjugation of the dye was checked by the appearance of peaks in the 7.5-8.5 ppm range (related to the rings and double bonds of the structure) and the number of conjugates was determined through the integration of the peak at 6.35 ppm. This peak was selected due to the fact that it is very isolated from other peaks and no overlap was observed. The integration of it showed the conjugation of 1.8 molecules of dye per dendrimer.

After the obtainment of the labeled dendrimer, it was reacted with mPEGCOOH (1,000 Da) and the purified macromolecule was analyzed through ^1H NMR. The conjugation of mPEG resulted in the appearance of a very intense peak at 3.51 ppm, which is correspondent to the $-\text{CH}_2$ units of the polymeric chain. To quantify the number of polymer chains connected, it was used the integration of the terminal methyl group ($-\text{CH}_3$) of mPEG at 3.24 ppm. It was determined that was conjugated 10.2 PEG chains per dendrimer. Additionally, in the spectrum of this final structure it is possible to observe the peaks of Cy5.5 showcasing that the dye was not affected by the reaction between dendrimer and mPEG.

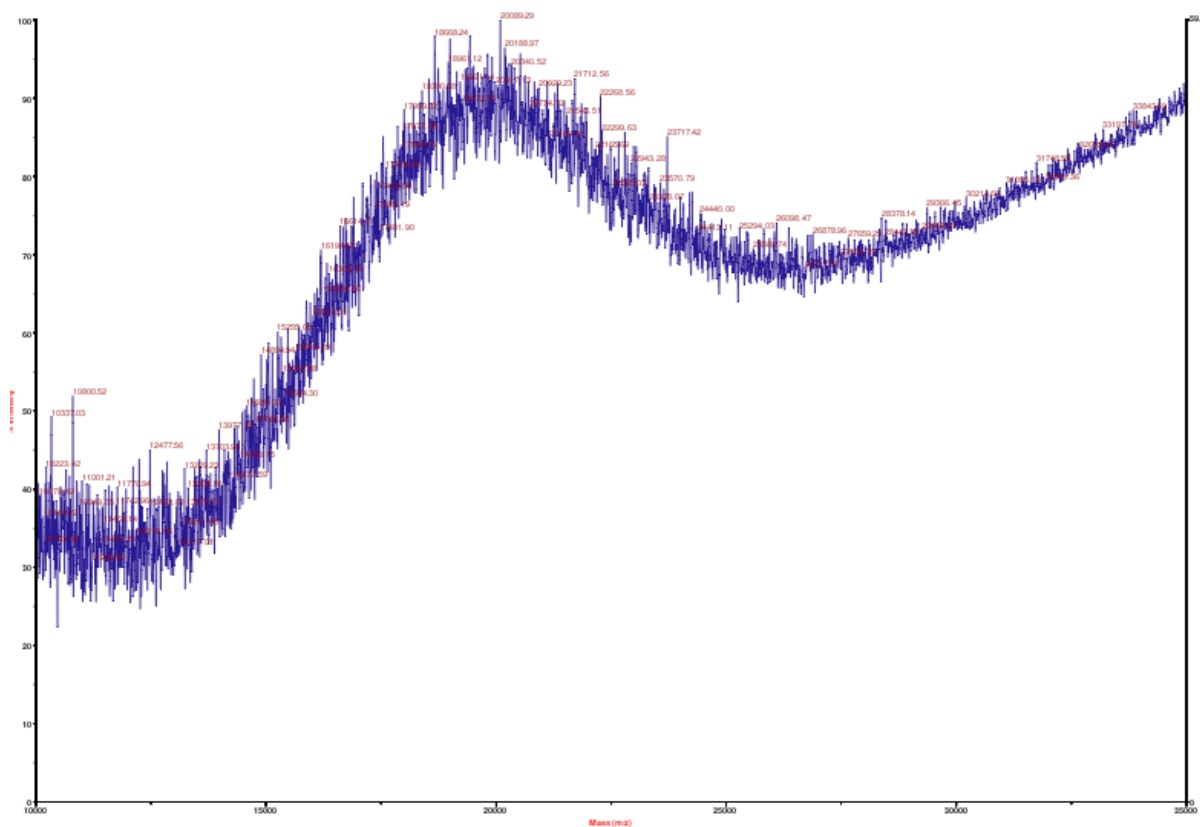


Figure S3.6 MALDI-ToF peak (**20089 Da**) showing the successful conjugation of HOOC-PEG-NH₂-BOC to the G4-CY.

REFERENCES

- Akbarzadeh, A., Rezaei-Sadabady, R., Davaran, S., Joo, S.W., Zarghami, N., Hanifehpour, Y., Samiei, M., Kouhi, M., Nejati-Koshki, K., 2013a. Liposome: classification, preparation, and applications. *Nanoscale Res Lett* 8, 102.
- Akbarzadeh, A., Rezaei-Sadabady, R., Davaran, S., Joo, S.W., Zarghami, N., Hanifehpour, Y., Samiei, M., Kouhi, M., Nejati-Koshki, K., 2013b. Liposome: classification, preparation, and applications. *Nanoscale research letters* 8, 102.
- Akour, A.A., Gerk, P., Kennedy, M.J., 2015a. Megalin expression in human term and preterm placental villous tissues: effect of gestational age and sample processing and storage time. *J Pharmacol Toxicol Methods* 71, 147-154.
- Akour, A.A., Kennedy, M.J., Gerk, P., 2013. Receptor-mediated endocytosis across human placenta: emphasis on megalin. *Mol Pharm* 10, 1269-1278.
- Akour, A.A., Kennedy, M.J., Gerk, P.M., 2015b. The Role of Megalin in the Transport of Gentamicin Across BeWo Cells, an In Vitro Model of the Human Placenta. *AAPS J* 17, 1193-1199.
- Al-Enazy, S., Ali, S., Albekairi, N., El-Tawil, M., Rytting, E., 2017. Placental control of drug delivery. *Advanced drug delivery reviews* 116, 63-72.
- Audus, K.L., 1999. Controlling drug delivery across the placenta. *European journal of pharmaceutical sciences* 8, 161-165.
- Bajoria, R., Contractor, S.F., 1997. Effect of the size of liposomes on the transfer and uptake of carboxyfluorescein by the perfused human term placenta. *J Pharm Pharmacol* 49, 675-681.
- Bajoria, R., Fisk, N.M., Contractor, S.F., 1997a. Liposomal thyroxine: a noninvasive model for transplacental fetal therapy. *J Clin Endocrinol Metab* 82, 3271-3277.
- Bajoria, R., Sooranna, S., Chatterjee, R., 2013. Effect of lipid composition of cationic SUV liposomes on materno-fetal transfer of warfarin across the perfused human term placenta. *Placenta* 34, 1216-1222.
- Bajoria, R., Sooranna, S.R., Contractor, S.F., 1997b. Endocytotic uptake of small unilamellar liposomes by human trophoblast cells in culture. *Hum Reprod* 12, 1343-1348.
- Bawa, R., 2008. Nanoparticle-based therapeutics in humans: a survey. *Nanotech. L. & Bus.* 5, 135.
- Bergamaschi, G., Bergamaschi, P., Carlevati, S., Cazzola, M., 1990. Transferrin receptor expression in the human placenta. *Haematologica* 75, 220-223.
- Bielski, E.R., Zhong, Q., Brown, M., da Rocha, S.R., 2015. Effect of the Conjugation Density of Triphenylphosphonium Cation on the Mitochondrial Targeting of Poly(amidoamine) Dendrimers. *Mol Pharm* 12, 3043-3053.

- Biswas, S., Dodwadkar, N.S., Piroyan, A., Torchilin, V.P., 2012. Surface conjugation of triphenylphosphonium to target poly(amidoamine) dendrimers to mitochondria. *Biomaterials* 33, 4773-4782.
- Bozzuto, G., Molinari, A., 2015a. Liposomes as nanomedical devices. *International journal of nanomedicine* 10, 975.
- Bozzuto, G., Molinari, A., 2015b. Liposomes as nanomedical devices. *International journal of nanomedicine* 10, 975-999.
- Burton, G.J., Jauniaux, E., 2015. What is the placenta? *American journal of obstetrics and gynecology* 213, S6. e1-S6. e4.
- Campeiro, J.D., Dam, W., Monte, G.G., Porta, L.C., de Oliveira, L.C.G., Nering, M.B., Viana, G.M., Carapeto, F.C., Oliveira, E.B., van den Born, J., 2019. Long term safety of targeted internalization of cell penetrating peptide crotamine into renal proximal tubular epithelial cells in vivo. *Scientific reports* 9, 3312.
- Carter, A.M., 2007. Animal models of human placentation—a review. *Placenta* 28, S41-S47.
- Cheng, Y., Xu, T., 2008. The effect of dendrimers on the pharmacodynamic and pharmacokinetic behaviors of non-covalently or covalently attached drugs. *Eur J Med Chem* 43, 2291-2297.
- Clarot, I., Chaimbault, P., Hasdenteufel, F., Netter, P., Nicolas, A., 2004. Determination of gentamicin sulfate and related compounds by high-performance liquid chromatography with evaporative light scattering detection. *J Chromatogr A* 1031, 281-287.
- Dashe, J.S., Gilstrap III, L.C., 1997. Antibiotic use in pregnancy. *Obstetrics and gynecology clinics of North America* 24, 617-629.
- Derycke, A.S., Kamuhabwa, A., Gijssens, A., Roskams, T., De Vos, D., Kasran, A., Huwyler, J., Missiaen, L., de Witte, P.A., 2004. Transferrin-Conjugated Liposome Targeting of Photosensitizer AlPcS 4 to Rat Bladder Carcinoma Cells. *Journal of the National Cancer Institute* 96, 1620-1630.
- Doane, T.L., Burda, C., 2012. The unique role of nanoparticles in nanomedicine: imaging, drug delivery and therapy. *Chemical Society Reviews* 41, 2885-2911.
- Donnelly, L., Campling, G., 2014. Functions of the placenta. *Anaesthesia & intensive care medicine* 15, 136-139.
- Duley, L., 2009. The global impact of pre-eclampsia and eclampsia. *Semin Perinatol* 33, 130-137.
- Duncan, R., Izzo, L., 2005. Dendrimer biocompatibility and toxicity. *Advanced drug delivery reviews* 57, 2215-2237.
- Duzgune, scedil, Nir, S., 1999. Mechanisms and kinetics of liposome-cell interactions. *Adv Drug Deliv Rev* 40, 3-18.

- Faber, K., Hvidberg, V., Moestrup, S.K., Dahlbäck, B.r., Nielsen, L.B., 2006. Megalin is a receptor for apolipoprotein M, and kidney-specific megalin-deficiency confers urinary excretion of apolipoprotein M. *Molecular endocrinology* 20, 212-218.
- Faraji, A.H., Wipf, P., 2009. Nanoparticles in cellular drug delivery. *Bioorg Med Chem* 17, 2950-2962.
- Forssen, E., Willis, M., 1998. Ligand-targeted liposomes. *Advanced drug delivery reviews* 29, 249-271.
- Friend, D.S., Papahadjopoulos, D., Debs, R.J., 1996. Endocytosis and intracellular processing accompanying transfection mediated by cationic liposomes. *Biochim Biophys Acta* 1278, 41-50.
- Fritze, A., Hens, F., Kimpfler, A., Schubert, R., Peschka-Süss, R., 2006. Remote loading of doxorubicin into liposomes driven by a transmembrane phosphate gradient. *Biochimica et Biophysica Acta (BBA)-Biomembranes* 1758, 1633-1640.
- Gabizon, A., Shmeeda, H., Horowitz, A.T., Zalipsky, S., 2004. Tumor cell targeting of liposome-entrapped drugs with phospholipid-anchored folic acid-PEG conjugates. *Adv Drug Deliv Rev* 56, 1177-1192.
- Gao, C., Liang, X., Mo, S., Zhang, N., Sun, D., Dai, Z., 2018. Near-infrared cyanine-loaded liposome-like nanocapsules of camptothecin–floxuridine conjugate for enhanced chemophotothermal combination cancer therapy. *ACS applied materials & interfaces* 10, 3219-3228.
- Gao, Z., Lukyanov, A.N., Singhal, A., Torchilin, V.P., 2002. Diacyllipid-polymer micelles as nanocarriers for poorly soluble anticancer drugs. *Nano letters* 2, 979-982.
- Garite, T.J., Clark, R., Thorp, J.A., 2004. Intrauterine growth restriction increases morbidity and mortality among premature neonates. *Am J Obstet Gynecol* 191, 481-487.
- Gberindyer, F.A., Abatan, M.O., Wiesner, L., 2017. Composition of Gentamicin C Components in Gentamicin Sulphate Generics Commonly Used in Small Animal Practice in Nigeria. *Journal of Pharmacy and Pharmacology* 5, 20-25.
- Georgiades, P., Ferguson-Smith, A., Burton, G., 2002. Comparative developmental anatomy of the murine and human definitive placentae. *Placenta* 23, 3-19.
- Goldenberg, R.L., Culhane, J.F., Iams, J.D., Romero, R., 2008. Epidemiology and causes of preterm birth. *Lancet* 371, 75-84.
- Grazia Calvagno, M., Celia, C., Paolino, D., Cosco, D., Iannone, M., Castelli, F., Doldo, P., Fresta, M., 2007. Effects of lipid composition and preparation conditions on physical-chemical properties, technological parameters and in vitro biological activity of gemcitabine-loaded liposomes. *Current drug delivery* 4, 89-101.
- Griffiths, S.K., Campbell, J.P., 2014. Placental structure, function and drug transfer. *Continuing Education in Anaesthesia, Critical Care & Pain* 15, 84-89.

- Gude, N.M., Roberts, C.T., Kalionis, B., King, R.G., 2004. Growth and function of the normal human placenta. *Thromb Res* 114, 397-407.
- Gulraze, A., Kurdi, W., Tulbah, M., Niaz, F.A., 2013. Prenatal diagnosis and treatment perspective of fetal hypothyroidism with goiter. *J Coll Physicians Surg Pak* 23, 216-218.
- Heath, T.D., Fraley, R.T., Papahadjopoulos, D., 1980. Antibody targeting of liposomes: cell specificity obtained by conjugation of F (ab')₂ to vesicle surface. *Science* 210, 539-541.
- Heath, T.D., Montgomery, J.A., Piper, J.R., Papahadjopoulos, D., 1983. Antibody-targeted liposomes: increase in specific toxicity of methotrexate-gamma-aspartate. *Proceedings of the National Academy of Sciences* 80, 1377-1381.
- Heyder, R.S., Zhong, Q., Bazito, R.C., da Rocha, S.R.P., 2017. Cellular internalization and transport of biodegradable polyester dendrimers on a model of the pulmonary epithelium and their formulation in pressurized metered-dose inhalers. *Int J Pharm* 520, 181-194.
- Heyne, G.W., Plisch, E.H., Melberg, C.G., Sandgren, E.P., Peter, J.A., Lipinski, R.J., 2015. A simple and reliable method for early pregnancy detection in inbred mice. *Journal of the American Association for Laboratory Animal Science* 54, 368-371.
- Hong, M., Zhu, S., Jiang, Y., Tang, G., Pei, Y., 2009. Efficient tumor targeting of hydroxycamptothecin loaded PEGylated niosomes modified with transferrin. *J Control Release* 133, 96-102.
- Huang, G., Zhou, Z., Srinivasan, R., Penn, M.S., Kottke-Marchant, K., Marchant, R.E., Gupta, A.S., 2008. Affinity manipulation of surface-conjugated RGD peptide to modulate binding of liposomes to activated platelets. *Biomaterials* 29, 1676-1685.
- Jansson, T., 2001. Amino acid transporters in the human placenta. *Pediatric research* 49, 141.
- Jim, B., Karumanchi, S.A., 2017. Preeclampsia: Pathogenesis, Prevention, and Long-Term Complications. *Semin Nephrol* 37, 386-397.
- John, R., Hemberger, M., 2012. A placenta for life. *Reprod Biomed Online* 25, 5-11.
- Juliano, R., Stamp, D., 1975. The effect of particle size and charge on the clearance rates of liposomes and liposome encapsulated drugs. *Biochemical and biophysical research communications* 63, 651-658.
- Keelan, J.A., Leong, J.W., Ho, D., Iyer, K.S., 2015a. Therapeutic and safety considerations of nanoparticle-mediated drug delivery in pregnancy. *Nanomedicine* 10, 2229-2247.
- Keelan, J.A., Leong, J.W., Ho, D., Iyer, K.S., 2015b. Therapeutic and safety considerations of nanoparticle-mediated drug delivery in pregnancy. *Nanomedicine (Lond)* 10, 2229-2247.
- Kesharwani, P., Iyer, A.K., 2015. Recent advances in dendrimer-based nanovectors for tumor-targeted drug and gene delivery. *Drug Discov Today* 20, 536-547.

- King, A., Ndifon, C., Lui, S., Widdows, K., Kotamraju, V.R., Agemy, L., Teesalu, T., Glazier, J.D., Cellesi, F., Tirelli, N., 2016a. Tumor-homing peptides as tools for targeted delivery of payloads to the placenta. *Science advances* 2, e1600349.
- King, A., Ndifon, C., Lui, S., Widdows, K., Kotamraju, V.R., Agemy, L., Teesalu, T., Glazier, J.D., Cellesi, F., Tirelli, N., Aplin, J.D., Ruoslahti, E., Harris, L.K., 2016b. Tumor-homing peptides as tools for targeted delivery of payloads to the placenta. *Sci Adv* 2, e1600349.
- Kolhe, P., Khandare, J., Pillai, O., Kannan, S., Lieh-Lai, M., Kannan, R.M., 2006. Preparation, cellular transport, and activity of polyamidoamine-based dendritic nanodevices with a high drug payload. *Biomaterials* 27, 660-669.
- Kooijmans, S., Fliervoet, L., Van Der Meel, R., Fens, M., Heijnen, H., en Henegouwen, P.v.B., Vader, P., Schiffelers, R., 2016. PEGylated and targeted extracellular vesicles display enhanced cell specificity and circulation time. *Journal of controlled release* 224, 77-85.
- Krishnan, L., Nguyen, T., McComb, S., 2013. From mice to women: the conundrum of immunity to infection during pregnancy. *Journal of reproductive immunology* 97, 62-73.
- Kulvietis, V., Zalgeviciene, V., Didziapetriene, J., Rotomskis, R., 2011. Transport of nanoparticles through the placental barrier. *The Tohoku journal of experimental medicine* 225, 225-234.
- Laouini, A., Jaafar-Maalej, C., Limayem-Blouza, I., Sfar, S., Charcosset, C., Fessi, H., 2012. Preparation, characterization and applications of liposomes: state of the art. *Journal of colloid Science and Biotechnology* 1, 147-168.
- Lee, R.J., Low, P.S., 1995. Folate-mediated tumor cell targeting of liposome-entrapped doxorubicin in vitro. *Biochim Biophys Acta* 1233, 134-144.
- Li, H., van Ravenzwaay, B., Rietjens, I.M., Louisse, J., 2013. Assessment of an in vitro transport model using BeWo b30 cells to predict placental transfer of compounds. *Archives of toxicology* 87, 1661-1669.
- Lim, S.B., Banerjee, A., Önyüksel, H., 2012. Improvement of drug safety by the use of lipid-based nanocarriers. *Journal of controlled release* 163, 34-45.
- Lybbert, J., Gullingsrud, J., Chesnokov, O., Turyakira, E., Dhorda, M., Guerin, P.J., Piola, P., Muehlenbachs, A., Oleinikov, A.V., 2016. Abundance of megalin and Dab2 is reduced in syncytiotrophoblast during placental malaria, which may contribute to low birth weight. *Scientific reports* 6, 24508.
- McCoy, S., Baldwin, K., 2009. Pharmacotherapeutic options for the treatment of preeclampsia. *American Journal of Health-System Pharmacy* 66, 337-344.
- McDonagh, S., Maidji, E., Ma, W., Chang, H.-T., Fisher, S., Pereira, L., 2004. Viral and bacterial pathogens at the maternal-fetal interface. *Journal of Infectious Diseases* 190, 826-834.

- Mehrotra, R., De Gaudio, R., Palazzo, M., 2004. Antibiotic pharmacokinetic and pharmacodynamic considerations in critical illness. *Intensive Care Med* 30, 2145-2156.
- Menjoge, A.R., Rinderknecht, A.L., Navath, R.S., Faridnia, M., Kim, C.J., Romero, R., Miller, R.K., Kannan, R.M., 2011. Transfer of PAMAM dendrimers across human placenta: prospects of its use as drug carrier during pregnancy. *Journal of controlled release* 150, 326-338.
- Miele, E., Spinelli, G.P., Miele, E., Tomao, F., Tomao, S., 2009. Albumin-bound formulation of paclitaxel (Abraxane® ABI-007) in the treatment of breast cancer. *International journal of nanomedicine* 4, 99.
- Miller, C.R., Bondurant, B., McLean, S.D., McGovern, K.A., O'Brien, D.F., 1998a. Liposome-cell interactions in vitro: effect of liposome surface charge on the binding and endocytosis of conventional and sterically stabilized liposomes. *Biochemistry* 37, 12875-12883.
- Miller, C.R., Bondurant, B., McLean, S.D., McGovern, K.A., O'Brien, D.F., 1998b. Liposome- cell interactions in vitro: effect of liposome surface charge on the binding and endocytosis of conventional and sterically stabilized liposomes. *Biochemistry* 37, 12875-12883.
- Mirza, A.Z., Siddiqui, F.A., 2014. Nanomedicine and drug delivery: a mini review. *International Nano Letters* 4, 94.
- Moghimi, S.M., Hunter, A.C., Murray, J.C., 2005. Nanomedicine: current status and future prospects. *FASEB J* 19, 311-330.
- Muggia, F.M., 2001. Liposomal encapsulated anthracyclines: new therapeutic horizons. *Curr Oncol Rep* 3, 156-162.
- Nagai, J., Takano, M., 2004. Molecular Aspects of Renal Handling of Aminoglycosides and Strategies for Preventing the Nephrotoxicity. *Drug Metabolism and Pharmacokinetics* 19, 159-170.
- Nanjwade, B.K., Bechra, H.M., Derkar, G.K., Manvi, F., Nanjwade, V.K., 2009. Dendrimers: emerging polymers for drug-delivery systems. *European Journal of Pharmaceutical Sciences* 38, 185-196.
- Natarajan, J.V., Nugraha, C., Ng, X.W., Venkatraman, S., 2014. Sustained-release from nanocarriers: a review. *Journal of Controlled Release* 193, 122-138.
- Nelson, D.M., 2015. How the placenta affects your life, from womb to tomb. *Am J Obstet Gynecol* 213, S12-13.
- Ohnishi, N., Yamamoto, E., Tomida, H., Hyodo, K., Ishihara, H., Kikuchi, H., Tahara, K., Takeuchi, H., 2013. Rapid determination of the encapsulation efficiency of a liposome formulation using column-switching HPLC. *International journal of pharmaceutics* 441, 67-74.

- Orlando, R.A., Rader, K., Authier, F., Yamazaki, H., Posner, B.I., Bergeron, J., Farquhar, M.G., 1998. Megalin is an endocytic receptor for insulin. *Journal of the American Society of Nephrology* 9, 1759-1766.
- Oroojalian, F., Rezayan, A.H., Shier, W.T., Abnous, K., Ramezani, M., 2017. Megalin-targeted enhanced transfection efficiency in cultured human HK-2 renal tubular proximal cells using aminoglycoside-carboxyalkyl-polyethylenimine-containing nanoplexes. *International journal of pharmaceutics* 523, 102-120.
- Oudijk, M.A., Michon, M.M., Kleinman, C.S., Kapusta, L., Stoutenbeek, P., Visser, G.H., Meijboom, E.J., 2000. Sotalol in the treatment of fetal dysrhythmias. *Circulation* 101, 2721-2726.
- Panwar, P., Pandey, B., Lakhera, P.C., Singh, K.P., 2010. Preparation, characterization, and in vitro release study of albendazole-encapsulated nanosize liposomes. *Int J Nanomedicine* 5, 101-108.
- Papahadjopoulos, D., Allen, T.M., Gabizon, A., Mayhew, E., Matthay, K., Huang, S.-K., Lee, K.D., Woodle, M.C., Lasic, D.D., Redemann, C., 1991. Sterically stabilized liposomes: improvements in pharmacokinetics and antitumor therapeutic efficacy. *Proceedings of the National Academy of Sciences* 88, 11460-11464.
- Parnham, M.J., Wetzig, H., 1993. Toxicity screening of liposomes. *Chemistry and physics of lipids* 64, 263-274.
- Pattni, B.S., Chupin, V.V., Torchilin, V.P., 2015. New Developments in Liposomal Drug Delivery. *Chem Rev* 115, 10938-10966.
- Paul, J.W., Hua, S., Ilicic, M., Tolosa, J.M., Butler, T., Robertson, S., Smith, R., 2017. Drug delivery to the human and mouse uterus using immunoliposomes targeted to the oxytocin receptor. *American journal of obstetrics and gynecology* 216, 283.e281-283. e214.
- Pechere, J.-C., Dugal, R., 1979. Clinical pharmacokinetics of aminoglycoside antibiotics. *Clinical Pharmacokinetics* 4, 170-199.
- Portnoy, E., Lecht, S., Lazarovici, P., Danino, D., Magdassi, S., 2011. Cetuximab-labeled liposomes containing near-infrared probe for in vivo imaging. *Nanomedicine: Nanotechnology, Biology and Medicine* 7, 480-488.
- Poulsen, M.S., Rytting, E., Mose, T., Knudsen, L.E., 2009. Modeling placental transport: correlation of in vitro BeWo cell permeability and ex vivo human placental perfusion. *Toxicology in vitro* 23, 1380-1386.
- Racicot, K., Mor, G., 2017. Risks associated with viral infections during pregnancy. *J Clin Invest* 127, 1591-1599.
- Refuerzo, J.S., Alexander, J.F., Leonard, F., Leon, M., Longo, M., Godin, B., 2015. Liposomes: a nanoscale drug carrying system to prevent indomethacin passage to the fetus in a pregnant mouse model. *Am J Obstet Gynecol* 212, 508 e501-507.

- Refuerzo, J.S., Leonard, F., Bulayeva, N., Gorenstein, D., Chiossi, G., Ontiveros, A., Longo, M., Godin, B., 2016. Uterus-targeted liposomes for preterm labor management: studies in pregnant mice. *Sci Rep* 6, 34710.
- Robbins, J.R., Skrzypczynska, K.M., Zeldovich, V.B., Kapidzic, M., Bakardjiev, A.I., 2010. Placental syncytiotrophoblast constitutes a major barrier to vertical transmission of *Listeria monocytogenes*. *PLoS Pathog* 6, e1000732.
- Roberts, D., Brown, J., Medley, N., Dalziel, S.R., 2017. Antenatal corticosteroids for accelerating fetal lung maturation for women at risk of preterm birth. *Cochrane database of systematic reviews*.
- Roberts, J.M., Gammill, H.S., 2005. Preeclampsia: recent insights. *Hypertension* 46, 1243-1249.
- Robson, A.L., Dastoor, P.C., Flynn, J., Palmer, W., Martin, A., Smith, D.W., Woldu, A., Hua, S., 2018. Advantages and Limitations of Current Imaging Techniques for Characterizing Liposome Morphology. *Front Pharmacol* 9, 80.
- Romo, A., Carceller, R., Tobajas, J., 2009. Intrauterine growth retardation (IUGR): epidemiology and etiology. *Pediatric endocrinology reviews: PER* 6, 332-336.
- Saito, A., Pietromonaco, S., Loo, A.K.-C., Farquhar, M.G., 1994. Complete cloning and sequencing of rat gp330/" megalin," a distinctive member of the low density lipoprotein receptor gene family. *Proceedings of the National Academy of Sciences* 91, 9725-9729.
- Seidl, G., Nerad, H., 1988. Gentamicin C: Separation of C 1, C 1a, C 2, C 2a and C 2b components by HPLC using Isocratic ion-exchange chromatography and post-column derivatisation. *Chromatographia* 25, 169-171.
- Šentjurc, M., Vrhovnik, K., Kristl, J., 1999. Liposomes as a topical delivery system: the role of size on transport studied by the EPR imaging method. *Journal of controlled release* 59, 87-97.
- Sercombe, L., Veerati, T., Moheimani, F., Wu, S.Y., Sood, A.K., Hua, S., 2015. Advances and challenges of liposome assisted drug delivery. *Frontiers in pharmacology* 6, 286.
- Shi, J., Votruba, A.R., Farokhzad, O.C., Langer, R., 2010. Nanotechnology in drug delivery and tissue engineering: from discovery to applications. *Nano letters* 10, 3223-3230.
- Sibai, B.M., 2004. Magnesium sulfate prophylaxis in preeclampsia: Lessons learned from recent trials. *American journal of obstetrics and gynecology* 190, 1520-1526.
- Silasi, M., Cardenas, I., Kwon, J.Y., Racicot, K., Aldo, P., Mor, G., 2015. Viral infections during pregnancy. *Am J Reprod Immunol* 73, 199-213.
- Simmons, L.E., Rubens, C.E., Darmstadt, G.L., Gravett, M.G., 2010. Preventing preterm birth and neonatal mortality: exploring the epidemiology, causes, and interventions. *Semin Perinatol* 34, 408-415.

- Soininen, S.K., Repo, J.K., Karttunen, V., Auriola, S., Vähäkangas, K.H., Ruponen, M., 2015. Human placental cell and tissue uptake of doxorubicin and its liposomal formulations. *Toxicology letters* 239, 108-114.
- Song, S., Liu, D., Peng, J., Sun, Y., Li, Z., Gu, J.R., Xu, Y., 2008. Peptide ligand-mediated liposome distribution and targeting to EGFR expressing tumor in vivo. *Int J Pharm* 363, 155-161.
- Storm, T., Christensen, E.I., Christensen, J.N., Kjaergaard, T., Ulbjerg, N., Larsen, A., Honoré, B., Madsen, M., 2016. Megalin is predominantly observed in vesicular structures in first and third trimester cytotrophoblasts of the human placenta. *Journal of Histochemistry & Cytochemistry* 64, 769-784.
- Straubinger, R.M., Hong, K., Friend, D.S., Papahadjopoulos, D., 1983. Endocytosis of liposomes and intracellular fate of encapsulated molecules: encounter with a low pH compartment after internalization in coated vesicles. *Cell* 32, 1069-1079.
- Sun, X., Liu, X., Analysis of Gentamicin Using a pH Stable Specialty Column for Aminoglycoside Antibiotics Separation.
- Swanson, J.A., King, J.S., 2018. The breadth of macropinocytosis research. The Royal Society.
- Tagalakis, A.D., He, L., Saraiva, L., Gustafsson, K.T., Hart, S.L., 2011. Receptor-targeted liposome-peptide nanocomplexes for siRNA delivery. *Biomaterials* 32, 6302-6315.
- Thornburg, K.L., Marshall, N., 2015. The placenta is the center of the chronic disease universe. *American Journal of Obstetrics & Gynecology* 213, S14-S20.
- Tiwari, G., Tiwari, R., Sriwastawa, B., Bhati, L., Pandey, S., Pandey, P., Bannerjee, S.K., 2012. Drug delivery systems: An updated review. *International journal of pharmaceutical investigation* 2, 2.
- Tuzel-Kox, S.N., Patel, H.M., Kox, W.J., 1995. Uptake of drug-carrier liposomes by placenta: transplacental delivery of drugs and nutrients. *J Pharmacol Exp Ther* 274, 104-109.
- Valero, L., Alhareth, K., Espinoza Romero, J., Viricel, W., Leblond, J., Chissey, A., Dhotel, H., Roques, C., Campiol Arruda, D., Escriou, V., 2018. Liposomes as Gene Delivery Vectors for Human Placental Cells. *Molecules* 23, 1085.
- Valero, L., Alhareth, K., Gil, S., Simasotchi, C., Roques, C., Scherman, D., Mignet, N., Fournier, T., Andrieux, K., 2017. Assessment of dually labelled PEGylated liposomes transplacental passage and placental penetration using a combination of two ex-vivo human models: The dually perfused placenta and the suspended villous explants. *International journal of pharmaceuticals* 532, 729-737.
- Velegrakis, A., Sfakiotaki, M., Sifakis, S., 2017. Human placental growth hormone in normal and abnormal fetal growth. *Biomedical reports* 7, 115-122.
- Verroust, P.J., Birn, H., Nielsen, R., Kozyraki, R., Christensen, E.I., 2002. The tandem endocytic receptors megalin and cubilin are important proteins in renal pathology. *Kidney international* 62, 745-756.

- Verroust, P.J., Christensen, E.I., 2002. Megalin and cubilin—the story of two multipurpose receptors unfolds. *Nephrology Dialysis Transplantation* 17, 1867-1871.
- Wagner, V., Dullaart, A., Bock, A.-K., Zweck, A., 2006. The emerging nanomedicine landscape. *Nature biotechnology* 24, 1211.
- Ward, K., Theiler, R.N., 2008. Once-daily dosing of gentamicin in obstetrics and gynecology. *Clin Obstet Gynecol* 51, 498-506.
- Weinstein, M.J., Luedemann, G.M., Oden, E.M., Wagman, G.H., Rosselet, J.P., Marquez, J.A., Coniglio, C.T., Charney, W., Herzog, H.L., Black, J., 1963. Gentamicin, 1 a new antibiotic complex from *Micromonospora*. *Journal of medicinal chemistry* 6, 463-464.
- Wijagkanalan, W., Kawakami, S., Hashida, M., 2011. Designing dendrimers for drug delivery and imaging: pharmacokinetic considerations. *Pharm Res* 28, 1500-1519.
- Wolfram, J., Suri, K., Yang, Y., Shen, J., Celia, C., Fresta, M., Zhao, Y., Shen, H., Ferrari, M., 2014. Shrinkage of pegylated and non-pegylated liposomes in serum. *Colloids and Surfaces B: Biointerfaces* 114, 294-300.
- Wooding, F., Flint, A., 1994. *Placentation, Marshall's physiology of reproduction*. Springer, pp. 233-460.
- Yamashita, K., Yoshioka, Y., Higashisaka, K., Mimura, K., Morishita, Y., Nozaki, M., Yoshida, T., Ogura, T., Nabeshi, H., Nagano, K., Abe, Y., Kamada, H., Monobe, Y., Imazawa, T., Aoshima, H., Shishido, K., Kawai, Y., Mayumi, T., Tsunoda, S., Itoh, N., Yoshikawa, T., Yanagihara, I., Saito, S., Tsutsumi, Y., 2011. Silica and titanium dioxide nanoparticles cause pregnancy complications in mice. *Nat Nanotechnol* 6, 321-328.
- Yang, Y., Yang, Y., Xie, X., Cai, X., Zhang, H., Gong, W., Wang, Z., Mei, X., 2014. PEGylated liposomes with NGR ligand and heat-activable cell-penetrating peptide-doxorubicin conjugate for tumor-specific therapy. *Biomaterials* 35, 4368-4381.
- Yellepeddi, V.K., Kumar, A., Maher, D.M., Chauhan, S.C., Vangara, K.K., Palakurthi, S., 2011. Biotinylated PAMAM dendrimers for intracellular delivery of cisplatin to ovarian cancer: role of SMVT. *Anticancer Res* 31, 897-906.
- Yu, J., Jia, J., Guo, X., Chen, R., Feng, L., 2017. Modulating circulating sFlt1 in an animal model of preeclampsia using PAMAM nanoparticles for siRNA delivery. *Placenta* 58, 1-8.
- Zeuzem, S., Feinman, S.V., Rasenack, J., Heathcote, E.J., Lai, M.-Y., Gane, E., O'grady, J., Reichen, J., Diago, M., Lin, A., 2000. Peginterferon alfa-2a in patients with chronic hepatitis C. *New England Journal of Medicine* 343, 1666-1672.
- Zhang, B., Tan, L., Yu, Y., Wang, B., Chen, Z., Han, J., Li, M., Chen, J., Xiao, T., Ambati, B.K., 2018. Placenta-specific drug delivery by trophoblast-targeted nanoparticles in mice. *Theranostics* 8, 2765.
- Zhang, H., Ma, Y., Sun, X.L., 2010. Recent developments in carbohydrate - decorated targeted drug/gene delivery. *Medicinal research reviews* 30, 270-289.

- Zhong, Q., Bielski, E.R., Rodrigues, L.S., Brown, M.R., Reineke, J.J., da Rocha, S.R., 2016a. Conjugation to Poly(amidoamine) Dendrimers and Pulmonary Delivery Reduce Cardiac Accumulation and Enhance Antitumor Activity of Doxorubicin in Lung Metastasis. *Mol Pharm* 13, 2363-2375.
- Zhong, Q., Merkel, O.M., Reineke, J.J., da Rocha, S.R., 2016b. Effect of the route of administration and PEGylation of poly (amidoamine) dendrimers on their systemic and lung cellular Biodistribution. *Molecular pharmaceuticals* 13, 1866-1878.
- Zhu, S., Hong, M., Tang, G., Qian, L., Lin, J., Jiang, Y., Pei, Y., 2010. Partly PEGylated polyamidoamine dendrimer for tumor-selective targeting of doxorubicin: the effects of PEGylation degree and drug conjugation style. *Biomaterials* 31, 1360-1371.
- Zidan, A.S., Aldawsari, H., 2015. Ultrasound effects on brain-targeting mannosylated liposomes: in vitro and blood-brain barrier transport investigations. *Drug Des Devel Ther* 9, 3885-3898.
- Zong, T., Mei, L., Gao, H., Shi, K., Chen, J., Wang, Y., Zhang, Q., Yang, Y., He, Q., 2014. Enhanced glioma targeting and penetration by dual-targeting liposome co-modified with T7 and TAT. *J Pharm Sci* 103, 3891-3901.
- Zuspan, F.P., 1966. Treatment of severe preeclampsia and eclampsia. *Clinical obstetrics and gynecology* 9, 954-972.

ABSTRACT**GENTAMICIN-MODIFIED NANOCARRIERS FOR PLACENTAL TARGETED
DRUG DELIVERY TO TREAT PREGNANCY-RELATED COMPLICATIONS**

by

ALI ALFAIFI**AUGUST 2019****Advisors:** Dr. Sandro R. P. da Rocha, Dr. Mahendra Kavdia**Major:** Biomedical Engineering**Degree:** Doctor of Philosophy

Diseases of pregnancy are the leading cause of maternal and neonatal morbidity and mortality affecting more than 20% of all pregnancies annually. Those diseases include preeclampsia, preterm labor, and intrauterine growth restriction, many of which are caused by placental dysfunctions. Placenta is a specialized organ that creates a maternal-fetal interface. It provides many functions that contribute to the fetal development. Unfortunately, there is currently no treatment for such diseases. Our work focuses on the development of a novel nanoplatform that can be used to target the placenta so as to deliver therapeutics, which can be encapsulated or conjugated to the nanoformulations.

In this work, we have established and characterized an *in vitro* placental model based on BeWo cell monolayers that mimic the placental barrier, the syncytiotrophoblast. Next, we synthesized lipid conjugates with gentamicin, as a targeting moiety that is a substrate to megalin receptors, which are expressed on the maternal (apical) side of the syncytiotrophoblast. Using those targeting lipids, we successfully prepared and characterized targeting liposomes nanocarriers and showed that they are more significantly taken up by the BeWo polarized

monolayers compared to liposomes lacking the targeting lipid. Furthermore, we tested our liposomal formulations under different conditions: 1) saturated megalin receptors 2) a different cell line (HepG2) that does not express megalin. Results reinforced the ability of the liposomes to target the *in vitro* syncytiotrophoblast model and that the internalization mechanism is megalin-mediated endocytosis. Subsequently, we established an *in vivo* model of the syncytiotrophoblast using timed-pregnant Balb/c mice. On gestational day 18.5, we administered the liposomal formulations and assessed the biodistribution in placentas, kidneys, and fetuses. Placental analysis showed significant accumulation of the targeting liposomes compared to the control non-targeting liposomes and the free Cy5.5 (drug model). Moreover, kidneys showed significant accumulation, which was expected because those organs also express megalin receptors. Fetal tissues showed no significant difference between the three groups suggesting that the fetus should experience no toxicity due to limited exposure to the nanocarriers. This conclusion confirms our hypothesis and satisfies our goal of successfully establishing a nanoplatform for the targeted delivery of therapeutics to the placenta.

AUTOBIOGRAPHICAL STATEMENT

Ali Alfaifi received his Bachelor of Science in 2011 from Wayne State University majoring in biological sciences. Beginning of 2012, Ali joined the biomedical engineering program at Wayne State University and earned his Master of Science degree in 2013. After graduation, he went back to his home country, Saudi Arabia, and worked in King Fahd Center for Medical Research. In 2015, Ali went back to Wayne State University to continue his PhD in the biomedical engineering department under the guidance of Prof. Sandro R. P da Rocha. Ali performed most of his PhD research in the Center for Pharmaceutical Engineering and Sciences in the Nanomedicine Group, under Prof. da Rocha a faculty in the Department of Pharmaceutics in School of Pharmacy at Virginia Commonwealth University, with support also from Dr. Mahendra Kadvia in Biomedical Engineering at WSU. During his PhD, Ali attended several conferences including Nanomedicine and Drug Delivery Symposium (NanoDDS) 2017 and 2018 and American Association for Pharmaceutical Scientists (AAPS) PharmSci 360, 2018 where he had an opportunity to disseminate the work being reported here.